Acoustic wave propagation in a multilayer composed of fluid, solid, and porous viscoelastic layers

Sandrine Matta

▶ **To cite this version:**

Sandrine Matta. Acoustic wave propagation in a multilayer composed of fluid, solid, and porous viscoelastic layers. Micro and nanotechnologies/Microelectronics. Université de Valenciennes et du Hainaut-Cambresis; Université de Balamand (Tripoli, Liban), 2018. English. NNT : 2018VALE0035 . tel-02398764

HAL Id: tel-02398764
https://theses.hal.science/tel-02398764

Submitted on 8 Dec 2019

HAL is a multi-disciplinary open access archive for the deposit and dissemination of scientific research documents, whether they are published or not. The documents may come from teaching and research institutions in France or abroad, or from public or private research centers.

L'archive ouverte pluridisciplinaire **HAL**, est destinée au dépôt et à la diffusion de documents scientifiques de niveau recherche, publiés ou non, émanant des établissements d'enseignement et de recherche français ou étrangers, des laboratoires publics ou privés.

Doctoral thesis

To obtain a Doctorate degree at

the POLYTECHNIC UNIVERSITY HAUTS-DE-FRANCE

and the UNIVERSITY OF BALAMAND

Specialty:
ELECTRONICS

Presented and defended by Sandrine, MATTA.

On 07/12/2018, at Valenciennes

Doctoral School:
Sciences for Engineering (ED SPI 072)

Research team, Laboratory:
Institute of Electronics, Microelectronics and Nanotechnology - Opto-Acousto-Electronic Department (IEMN DOAE – UMR 8520)

Acoustic Wave Propagation in a Multilayer Composed of Fluid, Solid, and Porous Viscoelastic Layers

JURY

President of jury
- LUPPÉ, Francine. Professor. University of Le Havre, France.

Reviewers
- NOURY, Norbert. Professor. University of Claude-Bernard Lyon 1, France.
- KAZAN, Michel. Assistant Professor. American University of Beirut, Lebanon.

Examiner
- FARAH, Wehbeh. Professor. Saint Joseph University, Lebanon.

Co-directors
- NASSAR, Georges. Associate Professor, HDR. Polytechnic University Hauts-de-France, France.
- ABCHE, Antoine. Professor. University of Balamand, Lebanon.

Supervisor
- XÜ, Wei-Jiang. Associate Professor. Polytechnic University Hauts-de-France, France.

Thèse de doctorat

Pour obtenir le grade de Docteur de

l'UNIVERSITÉ POLYTECHNIQUE HAUTS-DE-France

et l'UNIVERSITÉ DE BALAMAND

Spécialité :
ELECTRONIQUE

Présentée et soutenue par Sandrine, MATTA.

Le 07/12/2018, à Valenciennes

Ecole doctorale :
Sciences Pour l'Ingénieur (ED SPI 072)

Equipe de recherche, Laboratoire :
Institut d'Electronique de Microélectronique et de Nanotechnologie - Département Opto-Acousto-Electronique (IEMN DOAE – UMR 8520)

Propagation des Ondes Acoustiques dans une Multicouche Composée de Couches Viscoélastiques Liquides, Solides, et Poreuses

JURY

Président du jury
- LUPPÉ, Francine. Professeur. Université le Havre, France.

Rapporteurs
- NOURY, Norbert. Professeur. Université Claude-Bernard Lyon 1, France.
- KAZAN, Michel. Professeur. Université Américaine de Beyrouth, Liban.

Examinateur
- FARAH, Wehbeh. Professeur. Université Saint Joseph, Liban.

Co-directeurs de thèse
- NASSAR, Georges. Maître de conférences, HDR. Université Polytechnique Hauts-de-France, France.
- ABCHE, Antoine. Professeur. Université de Balamand, Liban.

Encadrant
- XÜ, Wei-Jiang. Maître de conférences. Université Polytechnique Hauts-de-France, France.

ACKNOWLEDGEMENTS

This manuscript is the outcome of four years of work under a collaboration between the Department of Opto-Acousto-Electronique (OAE) in the Institut d'Electronique, de Microélectronique et de Nanotechnologie (IEMN) at the Université Polytechnique Hauts-de-France (UPHF, previously Université de Valenciennes et du Hainaut-Cambrésis, UVHC), France, and the Department of Electrical Engineering at the University of Balamand (UOB), Lebanon. Hence, I would like first to thank my two supervisors from both institutions, Dr. Georges Nassar (UPHF) and Dr. Antoine Abche (UOB) for giving me the opportunity to start this PhD work, and for all the support and guidance they provided me during these four years.

My deepest gratitude goes to my co-supervisor Dr. Wei-Jiang Xü (UPHF), without whom none of this work could have been possible. Thank you for backing me up throughout the technical difficulties and analysis complexities, as well as for accommodating your schedule to suit my stays in France.

I would like also to thank all of the jury members for accepting this task and dedicating their time to go through my work.

For the time spent in France, I thank all of my colleagues and friends at UPHF who provided me with their enormous support and encouragement. I have to thank especially Hala, Tonia-Maria, Dany, Ahmad, Abdallah, Gilbert and Jamil for making my stays in Valenciennes much more bearable and memorable.

Outside of research, a gratitude from my heart goes to my mother, brother, sisters, and to the spirit of my father, from whom I have been always deriving my strength. Thank you for being always there for me and I hope I will always make you proud of me.

I also thank my cousins Dr. Sylvana El Khoury and Dr. Selim Mekdessi for their continuous moral support and guidance throughout these four years and before. Thank you for always being ready to hear me, share with me my problems and help me find solutions.

Last but not least, the biggest thanks go to my husband who supported me, in both the English and French meanings of the term, during these four years. Thank you for your infinite patience and for being always by my side, lifting me up from my downs, and making of me a better person. I hope the coming years would be much better than the previous ones.

ABSTRACT

This thesis proposes a general formalism to model the acoustic wave propagation in a multilayer consisting of any combination of fluid, isotropic elastic solid, and isotropic poro-elastic layers, the method having the flexibility to be extended to include other layer-natures.

At a first stage, a stable algorithm is developed, based on the recursive stiffness matrix approach, to model the propagation of a plane wave incident on the multilayer as a function of its incidence angle and frequency. This algorithm merges recursively the structure individual layers stiffness matrices into one total stiffness matrix and allows then the calculation of the reflection and transmission coefficients, as well as the displacement and stress components inside the multilayer for every incident plane wave direction.

Secondly, to model the propagation of a bounded incident wave beam, the angular spectrum technique is used which is based on the decomposition of this beam into a spectrum of plane waves traveling in different directions. The corresponding reflected wave beam in the incidence medium, and the transmitted wave beam in the transmission medium, as well as the fields distributions (displacement and stress components) inside the multilayer are obtained by summing the contribution of all the plane waves traveling in different directions.

As a numerical application, a three-layered solid-porous-solid structure immersed in water is simulated. The resulting reflection and transmission as well as the displacement and stress components in the multilayer corresponding to both, the incident plane wave in different directions and the incident bounded beam reveal the stability of the method and the continuity of the displacements and stresses at the interfaces.

Keywords: Wave propagation; layered media; stiffness matrix; porous media; Biot's theory; reflection and transmission coefficients; angular spectrum.

RÉSUMÉ

Cette thèse propose un formalisme général pour modéliser la propagation des ondes acoustiques dans une multicouche composée de toute combinaison de couches liquides, solides élastiques isotropes et poro-élastiques isotropes, la méthode ayant la flexibilité d'être développée pour inclure d'autres natures de couches.

Dans un premier lieu, un algorithme stable est développé, basé sur l'approche récursive de la matrice de rigidité, pour modéliser la propagation d'une onde plane incidente sur la multicouche en fonction de son angle d'incidence et de sa fréquence. Cet algorithme fusionne de manière récursive les matrices de rigidité des couches individuelles de la structure en une matrice de rigidité totale et permet ensuite le calcul des coefficients de réflexion et de transmission, ainsi que les composantes de déplacement et de contrainte à l'intérieur de la multicouche pour chaque direction d'incidence des ondes planes.

Deuxièmement, pour modéliser la propagation d'un faisceau délimité d'ondes incidentes, la technique du spectre angulaire est utilisée, basée sur la décomposition de ce faisceau en un spectre d'ondes planes se propageant dans des directions différentes. Par la suite, le faisceau d'onde réfléchi dans le milieu d'incidence et le faisceau d'onde transmis dans le milieu de transmission, ainsi que la distribution des champs (composantes de déplacement et de contrainte) à l'intérieur de la multicouche sont obtenus en superposant la contribution de toutes les ondes planes se propageant dans les différentes directions.

Comme application numérique, une tri-couche solide-poreuse-solide immergée dans l'eau est simulée. La réflexion et la transmission qui en résultent, ainsi que les composantes de déplacement et de contrainte dans la multicouche, correspondants à l'onde plane incidente et au faisceau limité incident, révèlent la stabilité du procédé et la continuité des déplacements et des contraintes aux interfaces.

Mots-clés: propagation des ondes; multicouches; matrice de rigidité; milieu poreux; théorie de Biot; coefficients de réflexion et de transmission; spectre angulaire.

TABLE OF CONTENTS

ACKNOWLEDGEMENTS i
ABSTRACT iii
RÉSUMÉ iv
TABLE OF CONTENTS v

GENERAL INTRODUCTION 1

CHAPTER 1 HISTORICAL AND THEORETICAL BACKGROUNDS 5
1.1 Modeling of a Plane Wave Propagation in a Multilayer 5
1.2 Plane Wave Propagation in an Isotropic Elastic Solid 11
1.2.1 Stress and Strain in a Deformable Solid 11
1.2.2 Stress Strain Relationship for an Isotropic Elastic Solid 13
1.2.3 Wave Equation in an Isotropic Elastic Solid 14
1.3 Plane Wave Propagation in a Fluid Medium 17
1.4 Plane Wave Propagation in an Isotropic Poro-elastic Medium 18
1.4.1 Background 18
1.4.2 Wave Equations in an Isotropic Poro-elastic Material - Biot's Theory 19
1.5 Conclusion 22

CHAPTER 2 DISPLACEMENTS AND STRESSES IN INDIVIDUAL LAYERS OF A MULTILAYERED STRUCTURE 24
2.1 Introduction 24
2.2 Layers Characteristic Matrices 24
2.2.1 Characteristic Matrix of an Isotropic Solid Layer 28
2.2.2 Characteristic Matrix of a Fluid Layer 30
2.2.3 Characteristic Matrix of a Poro-elastic Isotropic Layer 31
2.3 Layers Stiffness Matrices 40
2.3.1 Stiffness Matrix of a Fluid Layer 42
2.3.2 Stiffness Matrix of an Isotropic Elastic Solid Layer 43
2.3.3 Stiffness Matrix for an Isotropic Poro-elastic Layer 44
2.4 Conclusion 46

CHAPTER 3 DEVELOPED ALGORITHM FOR PLANE WAVE PROPAGATION IN MULTILAYERED MEDIA 47
3.1 Introduction 47
3.2 Interfaces Boundary Conditions 48
3.2.1 Fluid-Isotropic Elastic Solid Interface: 48
3.2.2 Fluid-Porous Interface: 48
3.2.3 Solid-Porous Interface: 49
3.3 Total Stiffness Matrix of Multilayered Media 49
3.3.1 Algorithm Concept 50
3.3.2 Computation of the Matrix $[V_i]$ 53
3.3.2.1 Interface Separating Two Layers of the Same Nature 54
3.3.2.2 Fluid - Isotropic Elastic Solid Interface 55
3.3.2.3 Isotropic Elastic Solid - Fluid Interface 56
3.3.2.4 Fluid - Isotropic Poro-elastic Interface 57
3.3.2.5 Isotropic Poro-elastic - Fluid Interface 58
3.3.2.6 Isotropic Elastic Solid - Isotropic Poro-elastic Interface 60
3.3.2.7 Isotropic Poro-elastic - Isotropic Elastic Solid Interface 61
3.4 Reflection and Transmission Coefficients 63
3.4.1 Layer 1 Fluid – Layer N Fluid 67
3.4.2 Layer 1 Fluid – Layer N Isotropic Elastic Solid 68
3.4.3 Layer 1 Fluid – Layer N Isotropic Poro-elastic Medium 68
3.4.4 Layer 1 Isotropic Elastic Solid – Layer N Fluid 69
3.4.5 Layer 1 Isotropic Elastic Solid – Layer N Isotropic Elastic Solid 70
3.4.6 Layer 1 Isotropic Elastic Solid – Layer N Isotropic Poro-elastic Medium 71
3.4.7 Layer 1 Isotropic Poro-elastic Medium – Layer N Fluid 72
3.4.8 Layer 1 Isotropic Poro-elastic Medium – Layer N Isotropic Elastic Solid 73
3.4.9 Layer 1 Isotropic Poro-elastic Medium – Layer N Isotropic Poro-elastic Medium 74
3.5 Wave Amplitudes Inside the Structure Layers 75
3.5.1 Wave Amplitudes Inside Layer N 76
3.5.2 Wave Amplitudes Inside Layers $N-1$ to 2 77
3.5.3 Wave Amplitudes Inside Layer 1 79
3.6 Conclusion 79

CHAPTER 4 WAVE BEAM PROPAGATION THROUGH LAYERED MEDIA USING THE ANGULAR SPECTRUM METHOD 80
4.1 Introduction 80
4.2 Modeling of the Wave Beam Propagation 80
4.2.1 Incident Wave Field 81
4.2.2 Reflected and Transmitted Wave Fields 83
4.2.3 Displacement and Stress Distribution in the Multilayer 87
4.3 Numerical Application 89
4.4 Conclusion 101

CONCLUSION 103

LIST OF REFERENCES 105

GENERAL INTRODUCTION

The topic of elastic waves propagation in layered media has been, for the past half century, the interest of many researchers working in several fields such as underwater acoustics, seismology, geophysics, biomedical engineering nondestructive testing, etc... Moreover, since many layered materials encountered in these fields include porous media, the inclusion of porous materials in the study of the waves propagation in layered media has gained considerable attention. Some of these studies have considered the case of multilayers consisting of layers of the same nature but with different characteristics, while others have dealt with a combination of a varied layer natures. However, the common point to all of them is their focus on how the involved layers interact with each other, due to the propagation of a plane wave through them, depending on their natures and properties, as well as the natures of the interfaces separating them. Hence, the established methods in these studies for modeling the plane wave propagation in a multilayer, whether analytical or numerical methods, have been developed from formulations that combine the physical and mechanical characteristics of each layer with the interaction conditions of the waves at the interfaces between every two adjacent layers, or the so-called boundary conditions. For a given incident plane wave on a multilayer, this interaction is usually investigated through the assessment of the amount of reflection obtained in the originating medium, and the amount of transmission in the continuing medium.

The purpose of this thesis is, first, to develop an analytical, stable, and general formalism for plane wave propagation in layered media that could consist of a combination of varied layer natures. The developed algorithm is based on the recursive stiffness matrix

method proposed by Rokhlin and Wang [1]. We consider only isotropic and homogeneous materials with three possible layer-natures: fluid, isotropic elastic solid, and isotropic poro-elastic material. However, this formalism has the ability to be extended and adapted to include anisotropy and other layer natures in the future. The investigation in the study of the plane wave propagation in the multilayer is not limited to the acquisition of the reflection and transmission coefficients, but the developed formalism allows also to evaluate the wave amplitudes inside the layers.

Then, since in real situations, an incident wave generated by an acoustic source is usually not a plane wave, but rather a bounded beam, the technique developed in this work for plane wave propagation in layered media is furthermore employed in the development of the modeling of an acoustic beam propagation in a multilayer using the angular spectrum method.

This manuscript is composed of four chapters.

In the first one, a historical background is presented for the different techniques that have been developed by researchers for modeling plane wave propagation in layered media. Then, a theoretical background is given for plane wave propagation in each of the three-considered layer-natures, the Biot's theory being used for the case of the porous material.

In the second chapter, the multilayer consisting of any combination of the three layer-natures is defined. The displacement and stress components are then expressed in terms of the partial plane waves amplitudes in every layer of the structure, depending on its nature. The factorization of these expressions allows to obtain the characteristic matrices of the individual layers of the structure, and subsequently their stiffness matrices, in terms of the layer mechanical properties as well as the incident plane wave frequency and incidence angle.

In the third chapter, a recursive algorithm is developed to obtain the total stiffness matrix of the multilayer. In this algorithm the individual layers stiffness matrices found in the

second chapter are combined into one total stiffness matrix, based on the boundary conditions at every interface separating two adjacent layers of the structure. Subsequently, the reflection and transmission coefficients are calculated considering the multilayer bounded by fluid materials. Then, having the reflection and transmission coefficients, a back recursive algorithm is developed in order to obtain the partial plane waves amplitudes inside the structure layers. This allows afterwards to evaluate the displacements and stresses components at any point in the multilayer. The expressions found for the reflection and transmission coefficients, the amplitudes of the waves inside the layers, as well as the displacement and stress components in the multilayer are all in terms of the incident plane wave frequency and incidence angle.

Having modeled the propagation of a plane wave incident on the multilayer at a given frequency and incidence angle, the propagation of an acoustic beam incident on the multilayer is modeled in the fourth chapter using the angular spectrum technique. The latter is based on the superposition of the contributions of monochromatic plane waves traveling in many directions. Hence for an incident acoustic beam, the reflected and transmitted beams in the incidence and transmission media are reconstructed. Furthermore, the displacement and stress components fields distributions are obtained inside the multilayer. A numerical example is applied in this chapter to simulate the algorithm, where the case of a three-layered solid-porous-solid structure immersed in water is considered. So, first, the formalism developed in the third chapter is applied in order to obtain the reflection and transmission coefficients as well as the displacement and stress components at any position in the multilayer, corresponding to each incident plane wave direction and at a given frequency. Then, using the angular spectrum method, the reflected, and transmitted wave fields along with the displacement and stress components fields distribution are obtained. Finally, the

presented work is summarized in the general conclusion, and perspectives for future works on the subject are proposed.

CHAPTER 1

HISTORICAL AND THEORETICAL BACKGROUNDS

1.1 Modeling of a Plane Wave Propagation in a Multilayer

A multilayer is, by definition, a medium consisting of a stack of a given number of media separated by interfaces. In particular, when these stacked layers or strata are homogeneous and planar with parallel interfaces, the structure is referred to as a stratified medium.

The investigation in modeling the propagation of elastic plane waves in stratified media had been triggered long time ago [2, 3, 4, 5], however it has got a remarkable push after the elaborated technique published by Thomson in 1950 [6]. In his method, Thomson studied theoretically the transmission of an elastic plane wave at an oblique incidence through a stratified medium consisting of an arbitrary number of parallel planar solid media of different characteristics and thicknesses. He defined a matrix called transfer matrix that relates the displacements and stresses at the bottom of a layer to the ones at the top of that layer. Then, for two consecutive solid layers, by applying the appropriate boundary conditions at the interface separating them, which are the continuity of particle velocities and normal and shearing stresses, the stresses and displacements of these two layers can be related. Therefore, the wave propagation across the layers of the structure is expressed through each layer transfer matrix, and its propagation across interfaces in the structure is expressed via the boundary conditions at each interface. In this manner, the displacements and stresses at the

bottom of the multilayer can be related to those at the top through a single matrix obtained via a process of individual layers matrices multiplication. The equations derived by Thomson were based on some assumptions such as that the shear modulus is the same in all the solid layers, which made the method of limited validity to some particular cases. This issue was fixed three years later by Haskell who proposed a more generalized formulation of Thomson's method [7], and since then it has been referred to as Thomson-Haskell method, transfer matrix method, or propagator matrix method. Shaw and Bugl published in 1969 a refined version of Thomson-Haskell matrix formalism [8], where they expressed the displacements and stresses in terms of the layers parameters and they introduced the effects of viscoelasticity by assigning complex values to the parameters of the solid layers. In parallel to Thomson's work, Brekhovskikh developed in 1960 another method for wave propagation in layered media based on the layers and interfaces impedances [9]. However, the equations he developed had also the problem of their limitation to the same particular cases as those of Thomson. Folds and Loggins reconsidered the previously published results from both methods and re-derived them in a more suitable and revealing way with few modifications. In their work, they obtained the reflection and transmission coefficients for the case of a plane elastic wave incident on a stratified structure consisting of viscoelastic layers [10].

Following Thomson-Haskell work, and with the availability of computer resources, there was an increasing interest of implementing the transfer matrix technique in numerical methods for modal calculations of plane wave propagation in layered media. This revealed an instability problem of the method when dealing with thick layers and at high frequencies. These numerical instabilities are due to a loss of precision when performing arithmetic calculations on the layers transfer matrices using computers. In fact, according to Thomson-Haskell method, the total transfer matrix of a layered medium consisting of solids is obtained

by multiplying the layers transfer matrices. The greater the number of layers, the greater the numerical loss of precision in the computer calculations due to its limited capacity (limited number of digits). Moreover, as shown by Dunkin [11], the transfer matrices of individual layers contain an exponential term whose power is proportional to the layer thickness and the wave frequency. Therefore, at high frequencies and for thick layers, these small precision errors will be considerably amplified by the exponential term. Consequently, an effort was put by researchers to solve for this problem that became known as the "large fd problem", and thus improve the performance of transfer matrix method. In his paper, as a solution to the issue, Dunkin introduced the delta operator approach which was used and improved later on by other researchers such as Kundu and Mal [12] and Lévesque and Piché [13]. In this method, delta matrices are calculated made up of 2×2 subdeterminants of individual layers transfer matrices in order to avoid the accumulation of errors when multiplying the transfer matrices to find the total one. The delta operator method, being only applied in previous works on wave propagation through isotropic media, Castaings and Hosten [14, 15] published an extension of this method to include anisotropic materials. In that case, the delta matrices are constructed from 3×3 subdeterminants of individual layers transfer matrices. The delta operator method has succeeded to heal the transfer matrix method from the loss of precision, nevertheless, its problem is in the considerable increase of the computational time because of the large number of subdeterminants introduced calculations. Balasubramaniam proposes an alternative solution that is simpler and not computationally intensive: the numerical truncation algorithm [16, 17]. The latter is an approximation algorithm that is based on setting a maximum threshold value for the exponential terms involved, which limits the amplification of the precision errors and prevents instabilities. This approach, which has been referred to as the modified transfer matrix approach, has been shown to stabilize the computation without requiring any extensive reformulation and without compromising the

original method efficiency. Nevertheless, this numerical truncation has exhibited instabilities for very high fd values.

While the above-mentioned works adopted the transfer matrix method and developed their own approaches to enhance it and make it robust, some other publications proposed quite different computationally stable matrix formulations, alternative to the transfer matrix method, for modeling wave propagation in layered media. Among these techniques we cite the global matrix method that was first proposed by Knopoff in 1964 [18] for layered structures consisting of isotropic solids, then implemented and validated by other researchers [19, 20, 21, 22, 23, 24]. This method consists of mapping the equations for individual layers into one global single matrix that includes all the unknowns related to the boundary conditions. This algorithm proved to be stable and efficient with the disadvantage of computation slowness in the case of several layers which increases the size of that global matrix. A review of the technique and its comparison to the transfer matrix method was done by Lowe [25].

A reformulated global matrix technique has been proposed by Kausel and Roesset [26] where the system global matrix was obtained for isotropic solid layered media in terms of the layers stiffness matrices rather than their transfer matrices. A stiffness matrix relates the stress components to the displacement components at the top and bottom surfaces of that layer. Thus, in this method, the total displacements and stresses are obtained instead of the waves amplitudes.

Another stable different approach was developed by Kennett and Kerry [27] and Kennett [28] for isotropic solid layered media, referred to as reflection matrix method or transmission reflection matrix method. It consists of creating reflection and transmission matrices for individual interfaces in the multilayer, then these matrices are mapped recursively into global reflection and transmission matrices. The approach was extended later

on to generally anisotropic layered media by Fryer and Frazer [29, 30] and Rokhlin and Huang [31]. This method has proven to be computationally stable and efficient and has been widely used for wave propagation modeling in layered media in the fields of seismology and geophysics.

An additional alternative stable method to the transfer matrix method was developed in the beginning of the twenty-first century by Rokhlin and Wang who presented a recursive algorithm they developed for the computation of a total stiffness matrix for layered elastic anisotropic media [1, 32, 33], based on individual layers stiffness matrices. They proved their method, referred to as stiffness matrix method, to be unconditionally stable at high frequencies and for thick layers, keeping at the same time the computational efficiency and simplicity of the transfer matrix method. A comparison was made between the stiffness matrix method and the transfer matrix method by Balasubramaniam et al. [17]. A detailed description of this approach will be provided later in this manuscript.

All of the above-mentioned techniques and their developments considered layered media consisting either of isotropic or anisotropic elastic solids. However, the researches in some specific fields such as geophysics and biomedical engineering necessitated modeling wave propagation in layered media including porous material. Thus, the need to adapt the previously developed techniques for the modeling of plane wave propagation in layered media to the case of multilayers composed of either porous layered media or a combination of various layer natures arose.

For instance, the sound propagation in layered porous media was described at normal incidence by Allard et al. [34] and at oblique incidence by Allard et al. [35] using the transfer matrix method. Schmitt [36] and Lauriks et al. [37] worked on the modeling of the propagation of plane waves in a multilayered medium including fluid, solid and porous layers based on the transfer matrix method as well. Vashishth et al. [38] studied the wave

propagation in a layered anisotropic poro-elastic structure bounded by an isotropic elastic solid and a fluid using the transfer matrix technique. Jocker et al. [39] proposed an extension of the Thomson-Haskell method to present closed-form analytical expressions for the reflection and transmission coefficients of a layered isotropic poro-elastic medium, and they investigated the stability of their approach.

Parra [40] calculated the dispersion and attenuation of acoustic waves in layered fluid filled porous media based on the global matrix method. Brouard et al. [41] and Allard and Atalla [42] presented a general method of modeling sound propagation in multi-layered media including fluid, elastic solid, and porous layers using also the transfer matrix method. In their approach, and in order to adapt the original method to the case of two adjacent layers of different natures, they defined two matrices for every interface that relate the acoustic fields from both sides of that interface.

Rajapakse and Senjuntichai used the global stiffness matrix method as proposed by Kaussel and Roesset to study the dynamic [43] and quasi-static [44] responses of a layered poro-elastic medium. Degrande et al. [45] studied the wave propagation in multi-layered dry, saturated and unsaturated isotropic poro-elastic media using also the global stiffness matrix method.

Moreover, Feng et al. [46] have recently proposed and extension of the transmission and reflection matrix method to investigate about the reflection and transmission of plane waves in a multilayered porous medium.

In this manuscript, we develop a general stable formalism for modeling plane wave propagation in a layered medium consisting of layers of different natures, based on the recursive stiffness matrix method. Three layer-natures will be considered in particular: fluid, isotropic elastic solid, and isotropic poro-elastic medium, the method having the flexibility to

be extended to include other layer-natures. Therefore, a background will be provided in the coming section for the plane wave propagation theories in each of these three layer-natures.

1.2 Plane Wave Propagation in an Isotropic Elastic Solid

1.2.1 Stress and Strain in a Deformable Solid

Consider a cubical volume in a deformable medium. If a force is applied on the top of the cube, this latter is compressed in the direction of the force, while the other sides are bulged. Hence this force is converted into stresses in different directions, the stress being obtained by dividing the force by the surface area on which it is acting. The normal stress components applied on the solid face in a direction i are denoted by σ_{ii}, while the tangential components acting on the plan j orthogonal to i are denoted by σ_{ij}. The first subscript refers to the direction of the stress component, while the second refers to the normal direction to the corresponding cube face. Hence, for example, the stress on the face xy of the cube in Figure 1-1 has three orthogonal components: the normal component σ_{zz} along the z direction, and the two tangential components σ_{xz} and σ_{yz} along x and y respectively. Considering also the stresses on the xz and yz faces, nine stress components are counted in total as shown in Figure 1-1, and the stress tensor is defined as:

$$\boldsymbol{\sigma} = \begin{bmatrix} \sigma_{xx} & \sigma_{xy} & \sigma_{xz} \\ \sigma_{yx} & \sigma_{yy} & \sigma_{yz} \\ \sigma_{zx} & \sigma_{zy} & \sigma_{zz} \end{bmatrix}. \tag{1.1}$$

An important property of this stress tensor is its symmetry, i.e.:

$$\sigma_{ij} = \sigma_{ji}\,, \tag{1.2}$$

which reduces the number of the stress components to six.

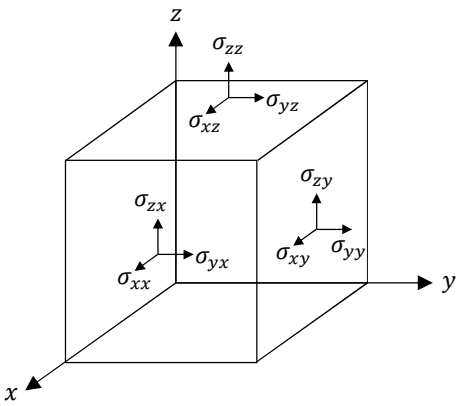

Figure 1-1: Applied stresses on the cube faces.

The strain is the deformation response of the volume to the applied force or stress in terms of relative displacement of particles in the given volume. It is by definition, the average change in two directions, i and j, of the deformed length within the volume that has undergone deformation, denoted by ε_{ij}. If the displacement due to the elastic wave vibration is defined by the vector $\boldsymbol{u}$, the strain can be related to the displacement by the Cauchy relationship as:

$$\varepsilon_{ij} = \frac{1}{2}\left(\frac{\partial u_i}{\partial j} + \frac{\partial u_j}{\partial i}\right). \tag{1.3}$$

It could be noticed from Eq. (1.3) that:

$$\varepsilon_{ij} = \varepsilon_{ji}, \tag{1.4}$$

which makes the strain tensor also symmetrical. In the following, the values of 1,2,3 will be attributed to each of the subscripts i and j representing the direction components of x, y, and z, respectively, under the Cartesian coordinates.

1.2.2 Stress Strain Relationship for an Isotropic Elastic Solid

The stress-stain relationships for an elastic solid are given by Hook's law to be:

$$\sigma_{ij} = C_{ijkl}\varepsilon_{kl}, \quad i,j,k,l = 1,2,3 \tag{1.5}$$

where C_{ijkl} is the elasticity or stiffness tensor of rank four, i.e. including 81 components. However, since, with reference to Eqs. (1.2) and (1.4), both of the stress and strain tensors are symmetrical, then, $C_{ijkl} = C_{jikl}$ and $C_{ijkl} = C_{ijlk}$, and the number of these components can then be reduced to 36. Using Voigt notation allows expressing Hook's law for elasticity in matrix form. In this notation, the subscripts ij are substituted by the subscript I, while kl are replaced by J, I and J varying from one to six, where the values of 1, 2, 3, 4, 5, 6 for I and J correspond respectively to the subscripts 11, 22, 33, 23, 31, 12 for ij and kl. Hence, Hook's law in Eq. (1.5) can be expressed in matrix form as:

$$[\boldsymbol{\sigma}_I] = [\boldsymbol{C}_{IJ}][\boldsymbol{\varepsilon}_J]. \tag{1.6}$$

In the case of an isotropic elastic solid, the number of independent elasticity coefficients is furthermore reduced to two: C_{11} and C_{22}. Therefore, the relationship in Eq. (1.6) can be explicitly expressed as:

$$\begin{bmatrix}\sigma_{11}\\ \sigma_{22}\\ \sigma_{33}\\ \sigma_{13}\\ \sigma_{23}\\ \sigma_{12}\end{bmatrix} = \begin{bmatrix} C_{11} & C_{12} & C_{12} & 0 & 0 & 0 \\ C_{12} & C_{11} & C_{12} & 0 & 0 & 0 \\ C_{12} & C_{12} & C_{11} & 0 & 0 & 0 \\ 0 & 0 & 0 & \frac{C_{11}-C_{12}}{2} & 0 & 0 \\ 0 & 0 & 0 & 0 & \frac{C_{11}-C_{12}}{2} & 0 \\ 0 & 0 & 0 & 0 & 0 & \frac{C_{11}-C_{12}}{2} \end{bmatrix} \begin{bmatrix}\varepsilon_{11}\\ \varepsilon_{22}\\ \varepsilon_{33}\\ \varepsilon_{13}\\ \varepsilon_{23}\\ \varepsilon_{12}\end{bmatrix}. \tag{1.7}$$

Thus, an isotropic elastic solid can be described by only the couple of coefficients C_{11} and C_{22}. Alternatively, the behavior of the isotropic elastic solid can be also described by other couples of coefficients related to C_{11} and C_{22}, such as the Lamé coefficients λ and μ,

where μ is sometimes denoted by G and is called the shear modulus of the material. Another used couple of coefficients to describe an isotropic elastic solid is the Young's modulus E and the Poisson ratio ν. These couples of coefficients are related together as summarized in Table 1-1 [47]. The bulk modulus K_s is another constant that describes the elastic property of a solid related to the Lamé coefficients by:

$$K_s = \lambda + \frac{2}{3}\mu\,. \tag{1.8}$$

Table 1-1: Conversion formulas among elastic properties of an isotropic elastic solid.

	(C_{11}, C_{12})	(λ, μ)	(E, ν)
λ	C_{12}	λ	$\frac{E\nu}{(1+\nu)(1-2\nu)}$
μ	$\frac{C_{11}-C_{12}}{2}$	μ	$\frac{E}{2(1+\nu)}$
E	$C_{11} - \frac{2{C_{12}}^2}{C_{11}+C_{12}}$	$\frac{\mu\,(3\lambda+2\mu)}{\lambda+\mu}$	E
ν	$\frac{C_{12}}{C_{11}+C_{12}}$	$\frac{\lambda}{2(\lambda+\mu)}$	ν

The stress-strain expression in Eq. (1.5) can be expressed for an isotropic elastic solid in terms of its Lamé coefficients as:

$$\sigma_{ij} = 2\mu\varepsilon_{ij} + \delta_{ij}\lambda\nabla.\boldsymbol{u},\;\; i,j = 1,2,3, \tag{1.9}$$

where $\nabla.$ is the divergence operator, and δ_{ij} is the Kronecker delta such that:

$$\begin{cases} \delta_{ij} = 1 \;\; if\; i = j, \\ \delta_{ij} = 0 \;\; if\; i \neq j. \end{cases} \tag{1.10}$$

1.2.3 Wave Equation in an Isotropic Elastic Solid

For a linear elastic solid having a constant density ρ, and neglecting the body forces applied to it, the equation of motion can be written as:

$$\rho \frac{\partial^2 u_i}{\partial t^2} = \frac{\partial \sigma_{ij}}{\partial x_j}. \tag{1.11}$$

Substituting Eqs. (1.3), (1.9), and (1.10) into Eq. (1.11) leads to the elasto-dynamic equation describing the displacement in an isotropic elastic solid which can be expressed as [47]:

$$\rho \frac{\partial^2 \boldsymbol{u}}{\partial t^2} = (\lambda + \mu)\nabla(\nabla . \boldsymbol{u}) + \mu \nabla^2 \boldsymbol{u}, \tag{1.12}$$

where ∇ is the gradient operator, $\nabla .$ is the divergence operator and ∇^2 is the Laplacian. In order to decouple the three displacement components u_x, u_y, and u_z, the displacement field $\boldsymbol{u}$ can be decomposed into a scalar potential ϕ and a vector potential $\boldsymbol{\psi}$ using Helmholtz decomposition, such that:

$$\boldsymbol{u} = \nabla \phi + \nabla \times \boldsymbol{\psi}, \tag{1.13}$$

with

$$\nabla \times (\nabla \phi) = \boldsymbol{0} \quad \text{and} \quad \nabla \boldsymbol{\psi} = 0, \tag{1.14}$$

where $\nabla \times$ is the curl operator.

Substituting the expressions in Eqs. (1.13) and (1.14) into Eq. (1.12) yields to:

$$\nabla \left(\rho \frac{\partial^2 \phi}{\partial t^2} - (\lambda + 2\mu)\nabla^2 \phi \right) + \nabla \times \left(\rho \frac{\partial^2 \boldsymbol{\psi}}{\partial t^2} - \mu \nabla^2 \boldsymbol{\psi} \right) = 0. \tag{1.15}$$

In order to satisfy Eq. (1.15), the latter could be replaced by the set of two decoupled equations in terms of ϕ and $\boldsymbol{\psi}$:

$$\begin{cases} \rho \dfrac{\partial^2 \phi}{\partial t^2} - (\lambda + 2\mu)\nabla^2 \phi = 0 \\ \rho \dfrac{\partial^2 \boldsymbol{\psi}}{\partial t^2} - \mu \nabla^2 \boldsymbol{\psi} = 0 \end{cases}. \tag{1.16}$$

These two equations show that two types of wave propagate in the isotropic elastic solid medium. The first equation corresponds to the propagation of longitudinal waves with a speed c_L such that:

$$c_L = \sqrt{\frac{\lambda + 2\mu}{\rho}}. \tag{1.17}$$

The second equation corresponds to the propagation of shear or transverse waves with a speed c_T such that:

$$c_T = \sqrt{\frac{\mu}{\rho}}. \tag{1.18}$$

For the longitudinal waves, the medium undergoes compression and rarefaction in the direction of propagation of the wave. Hence the direction of the displacement of the particles in the medium, called polarization, is parallel to the direction of propagation as illustrated in Figure 1-2 (a). As for the shear or transverse waves, the direction of the displacement of the particles in the medium (polarization) is orthogonal to the direction of propagation of the wave as shown in Figure 1-2 (b).

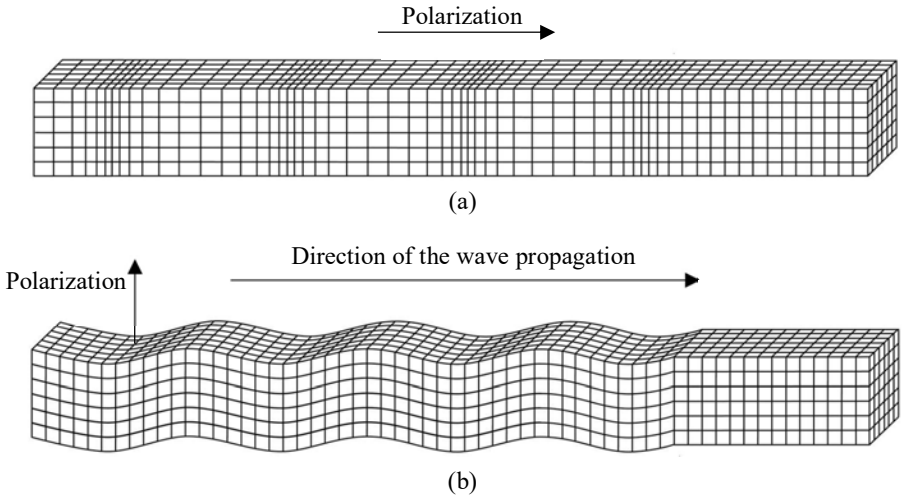

Figure 1-2: (a) Longitudinal and (b) Shear waves proagation in an isotropic elastic solid.

1.3 Plane Wave Propagation in a Fluid Medium

For the fluid medium, the equations could be deduced from the ones of the isotropic elastic solid for a vanished shear modulus, i.e. $\mu = 0$. Then, with reference to Eq. (1.8), the fluid bulk modulus is found to be:

$$K_f = \lambda\,. \tag{1.19}$$

If the body forces applied to it are neglected, the elasto-dynamic equation describing the displacement in a fluid can be expressed as:

$$\rho \frac{\partial^2 \boldsymbol{u}}{\partial t^2} = K\nabla(\nabla.\boldsymbol{u}). \tag{1.20}$$

The decomposition of the displacement field $\boldsymbol{u}$ in the case of the fluid includes only irrotational deformations such that:

$$\boldsymbol{u} = \nabla\phi, \tag{1.21}$$

with

$$\nabla \times (\nabla\phi) = \mathbf{0}. \tag{1.22}$$

Substituting Eqs. (1.21) and (1.22) into Eq. (1.20) leads to:

$$\rho \frac{\partial^2 \nabla\phi}{\partial t^2} = K_f\nabla(\nabla.\nabla\phi) = K\nabla(\nabla^2\phi). \tag{1.23}$$

Eq. (1.23) can be reduced to:

$$\nabla\left(\rho \frac{\partial^2 \phi}{\partial t^2} - K_f\nabla^2\phi\right) = 0. \tag{1.24}$$

Therefore, the displacement potential should verify the following equation:

$$\frac{\partial^2 \phi}{\partial t^2} - \frac{K_f}{\rho}\nabla^2\phi = 0, \tag{1.25}$$

which corresponds to the propagation of longitudinal waves with a speed c_L such that:

$$c_L = \sqrt{\frac{K_f}{\rho}}. \tag{1.26}$$

In an ideal compressible fluid, the nonzero stress elements are equal to $-P_f$ [42] where P_f is the pressure which is proportional to the dilatation of the fluid (that is the divergence of the displacement vector), i.e.:

$$P_f = -K_f(\nabla . \boldsymbol{u}). \tag{1.27}$$

1.4 Plane Wave Propagation in an Isotropic Poro-elastic Medium

1.4.1 Background

A porous material is a medium that consists of a solid frame, also called matrix or skeleton, that incorporates pores typically filled with a fluid. Hence, such a material includes two phases: solid and fluid. Interaction arises between these two phases when a sound wave propagates in the medium which leads to various physical properties that are not common for other classical media [48]. In real life porous materials are encountered in several fields, which made the researchers interested in the investigation about the behavior of acoustic waves in these media. For example, in the geophysics domain, the characterization of porous rocks by the mean of acoustic wave propagation gives information about the rock and soil constitution. In the biomedical field, the study of acoustic wave propagation in porous bones allows the diagnosis of some bone diseases such as osteoporosis.

In the developed models by researchers for acoustic wave propagation in porous media, two cases were distinguished regarding the rigidity of the porous structure. In the first case, when the porous material is filled by a lightweight fluid such as air, the skeleton is considered heavy with respect to that fluid. Hence, when an acoustic wave travels through the material, the skeleton does not vibrate (stationary), the reason why the porous structure is called rigid.

In this case, the wave propagates only in the fluid, with no displacement of the solid phase, and the porous medium is approximated to an equivalent fluid, similar to a free fluid whose characteristics are modified by the presence of the solid skeleton. The model developed to describe this case is called equivalent fluid model. It was established by Zwikker and Kosten in 1949 [49], who modeled the acoustic wave in materials incorporating air filled cylindrical pores, taking into consideration the thermal and viscous interactions in the medium: the viscous effects are taken into account by modifying the density of the fluid phase and the thermal effects by modifying its dynamic compressibility modulus.

The second case is when the porous structure is elastic, which means that the acoustic wave propagates in both the skeleton and the filling fluid. This case was elaborated by Biot [50, 51] few years later on; in his model, Biot considers the separate motions of the elastic solid skeleton and the fluid phase, taking into account the coupling between the two phases. Since then, Biot's model has been considered the most general model to describe the acoustic wave propagation in porous saturated media. Contributions to Biot's model were then brought by Attenbourgh [52, 53], Johnson et al. [54], Champoux and Allard [55], and Lafarge et al. [56], who introduced some parameters that extend the validity of Biot's model to include a larger frequency range, taking into account the thermal effects that develop when the fluid filling the pores is a gas [57].

In the following we consider only isotropic homogeneous poro-elastic media saturated by fluids (non-gazes), hence the viscous effects are only taken into consideration, while the thermal effects are neglected.

1.4.2 Wave Equations in an Isotropic Poro-elastic Material - Biot's Theory

As mentioned earlier, Biot's model considers separate motions of the solid and fluid phases in the porous material following an acoustic wave propagation. Thus, in Biot's theory,

the equations of motion for each of the fluid and solid phases are derived based on three types of coupling between these two phases: inertial, potential and viscous.

For an isotropic porous medium, three propagating modes are predicted: two longitudinal waves and one shear wave. One of the longitudinal waves is called first type or fast wave, while the other is called second type or slow wave.

Thus, consider an isotropic medium consisting of a porous solid whose connected pore space is saturated with a viscous compressible fluid. The fraction of the fluid volume over the total medium volume is the porosity ϕ, and it is assumed to have a constant value.

The fluid is characterized by its density ρ_f, its bulk modulus K_f, and its viscosity η_f, while the solid by ρ_s, K_s, and its shear modulus μ_s.

The solid grains are assumed to form an elastic porous dry frame and characterized by a mean bulk modulus K_m, a shear modulus μ_m and a permeability κ_m.

The bulk porous material is formed when the dry matrix is saturated by the fluid and it is characterized by its Lamé constants λ_c and μ.

Furthermore, it is assumed that the shear modulus μ of the porous saturated (wet) bulk material is equal to the shear modulus of the dry matrix μ_m.

The displacement of the solid matrix is designated by the vector $\boldsymbol{u}$, while that of the fluid by the vector $\boldsymbol{u}_f$. According to Biot's theory [50, 58, 59], the total mean displacement in the porous saturated bulk material is given by:

$$\phi \boldsymbol{u}_f + (1-\phi)\boldsymbol{u} = \phi(\boldsymbol{u}_f - \boldsymbol{u}) + \boldsymbol{u} = \boldsymbol{w} + \boldsymbol{u}, \tag{1.28}$$

where $\boldsymbol{w}$ is called the average fluid displacement relative to the frame measured in terms of volume per unit area of the bulk material and is expressed as:

$$\boldsymbol{w} = \phi(\boldsymbol{u}_f - \boldsymbol{u}). \tag{1.29}$$

The strain tensor of the solid $\varepsilon_{ij}(\boldsymbol{u})$ is related to the stress tensor of the bulk material $\sigma_{ij}(\boldsymbol{u}, \boldsymbol{w})$ by [50, 58]:

$$\sigma_{ij} = 2\mu\varepsilon_{ij} + \delta_{ij}(\lambda_c \nabla.\boldsymbol{u} + D\nabla.\boldsymbol{w}), \quad i,j = x,y,z. \tag{1.30}$$

Moreover, the liquid pressure $P_f(\boldsymbol{u}, \boldsymbol{w})$ can be expressed as:

$$P_f = -D\nabla.\boldsymbol{u} - M\nabla.\boldsymbol{w}\,. \tag{1.31}$$

The constants D and M in Eqs. (1.30) and (1.31) are expressed as [60, 61, 62]:

$$\begin{aligned} D &= \alpha M, \\ M &= \left(\frac{\alpha - \phi}{K_s} + \frac{\phi}{K_f}\right)^{-1}, \end{aligned} \tag{1.32}$$

where

$$\alpha = 1 - \frac{K_m}{K_s}. \tag{1.33}$$

The Lamé constant λ_c can be written as [58, 61]:

$$\lambda_c = K_c - \frac{2}{3}\mu\,, \tag{1.34}$$

where

$$K_c = K_m + \alpha^2 M\,. \tag{1.35}$$

The mass density ρ of the bulk material is defined as [59]:

$$\rho = (1-\phi)\rho_s + \phi\rho_f\,. \tag{1.36}$$

Moreover, let g and b be the mass and viscous coupling coefficients between fluid and solid phases, respectively, and S the structure factor. They are defined as [60, 63, 62]:

$$g = \frac{S\rho_f}{\phi}\,,$$

$$b = \frac{\eta_f}{\kappa_m}\,, \tag{1.37}$$

$$S = \frac{1}{2}\left(1 + \frac{1}{\phi}\right).$$

Then, assuming that the coefficients μ, λ_c, D, and M in Eqs. (1.30) and (1.31) are constant, Biot's equations of motion for fluid-filled porous medium can be written as [50, 58, 64, 62]:

$$\begin{aligned} \nabla.\sigma = H_c\nabla(\nabla.\boldsymbol{u}) - \mu\nabla\times(\nabla\times\boldsymbol{u}) + D\nabla(\nabla.\boldsymbol{w}) &= \rho\frac{\partial^2\boldsymbol{u}}{\partial t^2} + \rho_f\frac{\partial^2\boldsymbol{w}}{\partial t^2}\,, \\ -\nabla P_f = D\nabla(\nabla.\boldsymbol{u}) + M\nabla(\nabla.\boldsymbol{w}) &= \rho_f\frac{\partial^2\boldsymbol{u}}{\partial t^2} + g\frac{\partial^2\boldsymbol{w}}{\partial t^2} + b\frac{\partial\boldsymbol{w}}{\partial t}\,, \end{aligned} \tag{1.38}$$

where

$$H_c = \lambda_c + 2\mu\,. \tag{1.39}$$

1.5 Conclusion

In this chapter a historical background has been presented for the different methods that has been developed by researchers to model a plane wave propagation through a multilayered structure. Since our concern in this work is with three-layer natures that are fluid, isotropic solid, and isotropic poro-elastic, a theoretical background has been provided for the plane wave propagation in each of these types of media. For the porous material, the models developed by researchers for acoustic wave propagation in such a medium have been outlined, with a focus on the Biot's theory which will be employed in this work to model an isotropic poro-elastic material.

In this thesis, we present a robust and general method for modeling plane wave propagation in layered media including fluid, isotropic solid, and isotropic poro-elastic layers using the recursive stiffness matrix technique as described by Rokhlin and Wang, which proved to be computationally stable and efficient. The boundary conditions at the interfaces will be assumed perfect and Biot's theory will be used for the wave propagation in a fluid-filled poro-elastic material. In most of the previous work done on multi-layered structures including porous layers the porous media were modeled using the Biot's theory based on displacement potential rather than displacement amplitude, which limits some future extensibility of the methods. In this work, the equations in the developed matrix formulation will be expressed in terms of the displacement amplitudes.

Hence, at a first place, wave vector numbers will be calculated for each of the three natures of media in order to obtain their characteristic matrices. The stiffness matrix for each layer will be obtained afterwards and used to develop the recursive algorithm for obtaining the whole structure total stiffness matrix. The algorithm developed allows the fusion of consecutive layers stiffness matrices even if they were of different sizes, and it permits at the end relating the displacements and stresses at the top of the structure to those at the bottom. Having that total stiffness matrix, the reflection and transmission coefficients will be calculated assuming fluid incidence and transmission media, which allows then the calculation of the waves amplitudes inside each layer using a back recursive algorithm. The obtained results for a plane wave propagation in the layered media permits subsequently the modeling of an acoustic beam propagation through the layered media using the angular spectrum technique.

CHAPTER 2

DISPLACEMENTS AND STRESSES IN INDIVIDUAL LAYERS OF A MULTILAYERED STRUCTURE

2.1 Introduction

Given a structure consisting of many layers of various natures, in order to model the plane wave propagation in the whole multilayer, one should investigate first about the wave behavior in every layer of the structure. Thus, in this chapter, the displacement and stress components will be explicitly expressed inside each layer based on its physical nature. Three layer-natures will be considered: fluid, isotropic solid, and isotropic poro-elastic medium. These displacements and stresses are shown to be related to the amplitudes of the waves propagating in that layer through a matrix called layer characteristic matrix, that incorporates the medium physical parameters. Afterwards, another matrix, that is called layer stiffness matrix, and that relates the displacements to the stresses at the top and bottom of each layer, is derived as a function of its characteristic matrix.

2.2 Layers Characteristic Matrices

Consider a multilayer consisting of N layers of various material natures and thicknesses, bounded by two semi-spaces as shown in Figure 2-1. Each layer is assigned an index i, with i varying from 1 to N, while the upper and lower semi-spaces are allocated

indices 0 and $N+1$, respectively. The interface separating layers $i-1$ and i is attributed the index i.

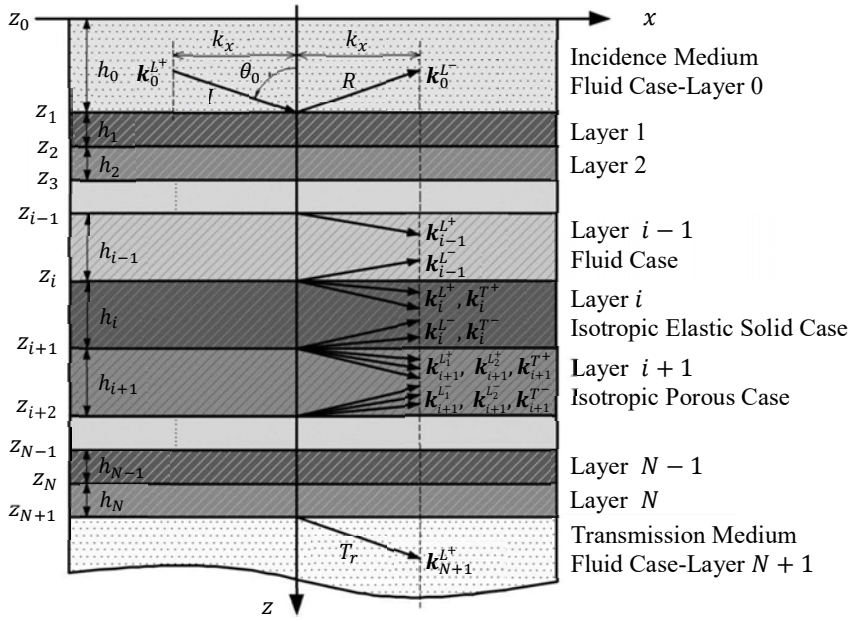

Figure 2-1: A Multilayered structure consisiting of N layers.

For an incident plane wave that hits the upper boundary or interface of the structure ($z = z_1$), scattered waves are generated: reflected waves propagate back in the incidence medium, and refracted waves are transmitted into the continuing medium to fall incident on the second interface at $z = z_2$, and so on. The number and type of the scattered waves at each interface depend on the natures of the two media around that interface and on its physical characteristics. In the following, we will be considering only flat (planar) interfaces, with rigid and smooth contacts. The superscript m is used to denote the corresponding excited partial plane wave propagating in each layer.

In general, the total displacement vector in a given layer i $(z_i \leq z \leq z_{i+1})$ is the summation of all displacements relative to each propagating partial wave, i.e.:

$$\boldsymbol{u}_i(x,y,z) = \sum_m a_i^m \, \boldsymbol{p}_i^m \, e^{j(\boldsymbol{k}_i^m \cdot \boldsymbol{r} - \omega t)} \,, \tag{2.1}$$

where,

$\boldsymbol{u_i} = \left[u_{x_i}, u_{y_i}, u_{z_i}\right]^{\mathrm{T}}$ is the displacement vector in the i^{th} layer;

$\boldsymbol{r} = [x, y, z]^{\mathrm{T}}$ is the position vector in the Cartesian coordinate system;

$\boldsymbol{k}_i^m = \left[k_{x_i}^m, k_{y_i}^m, k_{z_i}^m\right]^{\mathrm{T}}$ is the wave vector of the plane wave of index m in the i^{th} layer, and $k_i^m = \sqrt{(k_{x_i}^m)^2 + (k_{y_i}^m)^2 + (k_{z_i}^m)^2}$ is the corresponding wave number;

a_i^m is the amplitude of the displacement of index m in the i^{th} layer;

$\boldsymbol{p}_i^m = \left[p_{x_i}^m, p_{y_i}^m, p_{z_i}^m\right]^{\mathrm{T}}$ is the displacement normalized polarization vector of the plane wave of index m in the layer i;

T denotes a vector transpose.

In the following, the coordinate system is chosen such that the incident plane overlaps with the x, z plane. Hence, the components of all vectors will be expressed only in terms of x and z. Moreover, for each layer of the structure, a local coordinate origin is defined at the top of the i^{th} layer ($z = z_i$) for the waves propagating in the $+z$ direction, denoted by the superscript m^+, and at the bottom of the i^{th} layer ($z = z_{i+1}$) for the waves propagating in the $-z$ direction, denoted by the superscript m^- (i.e. $m = m^+, m^-$). The selection of this local coordinate system is important since it ensures that the exponential terms are normalized and that they are equal to unity at the interface where they are initiated, and decay to zero at the opposite surface of the layer [1].

The corresponding wave vectors are:

$$\boldsymbol{k}_i^{m^+} = \left[k_{x_i}^{m^+} \quad k_{z_i}^{m^+}\right]^{\mathrm{T}}, \quad \boldsymbol{k}_i^{m^-} = \left[k_{x_i}^{m^-} \quad k_{z_i}^{m^-}\right]^{\mathrm{T}}. \tag{2.2}$$

Applying Snell's law, the projection on the x-axis of these wave vectors for all the plane waves in all layers should be equal, which yields:

$$k_{x_i}^m = k_{x_0} = k_0 \sin\theta_0 = k_x \qquad \forall\, i, m, \tag{2.3}$$

where θ_0 is the plane wave incidence angle at the interface z_1, and k_0 is the wave number in the incidence medium. If the angles corresponding to the waves in a layer i are denoted by θ_i^m, these angles can be expressed using Eq. (2.3) in terms of the incidence angle θ_0 as:

$$\theta_i^m = \sin^{-1}\left(\frac{k_0 \sin\theta_0}{k_i^m}\right). \tag{2.4}$$

If a symmetry is considered around the z axis, then,

$$k_{z_i}^{m^+} = -k_{z_i}^{m^-} = \sqrt{(k_i^m)^2 - (k_x)^2}. \tag{2.5}$$

Consequently, Eq. (2.1) can be written as:

$$\boldsymbol{u}_i(x,z) = e^{j(k_x x - \omega t)}\left(\sum_{m^+} a_i^{m^+}\boldsymbol{p}_i^{m^+} e^{jk_{z_i}^{m^+}(z-z_i)} + \sum_{m^-} a_i^{m^-}\boldsymbol{p}_i^{m^-} e^{jk_{z_i}^{m^-}(z-z_{i+1})}\right). \tag{2.6}$$

It should be noted that the displacement amplitudes $a_i^{m^+}$ and $a_i^{m^-}$ in Eq. (2.6) differ from the amplitudes a_i^m in Eq. (2.1) by a constant term that is factorized from the exponential term due to the change of the coordinate system. However, for simplicity, the same symbol is kept in the adopted local coordinate system.

Let $\boldsymbol{A}_i$ be a column vector consisting of the displacements amplitudes a_i^m of the partial waves in the layer i, and $\boldsymbol{U}_i$ a displacement-stress column vector including the total displacement and stress components in the same layer. By factorizing the partial displacements amplitudes in the displacement and stress components expressions in each layer, the vector $\boldsymbol{U}_i$ could be expressed in terms of $\boldsymbol{A}_i$ as:

$$\boldsymbol{U}_i(x,z) = [\boldsymbol{B}_i][\boldsymbol{E}_i(z)]\,\boldsymbol{A}_i\, e^{j(k_x x - \omega t)} \quad \text{for } z_i \le z \le z_{i+1}\,, \tag{2.7}$$

where, $[\boldsymbol{E}_i(z)]$ is a diagonal square matrix in terms of z and that includes exponential powers of the partial wave numbers $\left(diag\,\{[\boldsymbol{E}_i(z)]\} = \left[e^{jk_{z_i}^{m^+}(z-z_i)} \quad e^{jk_{z_i}^{m^-}(z-z_{i+1})}\right]\right)$, while $[\boldsymbol{B}_i]$ is a square matrix called layer characteristic matrix since its components depend only on the layer physical characteristics and its orientation in the defined coordinate system. The

components and size of each of the vectors and matrices in Eq. (2.7) depend on the layer nature. The corresponding expressions will be developed in the following subsections for three material natures: isotropic elastic solid, fluid, and isotropic poro-elastic media.

2.2.1 Characteristic Matrix of an Isotropic Solid Layer

In an isotropic elastic solid with a density ρ_s and Lamé coefficients λ and μ, four partial waves can propagate: longitudinal and transverse (or shear) waves each in both positive and negative directions as shown in Figure 2-2. Hence, $m^+ = L^+, T^+$ and $m^- = L^-, T^-$ [42].

The angles relative to the longitudinal and transverse waves are denoted by θ_i^L and θ_i^T, respectively.

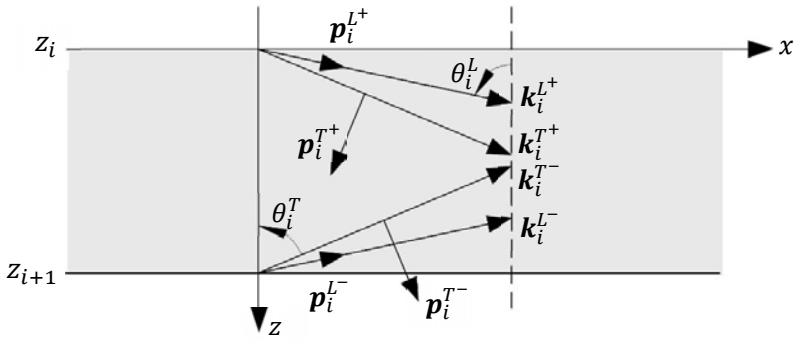

Figure 2-2: Wave propagation in an isotropic solid layer i.

The wave numbers of the longitudinal and transverse waves in the solid layer i can be expressed as:

$$k_i^m = \frac{\omega}{c_m}, \qquad m = L, T \tag{2.8}$$

where ω is the radial frequency and c_m is the corresponding wave velocity defined for the longitudinal and shear waves in Eqs. (1.17) and (1.18), respectively.

The components of the displacement normalized polarization vectors in this layer can be expressed in terms of θ_i^L and θ_i^T as:

$$\begin{aligned} \boldsymbol{p}_i^{L^+} &= [\sin\theta_i^L, 0, \cos\theta_i^L]^{\mathrm{T}}\ ;\ \boldsymbol{p}_i^{L^-} = [\sin\theta_i^L, 0, -\cos\theta_i^L]^{\mathrm{T}}; \\ \boldsymbol{p}_i^{T^+} &= [-\cos\theta_i^T, 0, \sin\theta_i^T]^{\mathrm{T}}\ ;\ \boldsymbol{p}_i^{T^-} = [\cos\theta_i^T, 0, \sin\theta_i^T]^{\mathrm{T}}. \end{aligned} \tag{2.9}$$

Since the boundary conditions at an interface that involves a solid layer reflects the continuity of the x and z components of the displacement and the continuity of each of the xz and zz components of the stress tensor [65], the displacement-stress column vector of a layer i being an isotropic elastic solid is:

$$\boldsymbol{U}_i(x,z) = [u_{x_i}(x,z) \quad u_{z_i}(x,z) \quad \sigma_{xz_i}(x,z) \quad \sigma_{zz_i}(x,z)]^{\mathrm{T}}\ . \tag{2.10}$$

The x and z components of the displacement vector can be expressed using Eq. (2.6) as:

$$\begin{aligned} u_{x_i}(x,z) &= e^{j(k_x x-\omega t)}\left(\sum_{m^+=L^+,T^+} a_i^{m^+}\, p_{x_i}^{m^+} e^{jk_{z_i}^{m^+}(z-z_i)} + \sum_{m^-=L^-,T^-} a_i^{m^-}\, p_{x_i}^{m^-} e^{jk_{z_i}^{m^-}(z-z_{i+1})}\right), \\ u_{z_i}(x,z) &= e^{j(k_x x-\omega t)}\left(\sum_{m^+=L^+,T^+} a_i^{m^+}\, p_{z_i}^{m^+} e^{jk_{z_i}^{m^+}(z-z_i)} + \sum_{m^-=L^-,T^-} a_i^{m^-}\, p_{z,i}^{m^-} e^{jk_{z_i}^{m^-}(z-z_{i+1})}\right). \end{aligned} \tag{2.11}$$

Using the stress-strain relationship of an elastic solid which is given in Eq. (1.9), the stress components could be expressed in terms of the displacements amplitudes as:

$$\begin{aligned} \sigma_{xz_i}(x,z) = j\mu_i e^{j(k_x x-\omega t)}\Bigg[&\left(\sum_{m^+} a_i^{m^+}\, p_{x_i}^{m^+} k_{z_i}^{m^+} e^{jk_{z_i}^{m^+}(z-z_i)} + \sum_{m^-} a_i^{m^-}\, p_{x_i}^{m^-} k_{z_i}^{m^-} e^{jk_{z_i}^{m^-}(z-z_{i+1})}\right) \\ &+k_x\left(\sum_{m^+} a_i^{m^+}\, p_{z_i}^{m^+} e^{jk_{z_i}^{m^+}(z-z_i)} + \sum_{m^-} a_i^{m^-}\, p_{z_i}^{m^-} e^{jk_{z_i}^{m^-}(z-z_{i+1})}\right)\Bigg], \\ \sigma_{zz_i}(x,z) = je^{j(k_x x-\omega t)}\Bigg[&(\lambda_i+2\mu_i)\left(\sum_{m^+} a_i^{m^+}\, p_{z_i}^{m^+} k_{z_i}^{m^+} e^{jk_{z,i}^{m^+}(z-z_i)} + \sum_{m^-} a_i^{m^-}\, p_{z_i}^{m^-} k_{z_i}^{m^-} e^{jk_{z_i}^{m^-}(z-z_{i+1})}\right) \\ &+\lambda_i k_x\left(\sum_{m^+} a_i^{m^+}\, p_{x_i}^{m^+} e^{jk_{z_i}^{m^+}(z-z_i)} + \sum_{m^-} a_i^{m^-}\, p_{x_i}^{m^-} e^{jk_{z_i}^{m^-}(z-z_{i+1})}\right)\Bigg]. \end{aligned} \tag{2.12}$$

The column vector $\boldsymbol{A}_i$ that consists of the displacements amplitudes associated with the four partial waves in the i^{th} isotropic elastic solid layer, is:

$$\boldsymbol{A}_i = \begin{bmatrix} a_i^{L^+} & a_i^{T^+} & a_i^{L^-} & a_i^{T^-} \end{bmatrix}^{\mathrm{T}}. \tag{2.13}$$

Thus, the factorization of the components of $\boldsymbol{A}_i$ in each of the components of $\boldsymbol{U}_i$ as expressed in Eqs. (2.11) and (2.12) leads to the 4×4 square matrices $[\boldsymbol{E}_i(z)]$ and $[\boldsymbol{B}_i]$ such that:

$$diag\,\{[E_i(z)]\} = \begin{bmatrix} e^{jk_{z_i}^{L^+}(z-z_i)} & e^{jk_{z_i}^{T^+}(z-z_i)} & e^{jk_{z_i}^{L^-}(z-z_{i+1})} & e^{jk_{z_i}^{T^-}(z-z_{i+1})} \end{bmatrix},$$

$$[\boldsymbol{B}_i]_{4\times4} = \begin{bmatrix} p_{x_i}^m \\ p_{z_i}^m \\ j\mu_i(p_{x_i}^m k_{z_i}^m + p_{z_i}^m k_x) \\ j\left[(\lambda_i + 2\mu_i)p_{z_i}^m k_{z_i}^m + \lambda_i p_{x_i}^m k_x\right] \end{bmatrix}, \quad m = L^+, T^+, L^-, T^-. \tag{2.14}$$

2.2.2 Characteristic Matrix of a Fluid Layer

For a fluid layer characterized by its bulk modulus K_f, only longitudinal waves propagate in the positive and negative directions ($m = L^+$, L^-) as illustrated in Figure 2-3.

The equations corresponding to the fluid layer could be deduced from those of the solid by assigning to the shear modulus a value of zero and by letting $\lambda = K_f$.

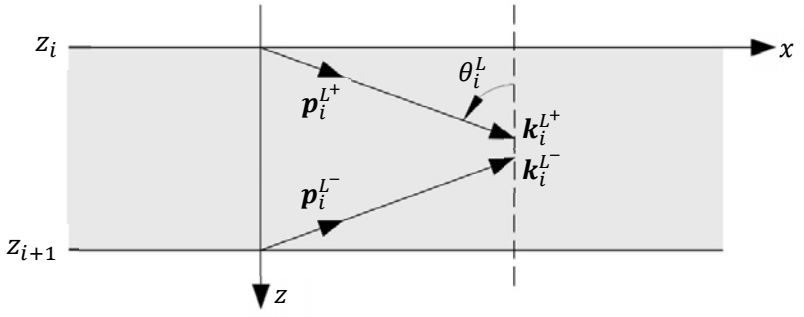

Figure 2-3: Wave propagation in a fluid layer *i*.

The system is then reduced to the size of two, the vectors $\boldsymbol{A}_i$ and $\boldsymbol{U}_i$ being:

$$\boldsymbol{A}_i = \begin{bmatrix} a_i^{L^+} & a_i^{L^-} \end{bmatrix}^{\mathrm{T}},$$
$$\boldsymbol{U}_i(x,z) = [\, u_{z_i}(x,z) \quad -P_{f_i}(x,z)]^{\mathrm{T}}, \tag{2.15}$$

where the pressure, P_f, in the fluid could be obtained in terms of the displacement vector components as defined in Eq. (1.27).

The matrices $[\boldsymbol{E}_i(z)]$ and $[\boldsymbol{B}_i]$ are 2×2 and defined as:

$$[\boldsymbol{E}_i(z)] = \begin{bmatrix} e^{jk_{z_i}^{L^+}(z-z_i)} & 0 \\ 0 & e^{jk_{z_i}^{L^-}(z-z_{i+1})} \end{bmatrix},$$
$$[\boldsymbol{B}_i] = \begin{bmatrix} p_{z_i}^{L^+} & p_{z_i}^{L^-} \\ jK_{f_i}\left(p_{z_i}^{L^+}k_{z_i}^{L^+} + p_{x_i}^{L^+}k_x\right) & jK_{f_i}\left(p_{z_i}^{L^-}k_{z_i}^{L^-} + p_{x_i}^{L^-}k_x\right) \end{bmatrix}. \tag{2.16}$$

2.2.3 Characteristic Matrix of a Poro-elastic Isotropic Layer

In this work, the porous medium is modeled based on the Biot's theory as defined in Section 1.4.2.

In a poro-elastic layer, six partial waves can propagate: two longitudinal waves each in both directions (L_1^+, L_1^-, L_2^+ and L_2^-), and shear waves in both directions as well (T^+ and T^-) as shown in Figure 2-4. Accordingly, the waves angles are denoted by θ^{L_1}, θ^{L_2} and θ^T. The partial waves $L_1^{\pm}$ and $T^{\pm}$ are associated with the solid phase, while the partial waves $L_2^{\pm}$ are related to the liquid phase in the bulk porous material.

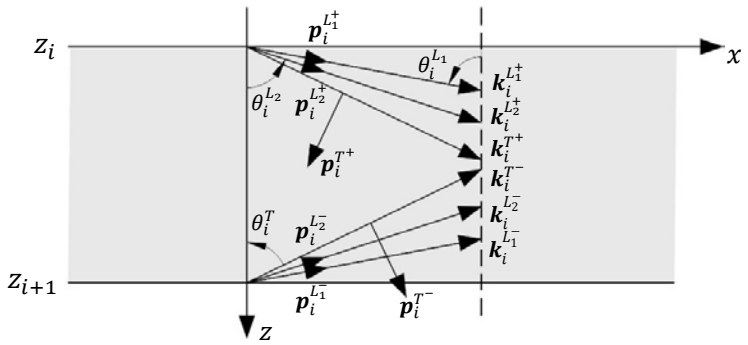

Figure 2-4: Wave propagation in an isotropic poro-elastic layer *i*.

In order to obtain the medium characteristic matrix, the wave numbers must be calculated first. For calculations simplicity purpose, and since the medium is considered to be isotropic, the waves will be represented by their displacement potentials [64] instead of the displacement vectors only to derive the wave numbers.

Wave numbers of longitudinal waves

Let φ^L and ψ^L be the potentials of the solid and the relative fluid displacements, respectively, associated with the longitudinal waves:

$$\begin{aligned} \varphi^{L^+_{1,2}} &= X^{L^+_{1,2}} e^{j\left[k_x x + k_z^{L^+_{1,2}}(z-z_i)-\omega t\right]}, \varphi^{L^-_{1,2}} = X^{L^-_{1,2}} e^{j\left[k_x x + k_z^{L^-_{1,2}}(z-z_{i+1})-\omega t\right]}, \\ \psi^{L^-_{1,2}} &= Y^{L^+_{1,2}} e^{j\left[k_x x + k_z^{L^+_{1,2}}(z-z_i)-\omega t\right]}, \psi^{L^-_{1,2}} = Y^{L^-_{1,2}} e^{j\left[k_x x + k_z^{L^-_{1,2}}(z-z_{i+1})-\omega t\right]}, \end{aligned} \tag{2.17}$$

where $X^{L^{\pm}_{1,2}}$ and $Y^{L^{\pm}_{1,2}}$ are the amplitudes of the potentials of the solid and the relative fluid displacements, respectively.

For longitudinal waves, the displacement vectors are related to their potentials by:

$$\begin{aligned} \boldsymbol{u^L} &= \nabla\varphi^L, \\ \boldsymbol{w^L} &= \nabla\psi^L. \end{aligned} \tag{2.18}$$

After expressing the displacement vectors for the longitudinal waves in terms of their potentials amplitudes, and then replacing them in the Biot's equations of motion, i.e. in Eq. (1.38), the following system of equations is obtained:

$$\begin{bmatrix} -H_c(k^L)^2 + \rho\omega^2 & -D(k^L)^2 + \rho_f\omega^2 \\ -D(k^L)^2 + \rho_f\omega^2 & -M(k^L)^2 + g\omega^2 - jb\omega \end{bmatrix} \begin{bmatrix} X^L \\ Y^L \end{bmatrix} = \begin{bmatrix} 0 \\ 0 \end{bmatrix}. \tag{2.19}$$

For the system to have non-trivial solutions X^L and Y^L, the matrix determinant shall be zero:

$$\begin{vmatrix} -H_c(k^L)^2 + \rho\omega^2 & -D(k^L)^2 + \rho_f\omega^2 \\ -D(k^L)^2 + \rho_f\omega^2 & -M(k^L)^2 + g\omega^2 - jb\omega \end{vmatrix} = 0. \tag{2.20}$$

The expression in Eq. (2.20) leads to a fourth order equation of the following form:

$$G(k^L)^4 + F(k^L)^2 + O = 0\,, \tag{2.21}$$

where

$$\begin{aligned} G &= H_c M - D^2\,, \\ F &= \omega^2\left(-H_c g - M\rho + 2D\rho_f\right) + j\omega H_c b, \\ O &= \omega^4\left(\rho g - \rho_f^2\right) - j\omega^3\rho b. \end{aligned} \tag{2.22}$$

Eq. (2.21) could be expressed as a quadratic equation with a discriminant Δ such that:

$$\Delta = F^2 - 4GO\,, \tag{2.23}$$

which leads to two distinct solutions of the equation, that are the wavenumbers of the longitudinal waves of types 1 and 2, respectively:

$$k^{L_{1,2}} = \sqrt{\frac{-F \pm \sqrt{F^2 - 4GO}}{2G}}. \tag{2.24}$$

Subsequently, the z-component of the wave vectors of the longitudinal waves can be obtained as follows:

$$k_z^{L_{1,2}^+} = -k_z^{L_{1,2}^-} = k^{L_{1,2}} \cos\theta^{L_{1,2}}. \tag{2.25}$$

Besides obtaining the wavenumbers and the wave vector components, the system of equations in Eq. (2.19) allows to determine a relationship between the amplitudes of the potentials of the solid and the relative fluid displacements associated with the longitudinal waves. This relationship is expressed as:

$$Y^L = \gamma^L X^L, \qquad \gamma^L = \frac{-H_c(k^L)^2 + \rho\omega^2}{D(k^L)^2 - \rho_f\omega^2}. \tag{2.26}$$

Wave numbers of shear waves

Let φ^T and ψ^T be the potentials of the solid and the relative fluid displacements, respectively, associated with the transverse or shear waves:

$$\begin{aligned}\varphi^{T^+} &= X^{T^+} e^{j\left[k_x x + k_z^{T^+}(z-z_{i-1})-\omega t\right]}, \varphi^{T^-} = X^{T^-} e^{j\left[k_x x + k_z^{T^-}(z-z_i)-\omega t\right]},\\ \psi^{T^+} &= Y^{T^+} e^{j\left[k_x x + k_z^{T^+}(z-z_{i-1})-\omega t\right]}, \psi^{T^-} = Y^{T^-} e^{j\left[k_x x + k_z^{T^-}(z-z_i)-\omega t\right]},\end{aligned} \tag{2.27}$$

where $X^{T^\pm}$ and $Y^{T^\pm}$ are the amplitudes of the potentials of the solid and the relative fluid displacements, respectively.

For shear waves, the displacement vectors are related to their potentials by:

$$\begin{aligned}\boldsymbol{u^T} &= \nabla \times \varphi^T = \left[-\frac{\partial \varphi^T}{\partial z} \quad 0 \quad \frac{\partial \varphi^T}{\partial x}\right]^{\mathrm{T}},\\ \boldsymbol{w^T} &= \nabla \times \psi^T = \left[-\frac{\partial \psi^T}{\partial z} \quad 0 \quad \frac{\partial \psi^T}{\partial x}\right]^{\mathrm{T}}.\end{aligned} \tag{2.28}$$

After expressing the displacement vectors for the shear waves in terms of their potentials amplitudes, and then replacing them in the Biot's equations of motion, i.e. in Eq. (1.38), the following system of equations is obtained:

$$\begin{bmatrix}\mu(k^T)^2 - \rho\omega^2 & -\rho_f\omega^2 \\ \rho_f\omega & g\omega - jb\end{bmatrix}\begin{bmatrix}X^T \\ Y^T\end{bmatrix} = \begin{bmatrix}0 \\ 0\end{bmatrix}. \tag{2.29}$$

For the system to have non-trivial solutions X^T and Y^T, the matrix determinant shall be zero:

$$\begin{vmatrix}\mu(k^T)^2 - \rho\omega^2 & -\rho_f\omega^2 \\ \rho_f\omega & g\omega - jb\end{vmatrix} = 0, \tag{2.30}$$

which yields:

$$(k^T)^2 = \frac{\omega^2}{\mu}\left(\rho - \frac{\rho_f^2}{g - jb/\omega}\right). \tag{2.31}$$

Thus, the wavenumber of the shear wave propagating in the porous medium is:

$$k^T = \sqrt{\frac{\omega^2}{\mu}\left(\rho - \frac{\rho_f^2}{g - jb/\omega}\right)}. \tag{2.32}$$

Subsequently, the wave vector z-component of the shear wave could be obtained as follows:

$$k_z^{T^+} = -k_z^{T^-} = k^T \cos\theta^T . \tag{2.33}$$

Moreover, the relationship between the amplitudes of the potentials of the solid and the relative fluid displacements associated with the shear waves can be derived from the system in Eq. (2.29), that is,

$$Y^T = \gamma^T X^T, \qquad \gamma^T = \frac{\mu(k^T)^2 + \rho\omega^2}{\rho_f \omega^2}. \tag{2.34}$$

Having determined the wave numbers in the poro-elastic layer i, the total solid displacement vector in that layer can be expressed as:

$$\begin{aligned} \boldsymbol{u}_i(x,z) &= \sum_m \boldsymbol{u}_i^m(x,z) \quad , \qquad m = L_1^+, L_2^+, T^+, L_1^-, L_2^-, T^- \\ &= \nabla\varphi_i^{L_1^+} + \nabla\varphi_i^{L_2^+} + \nabla\times\varphi_i^{T^+} + \nabla\varphi_i^{L_1^-} + \nabla\varphi_i^{L_2^-} + \nabla\times\varphi_i^{T^-}. \end{aligned} \tag{2.35}$$

The corresponding vector components are thus:

$$\begin{aligned} u_{x_i}(x,z) = je^{j(k_x x-\omega t)}\Bigg[& k_x\left(\sum_{L^+=L_1^+,L_2^+} X_i^{L^+} e^{jk_{z_i}^{L^+}(z-z_i)} + \sum_{L^-=L_1^-,L_2^-} X_i^{L^-} e^{jk_{z_i}^{L^-}(z-z_{i+1})}\right) \\ & - k_{z_i}^{T^+} X_i^{T^+} e^{jk_{z_i}^{T^+}(z-z_i)} - k_{z_i}^{T^-} X_i^{T^-} e^{jk_{z_i}^{T^-}(z-z_{i+1})}\Bigg], \\ u_{z_i}(x,z) = je^{j(k_x x-\omega t)}\Bigg[& \sum_{L^+=L_1^+,L_2^+} k_{z_i}^{L^+} X_i^{L^+} e^{jk_{z_i}^{L^+}(z-z_i)} + \sum_{L^-=L_1^-,L_2^-} k_{z_i}^{L^-} X_i^{L^-} e^{jk_{z_i}^{L^-}(z-z_{i+1})} \\ & + k_x\left(X_i^{T^+} e^{jk_{z_i}^{T^+}(z-z_i)} + X_i^{T^-} e^{jk_{z_i}^{T^-}(z-z_{i+1})}\right)\Bigg]. \end{aligned} \tag{2.36}$$

Similarly, the total relative fluid displacement in the poro-elastic layer i is expressed as:

$$\begin{aligned}\boldsymbol{w}_i(x,z) &= \sum_m \boldsymbol{w}_i^m(x,z) \quad , \qquad m = L_1^+, L_2^+, T^+, L_1^-, L_2^-, T^- \\ &= \nabla\psi_i^{L_1^+} + \nabla\psi_i^{L_2^+} + \nabla\times\psi_i^{T^+} + \nabla\psi_i^{L_1^-} + \nabla\psi_i^{L_2^-} + \nabla\times\psi_i^{T^-} ,\end{aligned} \tag{2.37}$$

The corresponding vector components are thus:

$$\begin{aligned}w_{x_i}(x,z) = je^{j(k_x x-\omega t)}\Bigg[k_x\Bigg(&\sum_{L^+=L_1^+,L_2^+} Y_i^{L^+} e^{jk_{z_i}^{L^+}(z-z_i)} + \sum_{L^-=L_1^-,L_2^-} Y_i^{L^-} e^{jk_{z_i}^{L^-}} e^{jk_{z_i}^{L^-}(z-z_{i+1})}\Bigg) \\ &- k_{z_i}^{T^+} Y_i^{T^+} e^{jk_{z_i}^{T^+}(z-z_i)} - k_{z_i}^{T^-} Y_i^{T^-} e^{jk_{z_i}^{T^-}} e^{jk_{z_i}^{L^-}(z-z_{i+1})}\Bigg],\end{aligned} \tag{2.38}$$

$$\begin{aligned}w_{z_i}(x,z) = je^{j(k_x x-\omega t)}\Bigg[&\sum_{L^+=L_1^+,L_2^+} k_{z_i}^{L^+} Y_i^{L^+} e^{jk_{z_i}^{L^+}(z-z_i)} + \sum_{L^-=L_1^-,L_2^-} k_{z_i}^{L^-} Y_i^{L^-} e^{jk_{z_i}^{L^-}} e^{jk_{z_i}^{L^-}(z-z_{i+1})} \\ &+ k_x\left(Y_i^{T^+} e^{jk_{z_i}^{T^+}(z-z_i)} + Y_i^{T^-} e^{jk_{z_i}^{T^-}} e^{jk_{z_i}^{L^-}(z-z_{i+1})}\right)\Bigg].\end{aligned}$$

Since the boundary conditions at an interface involving a poro-elastic layer reflect the continuity of the x and z components of the solid displacement, the continuity of the z component of the relative fluid displacement, the continuity of each of the xz and zz components of the stress tensor, and the continuity of the fluid pressure [60], the displacement-stress column vector of a poro-elastic layer i is:

$$\boldsymbol{U}_i(x,z) = [u_{x_i}(x,z) \quad u_{z_i}(x,z) \quad w_{z_i}(x,z) \quad \sigma_{xz_i}(x,z) \quad \sigma_{zz_i}(x,z) \quad P_{f_i}(x,z)]^{\mathrm{T}} . \tag{2.39}$$

By substituting Eqs. (2.36) and (2.38) in Eqs. (1.30) and (1.31), and taking into account the amplitudes relationship as defined in Eqs. (2.26) and (2.34), the stresses are expressed can be expressed as follows:

$$\sigma_{xz_i}(x,z) = e^{j(k_x x-\omega t)}\left[-2\mu_i k_x\left(\sum_{L^+} k_{z_i}^{L^+} X_i^{L^+} e^{jk_{z_i}^{L^+}(z-z_i)} + \sum_{L^-} k_{z_i}^{L^-} X_i^{L^-} e^{jk_{z_i}^{L^-}(z-z_{i+1})}\right)\right.$$
$$\left. + \mu_i\left(\left[\left(k_{z_i}^{T^+}\right)^2 - k_x^2\right] X_i^{T^+} e^{jk_{z_i}^{T^+}(z-z_i)} + \left[\left(k_{z_i}^{T^-}\right)^2 - k_x^2\right] X_i^{T^-} e^{jk_{z_i}^{T^-}(z-z_{i+1})}\right)\right],$$

$$\sigma_{zz_i}(x,z) = e^{j(k_x x-\omega t)}\left[\sum_{L^+}\left(\left[-2\mu_{\mathrm{i}}\left(k_{z_i}^{L^+}\right)^2 - \left(k_i^{L^+}\right)^2\left(\lambda_{c_i} + \gamma_i^{L^+} D_i\right)\right] X_i^{L^+} e^{jk_{z_i}^{L^+}(\mathrm{z}-\mathrm{z_i})}\right)\right.$$
$$+ \sum_{L^-}\left(\left[-2\mu_{\mathrm{i}}\left(k_{z_i}^{L^-}\right)^2 - (k_i^{L^-})^2\left(\lambda_{c_i} + \gamma_i^{L^-} D_i\right)\right] X_i^{L^-} e^{jk_{z_i}^{L^-}(\mathrm{z}-\mathrm{z_{i+1}})}\right) \qquad (2.40)$$
$$\left. - 2\mu_{\mathrm{i}} k_x\left(k_{z_i}^{T^+} X_i^{T^+} e^{jk_{z_i}^{T^+}(\mathrm{z}-\mathrm{z_i})} + k_{z_i}^{T^-} X_i^{T^-} e^{jk_{z_i}^{T^-}(\mathrm{z}-\mathrm{z_{i+1}})}\right)\right],$$

$$P_{f_i}(x,z) = e^{j(k_x x-\omega t)}\left(\sum_{L^+}\left(D_i + \gamma_i^{L^+} M_i\right)\left(k_i^{L^+}\right)^2 X_i^{L^+} e^{jk_{z_i}^{L^+}(z-z_i)}\right.$$
$$\left. + \sum_{L^-}\left(D_i + \gamma_i^{L^-} M_i\right)(k_i^{L^-})^2 X_i^{L^-} e^{jk_{z_i}^{L^-}(z-z_{i+1})}\right).$$

The terms of Eq. (2.36) can be rearranged as follows:

$$u_{x_i}(x,z) = e^{j(k_x x-\omega t)}\left(\sum_{L^+} jk_i^{L^+}\sin\theta_i^{L^+} X_i^{L^+} e^{jk_{z_i}^{L^+}(\mathrm{z}-\mathrm{z_i})} + \sum_{L^-} jk_i^{L^-}\sin\theta_i^{L^-} X_i^{L^-} e^{jk_{z_i}^{L^-}(z-z_{i+1})}\right.$$
$$\left. - jk_i^T\cos\theta_i^T\left(X_i^{T^+} e^{jk_{z_i}^{T^+}(\mathrm{z}-\mathrm{z_i})} - X_i^{T^-} e^{jk_{z_i}^{T^-}(z-z_{i+1})}\right)\right), \qquad (2.41)$$

$$u_{z_i}(x,z) = e^{j(k_x x-\omega t)}\left(\sum_{L^+} jk_i^{L^+}\cos\theta_i^{L^+} X_i^{L^+} e^{jk_{z_i}^{L^+}(\mathrm{z}-\mathrm{z_i})} - \sum_{L^-} jk_i^{L^-}\cos\theta_i^{L^-} X_i^{L^-} e^{jk_{z_i}^{L^-}(z-z_{i+1})}\right.$$
$$\left. + jk_i^T\sin\theta_i^T\left(X_i^{T^+} e^{jk_{z_i}^{T^+}(\mathrm{z}-\mathrm{z_i})} + X_i^{T^-} e^{jk_{z_i}^{T^-}(z-z_{i+1})}\right)\right).$$

With reference to Eq. (2.6), the displacement vector components in Eq. (2.41) can be expressed as:

$$u_{x_i}(x,z) = e^{j(k_x x-\omega t)}\left(\sum_{L^+} a_i^{L^+} p_{x_i}^{L^+} e^{jk_{z_i}^{L^+}(z-z_i)} + \sum_{L^-} a_i^{L^-} p_{x_i}^{L^-} e^{jk_{z_i}^{L^-}(z-z_{i+1})}\right.$$
$$\left. + a_i^{T^+} p_{x_i}^{T^+} e^{jk_{z_i}^{T^+}(z-z_i)} + a_i^{T^-} p_{x_i}^{T^-} e^{jk_{z_i}^{T^-}(z-z_{i+1})}\right),$$
$$u_{z_i}(x,z) = e^{j(k_x x-\omega t)}\left(\sum_{L^+} a_i^{L^+} p_{z_i}^{L^+} e^{jk_{z_i}^{L^+}(z-z_i)} + \sum_{L^-} a_i^{L^-} p_{z_i}^{L^-} e^{jk_{z_i}^{L^-}(z-z_{i+1})}\right. \quad (2.42)$$
$$\left. + a_i^{T^+} p_{z_i}^{T^+} e^{jk_{z_i}^{T^+}(z-z_i)} + a_i^{T^-} p_{z_i}^{T^-} e^{jk_{z_i}^{T^-}(z-z_{i+1})}\right).$$

By comparing Eqs. (2.41) and (2.42), and identifying the terms, the displacement vectors amplitudes and the waves polarization vectors can be expressed as:

$$a^L = jk^L X^L, \quad a^T = jk^T X^T,$$
$$\boldsymbol{p}^{L_{1,2}^+} = [\sin\theta^{L_{1,2}} \quad 0 \quad \cos\theta^{L_{1,2}}]^{\mathrm{T}}; \ \boldsymbol{p}^{L_{1,2}^-} = [\sin\theta^{L_{1,2}} \quad 0 \quad -\cos\theta^{L_{1,2}}]^{\mathrm{T}}; \quad (2.43)$$
$$\boldsymbol{p}^{T^+} = [-\cos\theta^T \quad 0 \quad \sin\theta^T]^{\mathrm{T}}; \ \boldsymbol{p}^{T^-} = [\cos\theta^T \quad 0 \quad \sin\theta^T]^{\mathrm{T}}.$$

Hence, the remaining components of the displacement-stress vector of the poro-elastic layer i, $\boldsymbol{U}_i(x,z)$, can be expressed in terms of the displacement vectors amplitudes rather than the potentials amplitudes as follows:

$$w_{z_i}(x,z) = je^{j(k_x x-\omega t)}\Bigg[\sum_{L^+=L_1^+,L_2^+} a_i^{L^+}\gamma_i^{L^+}p_{z_i}^{L^+}e^{jk_{z_i}^{L^+}(z-z_i)} + \sum_{L^-=L_1^-,L_2^-} a_i^{L^-}\gamma_i^{L^-}p_{z_i}^{L^-}e^{jk_{z_i}^{L^-}(z-z_{i+1})}$$

$$+\left(a_i^{T^+}\gamma_i^{T^+}p_{z_i}^{T^+}e^{jk_{z_i}^{T^+}(z-z_i)} + a_i^{T^-}\gamma_i^{T^-}p_{z_i}^{T^-}e^{jk_{z_i}^{T^-}(z-z_{i+1})}\right)\Bigg],$$

$$\sigma_{xz_i}(x,z) = e^{j(k_x x-\omega t)}\Bigg[j2\mu_i\left(\sum_{L^+} k_i^{L^+}a_i^{L^+}p_{x_i}^{L^+}p_{z_i}^{L^+}e^{jk_{z_i}^{L^+}(z-z_i)} + \sum_{L^-} k_i^{L^-}a_i^{L^-}p_{x_i}^{L^-}p_{z_i}^{L^-}e^{jk_{z_i}^{L^-}(z-z_{i+1})}\right)$$

$$+j\mu_i k_i^T\left(\left[\left(p_{z_i}^{T^+}\right)^2-\left(p_{x_i}^{T^+}\right)^2\right]a_i^{T^+}e^{jk_{z_i}^{T^+}(z-z_i)} + \left[\left(p_{z_i}^{T^-}\right)^2-\left(p_{x_i}^{T^-}\right)^2\right]a_i^{T^-}e^{jk_{z_i}^{T^-}(z-z_{i+1})}\right)\Bigg],$$

$$\sigma_{zz_i}(x,z) = e^{j(k_x x-\omega t)}\Bigg[\sum_{L^+} jk_i^{L^+}\left[2\mu_i\left(p_{z_i}^{L^+}\right)^2+\lambda_{c_i}+\gamma_i^{L^+}D_i\right]a_i^{L^+}e^{jk_{z_i}^{L^+}(z-z_i)}$$

$$+\sum_{L^-}\left(jk_i^{L^-}\left[2\mu_i\left(p_{z_i}^{L^-}\right)^2+\lambda_{c_i}+\gamma_i^{L^-}D_i\right]a_i^{L^-}e^{jk_{z_i}^{L^-}(z-z_{i+1})}\right) \qquad (2.44)$$

$$-j2\mu_i k_i^T\left(p_{z_i}^{T^+}p_{x_i}^{T^+}a_i^{T^+}e^{jk_{z_i}^{T^+}(z-z_i)} + p_{z_i}^{T^-}p_{x_i}^{T^-}a_i^{T^-}e^{jk_{z_i}^{T^-}(z-z_{i+1})}\right)\Bigg],$$

$$P_{f_i}(x,z) = e^{j(k_x x-\omega t)}\Bigg(\sum_{L^+} -j\left(D_i+\gamma_i^{L^+}M_i\right)k_i^{L^+}a_i^{L^+}e^{jk_{z_i}^{L^+}(z-z_i)}$$

$$+\sum_{L^-} -j\left(D_i+\gamma_i^{L^-}M_i\right)k_i^{L^-}a_i^{L^-}e^{jk_{z_i}^{L^-}(z-z_{i+1})}\Bigg).$$

The column vector $\boldsymbol{A}_i$, consisting of the displacements amplitudes associated with the six partial waves in the i^{th} isotropic poro-elastic layer, is:

$$\boldsymbol{A}_i = \begin{bmatrix} a_i^{L_1^+} & a_i^{L_2^+} & a_i^{T^+} & a_i^{L_2^+} & a_i^{L_2^-} & a_i^{T^-}\end{bmatrix}^{\mathrm{T}}. \qquad (2.45)$$

Thus, the factorization of the components of $\boldsymbol{A}_i$ in each of the components of $\boldsymbol{U}_i$ as expressed in Eqs. (2.42) and (2.44) leads to the 6×6 square matrices $[\boldsymbol{E}_i(z)]$ and $[\boldsymbol{B}_i]$ such that:

$$diag\,\{[\boldsymbol{E}_i(z)]\} = \left[e^{jk_{z_i}^{L_1^+}(z-z_i)} \quad e^{jk_{z_i}^{L_2^+}(z-z_i)} \quad e^{jk_{z_i}^{T^+}(z-z_i)} \right.$$
$$\left. e^{jk_{z_i}^{L_1^-}(z-z_{i+1})} \quad e^{jk_{z_i}^{L_2^-}(z-z_{i+1})} \quad e^{jk_{z_i}^{T^-}(z-z_{i+1})}\right],$$

$$[\boldsymbol{B}_i] = \begin{bmatrix} p_{x_i}^m \\ p_{z_i}^m \\ \gamma_i^m p_{z_i}^m \\ [\boldsymbol{C}_i^m] \end{bmatrix}, m = L_1^{\pm}, L_2^{\pm}, T^{\pm}, \tag{2.46}$$

where:

$$[\boldsymbol{C}_i^m] = \begin{cases} \begin{bmatrix} j2\mu_i k_i^m p_{x_i}^m p_{z_i}^m \\ jk_i^m\left(2\mu_i\left(p_{z_i}^m\right)^2 + \lambda_{c_i} + D_i\gamma_i^m\right) \\ -j(D_i + \gamma_i^m M_i)k_i^m \end{bmatrix}, \text{for } m = L_1^{\pm}, L_2^{\pm}, \\ \begin{bmatrix} j\mu_i k_i^m\left(\left(p_{z_i}^m\right)^2 - \left(p_{x_i}^m\right)^2\right) \\ -j2\mu_i k_i^m p_{x_i}^m p_{z_i}^m \\ 0 \end{bmatrix}, \text{for } m = T^{\pm}. \end{cases} \tag{2.47}$$

2.3 Layers Stiffness Matrices

In this section, the stiffness matrix of a layer i will be derived. By definition, this matrix relates the stress components to the displacement components at the top and bottom surfaces of that layer. It is to be noted that the time harmonic dependence term e^{-j} will be suppressed in the subsequent expressions intentionally without any loss of generality.

In the following, the displacement-stress vector $\boldsymbol{U}_i$ will be subdivided into two column vectors each of length n_i: $\boldsymbol{U}_i(x,z) = [\boldsymbol{v}_i(x,z) \quad \boldsymbol{T}_i(x,z)]^{\mathrm{T}}$, $\boldsymbol{v}_i$ consisting of the displacement vectors components, and $\boldsymbol{T}_i$ comprising the stress components. It is to be noted that the variable n_i takes the value of 1, 2, or 3 for fluid, isotropic solid, and porous layers,

respectively. Hence, if the square characteristic matrices obtained in Section 2.2 are subdivided into four square matrices of the same size, i.e.:

$$[\boldsymbol{B}_i]_{2n_i\times 2n_i} = \begin{bmatrix} [\boldsymbol{B}_i^{11}]_{n_i\times n_i} & [\boldsymbol{B}_i^{12}]_{n_i\times n_i} \\ [\boldsymbol{B}_i^{21}]_{n_i\times n_i} & [\boldsymbol{B}_i^{22}]_{n_i\times n_i} \end{bmatrix}, \tag{2.48}$$

$\boldsymbol{v}_i$ and $\boldsymbol{T}_i$ can be expressed with reference to Eq. (2.7) as:

$$\begin{aligned} \boldsymbol{v}_i(x,z) &= [[\boldsymbol{B}_i^{11}] \quad [\boldsymbol{B}_i^{12}]]\,[\boldsymbol{E}_i(z)]\,\boldsymbol{A}_i\, e^{j(k_x x)}\,, \\ \boldsymbol{T}_i(x,z) &= [[\boldsymbol{B}_i^{21}] \quad [\boldsymbol{B}_i^{22}]]\,[\boldsymbol{E}_i(z)]\,\boldsymbol{A}_i\, e^{j(k_x x)},\ \text{for } z_i \le z \le z_{i+1}\,. \end{aligned} \tag{2.49}$$

The displacement components vector at the upper ($z = z_i$) and lower ($z = z_{i+1}$) surfaces of the layer i can be then expressed as:

$$\begin{bmatrix} \boldsymbol{v}_i(x,z_i) \\ \boldsymbol{v}_i(x,z_{i+1}) \end{bmatrix} = \begin{bmatrix} [\boldsymbol{B}_i^{11}] & [\boldsymbol{B}_i^{12}][\boldsymbol{H}_i^{-}] \\ [\boldsymbol{B}_i^{11}][\boldsymbol{H}_i^{+}] & [\boldsymbol{B}_i^{12}] \end{bmatrix} \begin{bmatrix} \boldsymbol{A}_i^{+} \\ \boldsymbol{A}_i^{-} \end{bmatrix} e^{j(k_x x)} = [\boldsymbol{E}_i^{v}]\boldsymbol{A}_i e^{jk_x x}\,, \tag{2.50}$$

where $[\boldsymbol{H}_i^{+}]$ and $[\boldsymbol{H}_i^{-}]$ are square $n \times n$ diagonal matrices whose elements are $diag\{[\boldsymbol{H}_i^{+}]\} = e^{jk_{z_i}^{m^+}h_i}$ and $diag\{[\boldsymbol{H}_i^{-}]\} = e^{-jk_{z_i}^{m^-}h_i}$, h_i is the layer thickness i.e. $h_i = z_{i+1} - z_i$, and $\boldsymbol{A}_i^{+}$ and $\boldsymbol{A}_i^{-}$ are column vectors of length n_i whose elements are the displacement amplitudes of the partial plane waves in the $+z$ and $-z$ directions, respectively. If a symmetry is considered around the z axis and by referring to Eq. (2.5), $e^{jk_{z_i}^{m^+}h_i} = e^{-jk_{z_i}^{m^-}h_i}$, and $[\boldsymbol{H}_i^{+}] = [\boldsymbol{H}_i^{-}]$.

Similarly, the stress components vectors obtained in Section 2.2 for the three layer-natures can be expressed at the top and bottom surfaces of the layer i in terms of $\boldsymbol{A}_i^{+}$ and $\boldsymbol{A}_i^{-}$, which yields:

$$\begin{bmatrix} \boldsymbol{T}_i(x,z_i) \\ \boldsymbol{T}_i(x,z_{i+1}) \end{bmatrix} = \begin{bmatrix} [\boldsymbol{B}_i^{21}] & [\boldsymbol{B}_i^{22}][\boldsymbol{H}_i^{-}] \\ [\boldsymbol{B}_i^{21}][\boldsymbol{H}_i^{+}] & [\boldsymbol{B}_i^{22}] \end{bmatrix} \begin{bmatrix} \boldsymbol{A}_i^{+} \\ \boldsymbol{A}_i^{-} \end{bmatrix} e^{j(k_x x)} = [\boldsymbol{E}_i^{T}]\boldsymbol{A}_i e^{jk_x x}\,. \tag{2.51}$$

If the term $\boldsymbol{A_i} e^{jk_x x}$ in Eq. (2.50) is substituted into Eq. (2.51), either the layer stiffness matrix $[\boldsymbol{K}_i]_{2n\times 2n}$ or the compliance matrix $[\boldsymbol{S}_i]_{2n\times 2n}$ can be obtained. These matrices relate

the stresses to the displacements at the top and bottom surfaces of layer i as follows:

$$\begin{aligned}\begin{bmatrix}\boldsymbol{T}_i(x,z_i)\\ \boldsymbol{T}_i(x,z_{i+1})\end{bmatrix} &= [\boldsymbol{E}_i^T][\boldsymbol{E}_i^v]^{-1}\begin{bmatrix}\boldsymbol{v}_i(x,z_i)\\ \boldsymbol{v}_i(x,z_{i+1})\end{bmatrix} = [\boldsymbol{K}_i]\begin{bmatrix}\boldsymbol{v}_i(x,z_i)\\ \boldsymbol{v}_i(x,z_{i+1})\end{bmatrix},\\ \begin{bmatrix}\boldsymbol{v}_i(x,z_i)\\ \boldsymbol{v}_i(x,z_{i+1})\end{bmatrix} &= [\boldsymbol{E}_i^v][\boldsymbol{E}_i^T]^{-1}\begin{bmatrix}\boldsymbol{T}_i(x,z_i)\\ \boldsymbol{T}_i(x,z_{i+1})\end{bmatrix} = [\boldsymbol{S}_i]\begin{bmatrix}\boldsymbol{T}_i(x,z_i)\\ \boldsymbol{T}_i(x,z_{i+1})\end{bmatrix},\end{aligned} \tag{2.52}$$

where

$$[\boldsymbol{S}_i] = [\boldsymbol{K}_i]^{-1}. \tag{2.53}$$

In the following subsections, the stiffness matrix derivation will be presented in details for each layer nature based on the layers physical parameters and characteristic matrices obtained in Section 2.2.

2.3.1 Stiffness Matrix of a Fluid Layer

For a fluid layer i, the displacements and stress components vectors are respectively:

$$\begin{aligned}\boldsymbol{v}_i(x,z) &= u_{z_i}(x,z),\\ \boldsymbol{T}_i(x,z) &= -P_{f_i}(x,z).\end{aligned} \tag{2.54}$$

Then, the stiffness matrix of the fluid layer relates the (z,z) component of the stress tensor to the z component of the displacement vector at the top and bottom surfaces of the layer as follows:

$$\begin{aligned}\begin{bmatrix}\boldsymbol{T}_i(x,z_i)\\ \boldsymbol{T}_i(x,z_{i+1})\end{bmatrix} = \begin{bmatrix}-P_{f_i}(x,z_i)\\ -P_{f_i}(x,z_{i+1})\end{bmatrix} &= [\boldsymbol{K}_i]_{2\times 2}\begin{bmatrix}\boldsymbol{v}_i(x,z_i)\\ \boldsymbol{v}_i(x,z_{i+1})\end{bmatrix}\\ &= [\boldsymbol{K}_i]_{2\times 2}\begin{bmatrix}u_{z_i}(x,z_i)\\ u_{z_i}(x,z_{i+1})\end{bmatrix}.\end{aligned} \tag{2.55}$$

If the fluid characteristic matrix in Eq. (2.16) is written as:

$$[\boldsymbol{B}_i]_{2\times 2} = \begin{bmatrix} B_i^{11} & B_i^{12} \\ B_i^{21} & B_i^{22} \end{bmatrix}, \tag{2.56}$$

its stiffness matrix $[\boldsymbol{K}_i]$ can be expressed as:

$$\begin{aligned} [\boldsymbol{K}_i]_{2\times 2} &= [\boldsymbol{E}_i^{\sigma}][\boldsymbol{E}_i^{u}]^{-1} \\ &= \begin{bmatrix} B_i^{21} & B_i^{22} e^{-jk_{z_i}^{L^-} h_i} \\ B_i^{21} e^{jk_{z_i}^{L^+} h_i} & B_i^{22} \end{bmatrix} \begin{bmatrix} B_i^{11} & B_i^{12} e^{-jk_{z_i}^{L^-} h_i} \\ B_i^{11} e^{jk_{z_i}^{L^+} h_i} & B_i^{12} \end{bmatrix}^{-1}. \end{aligned} \tag{2.57}$$

2.3.2 Stiffness Matrix of an Isotropic Elastic Solid Layer

For an isotropic elastic solid layer i, the displacements and stress components vectors are respectively:

$$\begin{aligned} \boldsymbol{v}_i(x,z) &= \begin{bmatrix} u_{x_i}(x,z) \\ u_{z_i}(x,z) \end{bmatrix}, \\ \boldsymbol{T}_i(x,z) &= \begin{bmatrix} \sigma_{xz_i}(x,z) \\ \sigma_{zz_i}(x,z) \end{bmatrix}. \end{aligned} \tag{2.58}$$

Then, the stiffness matrix of the isotopic elastic solid layer relates the (x,z) and (z,z) components of the stress tensor to the x and z components of the displacement vector, respectively, at the top and bottom surfaces of the layer, as follows:

$$\begin{bmatrix} \boldsymbol{T}_i(x,z_i) \\ \boldsymbol{T}_i(x,z_{i+1}) \end{bmatrix} = \begin{bmatrix} \sigma_{xz_i}(x,z_i) \\ \sigma_{zz_i}(x,z_i) \\ \sigma_{xz_i}(x,z_{i+1}) \\ \sigma_{zz_i}(x,z_{i+1}) \end{bmatrix} = [\boldsymbol{K}_i]_{4\times 4} \begin{bmatrix} \boldsymbol{v}_i(x,z_i) \\ \boldsymbol{v}_i(x,z_{i+1}) \end{bmatrix} \tag{2.59}$$

$$= [\boldsymbol{K}_i]_{4\times4} \begin{bmatrix} u_{x_i}(x, z_i) \\ u_{z_i}(x, z_i) \\ u_{x_i}(x, z_{i+1}) \\ u_{z_i}(x, z_{i+1}) \end{bmatrix}.$$

If the isotropic elastic solid characteristic matrix in Eq. (2.14) is subdivided into four square matrices of the same size, i.e.:

$$[\boldsymbol{B}_i]_{4\times4} = \begin{bmatrix} [\boldsymbol{B}_i^{11}]_{2\times2} & [\boldsymbol{B}_i^{12}]_{2\times2} \\ [\boldsymbol{B}_i^{21}]_{2\times2} & [\boldsymbol{B}_i^{22}]_{2\times2} \end{bmatrix}, \tag{2.60}$$

its stiffness matrix $[\boldsymbol{K}_i]$ can be expressed as:

$$\begin{aligned} &[\boldsymbol{K}_i]_{4\times4} = [\boldsymbol{E}_i^{\sigma}][\boldsymbol{E}_i^{u}]^{-1} \\ &= \begin{bmatrix} [\boldsymbol{B}_i^{21}]_{2\times2} & [\boldsymbol{B}_i^{22}]_{2\times2}[\boldsymbol{H}_i^{-}]_{2\times2} \\ [\boldsymbol{B}_i^{21}]_{2\times2}[\boldsymbol{H}_i^{+}]_{2\times2} & [\boldsymbol{B}_i^{22}]_{2\times2} \end{bmatrix} \begin{bmatrix} [\boldsymbol{B}_i^{11}]_{2\times2} & [\boldsymbol{B}_i^{12}]_{2\times2}[\boldsymbol{H}_i^{-}]_{2\times2} \\ [\boldsymbol{B}_i^{11}]_{2\times2}[\boldsymbol{H}_i^{+}]_{2\times2} & [\boldsymbol{B}_i^{12}]_{2\times2} \end{bmatrix}^{-1} \end{aligned} \tag{2.61}$$

where $[\boldsymbol{H}_i^{+}]$ and $[\boldsymbol{H}_i^{-}]$ are 2×2 diagonal square matrices whose elements are:

$$\begin{aligned} diag\{[\boldsymbol{H}_i^{+}]\} &= \left[e^{jk_{z_i}^{L^+}h_i} \quad e^{jk_{z_i}^{T^+}h_i}\right], \\ diag\{[\boldsymbol{H}_i^{-}]\} &= \left[e^{-jk_{z_i}^{L^-}h_i} \quad e^{-jk_{z_i}^{T^-}h_i}\right]. \end{aligned} \tag{2.62}$$

2.3.3 Stiffness Matrix for an Isotropic Poro-elastic Layer

For an isotropic poro-elastic layer i, the displacements and stress components vectors are respectively:

$$\boldsymbol{v}_i(x,z) = \begin{bmatrix} u_{x_i}(x,z) \\ u_{z_i}(x,z) \\ w_{z_i}(x,z) \end{bmatrix},$$
$$\boldsymbol{T}_i(x,z) = \begin{bmatrix} \sigma_{xz_i}(x,z) \\ \sigma_{zz_i}(x,z) \\ P_{f_i}(x,z) \end{bmatrix}. \tag{2.63}$$

Then, the stiffness matrix of the isotropic poro-elastic layer relates the (x,z) and (z,z) components of the stress tensor and the fluid pressure to the x and z components of the solid displacement and the z component of the relative fluid displacement respectively, at the top and bottom surfaces of the layer, as follows:

$$\begin{bmatrix} \boldsymbol{T}_i(x,z_i) \\ \boldsymbol{T}_i(x,z_{i+1}) \end{bmatrix} = \begin{bmatrix} \sigma_{xz_i}(x,z_i) \\ \sigma_{zz_i}(x,z_i) \\ \mathrm{P_{f_i}}(x,z_i) \\ \sigma_{xz_i}(x,z_{i+1}) \\ \sigma_{zz_i}(x,z_{i+1}) \\ P_{f_i}(x,z_{i+1}) \end{bmatrix} = [\boldsymbol{K}_i]_{6\times 6} \begin{bmatrix} \boldsymbol{v}_i(x,z_i) \\ \boldsymbol{v}_i(x,z_{i+1}) \end{bmatrix}$$
$$= [\boldsymbol{K}_i]_{6\times 6} \begin{bmatrix} u_{x_i}(x,z_i) \\ u_{z_i}(x,z_i) \\ w_{z_i}(x,z_i) \\ u_{x_i}(x,z_{i+1}) \\ u_{z_i}(x,z_{i+1}) \\ w_{z_i}(x,z_{i+1}) \end{bmatrix}. \tag{2.64}$$

If the isotropic poro-elastic layer characteristic matrix in Eq. (2.46) is subdivided into four square matrices of the same size, i.e.:

$$[\boldsymbol{B}_i]_{6\times6} = \begin{bmatrix} [\boldsymbol{B}_i^{11}]_{3\times3} & [\boldsymbol{B}_i^{12}]_{3\times3} \\ [\boldsymbol{B}_i^{21}]_{3\times3} & [\boldsymbol{B}_i^{22}]_{3\times3} \end{bmatrix}, \tag{2.65}$$

its stiffness matrix $[\boldsymbol{K}_i]$ can be expressed as:

$$\begin{aligned} [\boldsymbol{K}_i]_{6\times6} &= [\boldsymbol{E}_i^{\sigma}][\boldsymbol{E}_i^{u}]^{-1} \\ &= \begin{bmatrix} [\boldsymbol{B}_i^{21}]_{3\times3} & [\boldsymbol{B}_i^{22}]_{3\times3}[\boldsymbol{H}_i^{-}]_{3\times3} \\ [\boldsymbol{B}_i^{21}]_{3\times3}[\boldsymbol{H}_i^{+}]_{3\times3} & [\boldsymbol{B}_i^{22}]_{3\times3} \end{bmatrix} \begin{bmatrix} [\boldsymbol{B}_i^{11}]_{3\times3} & [\boldsymbol{B}_i^{12}]_{3\times3}[\boldsymbol{H}_i^{-}]_{3\times3} \\ [\boldsymbol{B}_i^{11}]_{3\times3}[\boldsymbol{H}_i^{+}]_{3\times3} & [\boldsymbol{B}_i^{12}]_{3\times3} \end{bmatrix}^{-1} \end{aligned} \tag{2.66}$$

where $[\boldsymbol{H}_i^{+}]$ and $[\boldsymbol{H}_i^{-}]$ are 3×3 diagonal square matrices whose elements are:

$$\begin{aligned} diag\{[\boldsymbol{H}_i^{+}]\} &= \begin{bmatrix} e^{jk_{z_i}^{L_1^{+}}h_i} & e^{jk_{z_i}^{L_2^{+}}h_i} & e^{jk_{z_i}^{T^{+}}h_i} \end{bmatrix}, \\ diag\{[\boldsymbol{H}_i^{-}]\} &= \begin{bmatrix} e^{-jk_{z_i}^{L_1^{-}}h_i} & e^{-jk_{z_i}^{L_2^{-}}h_i} & e^{-jk_{z_i}^{T^{-}}h_i} \end{bmatrix}. \end{aligned} \tag{2.67}$$

2.4 Conclusion

The characteristic matrix of a layer has been derived for three layer-natures: fluid, isotropic elastic solid, and isotropic poro-elastic. This matrix relates the displacements and stresses in that layer to the displacement amplitudes of the partial plane waves propagating in the layer. Its components have been found to be dependent on the layer physical characteristics, as well as on the incident plane wave frequency ω, and its incidence angle θ_0 at the interface z_1. Having determined the layer characteristic matrix, its stiffness matrix has been derived and it relates the displacements to the stresses at the top of the layer to those at its bottom.

CHAPTER 3

DEVELOPED ALGORITHM FOR PLANE WAVE PROPAGATION IN MULTILAYERED MEDIA

3.1 Introduction

In this chapter, a recursive algorithm is developed to model the propagation of a plane wave that is incident on a multilayer with an incidence angle θ_0 and a frequency ω. All the layers of the structure are merged into a single equivalent layer by coupling the individual layers stiffness matrices into one total stiffness matrix. This latter relates the displacement and stress components at the top of the multilayer to those at the bottom and incorporates the physical parameters of all the layers, taking into account the boundary conditions at every interface separating two consecutive layers. Having computed the total stiffness matrix of the multilayered structure, the reflection coefficient in the incidence medium and the transmission coefficient in the transmission medium are calculated. Subsequently, the displacement amplitudes of the partial plane waves inside each layer are calculated through a back recursive algorithm.

Before proceeding with the derivation in details, the boundary conditions at interfaces separating any two layers of the three considered natures (fluid, isotropic elastic solid, and isotropic poro-elastic medium) are presented.

3.2 Interfaces Boundary Conditions

Consider the interface z_i between two consecutive layers $i-1$ and i. If these layers are of the same nature, the boundary conditions are expressed as the continuity of all the components of the displacement-stress vector, i.e. $\boldsymbol{U}_{i-1}(z_i) = \boldsymbol{U}_i(z_i)$.

However, when the two layers are of distinct natures, the boundary conditions are expressed as listed hereinafter [46, 61, 66, 67].

3.2.1 Fluid-Isotropic Elastic Solid Interface:

The subscript F denotes the fluid layer, and S the solid layer. Hence, the boundary conditions at the interface separating fluid and isotropic elastic solid layers are:

$$\begin{cases} u_{z_S}(z_i) = u_{z_F}(z_i), \\ \sigma_{xz_S}(z_1) = 0, \\ \sigma_{zz_S}(z_i) = -P_{f_F}(z_i). \end{cases} \tag{3.1}$$

3.2.2 Fluid-Porous Interface:

In this work, a free flow is considered across the fluid-porous interface. In other words, the fluid-porous interface is considered as an open-pores interface. The subscript F denotes the fluid layer, and P the porous layer; P_{f_F} refers to the fluid pressure in the fluid layer, while P_{f_P} designates the pressure of the fluid phase in the porous layer. The boundary conditions at the interface separating the fluid and isotropic poro-elastic layers are expressed as:

$$\begin{cases} u_{z_P}(z_i) + w_{z_P}(z_i) = u_{z_F}(z_i), \\ \sigma_{xz_P}(z_i) = 0, \\ \sigma_{zz_P}(z_i) = -P_{f_F}(z_i), \\ P_{f_P}(z_i) = P_{f_F}(z_i). \end{cases} \tag{3.2}$$

3.2.3 Solid-Porous Interface:

The solid is impermeable and there is no free flow across the solid-porous interface. That is, this latter is considered as a closed-pores interface. The subscript S denotes the solid layer, and P the porous layer. Therefore, the boundary conditions at the interface separating isotropic elastic solid and isotropic poro-elastic layers are given by:

$$\begin{cases} u_{x_P}(z_i) = u_{x_S}(z_i), \\ u_{z_P}(z_i) = u_{z_S}(z_i), \\ \dfrac{\partial w_{z_P}(z_i)}{\partial t} = 0 \implies w_{z_P}(z_i) = 0, \\ \sigma_{xz_P}(z_i) = \sigma_{xz_S}(z_i), \\ \sigma_{zz_P}(z_i) = \sigma_{zz_S}(z_i). \end{cases} \tag{3.3}$$

3.3 Total Stiffness Matrix of Multilayered Media

In this section, the recursive stiffness matrix method proposed by Rokhlin and Wang [1] is applied in order to merge the stiffness matrices of the structure individual layers obtained in Section 2.3 into one total stiffness matrix.

In the original work, a recursive algorithm was developed to build the total stiffness matrix of a multilayered structure based on the stiffness matrices of individual layers that have the same nature, i.e. the sizes of these stiffness matrices should be equal and there is a continuity of all the components of the displacement-stress vector at every interface. However, in this work, a more general algorithm is developed that computes the global stiffness matrix of a multilayer whose layers could be of any of the three types of physical media (i.e. fluid, isotropic solid and isotropic poro-elastic media). Moreover, the developed approach could be extended in the future to include more general cases such as anisotropic or piezoelectric media.

3.3.1 Algorithm Concept

Starting with layer 1, since no other precedes it, the first total stiffness matrix $[\boldsymbol{K}_{\boldsymbol{G}_1}]$ will be nothing but the stiffness matrix of the layer 1 $[\boldsymbol{K}_1]$, i.e.:

$$[\boldsymbol{K}_{\boldsymbol{G}_1}] = [\boldsymbol{K}_1]. \tag{3.4}$$

Then, moving to the interface at $z = z_2$, as shown in Figure 3-1, each of the displacements and stresses in layers 1 and 2, around that interface, ($\boldsymbol{v}_1(x, z_2)$, $\boldsymbol{v}_2(x, z_2)$ and $\boldsymbol{T}_1(x, z_2)$, $\boldsymbol{T}_2(x, z_2)$) can be related using the corresponding boundary conditions. Hence, the displacements and stresses at the top of the layer 1 ($\boldsymbol{v}_1(x, z_1)$ and $\boldsymbol{T}_1(x, z_1)$) and those at the bottom of the layer 2 ($\boldsymbol{v}_2(x, z_3)$ and $\boldsymbol{T}_2(x, z_3)$) can be related by excluding the previously mentioned components at the interface.

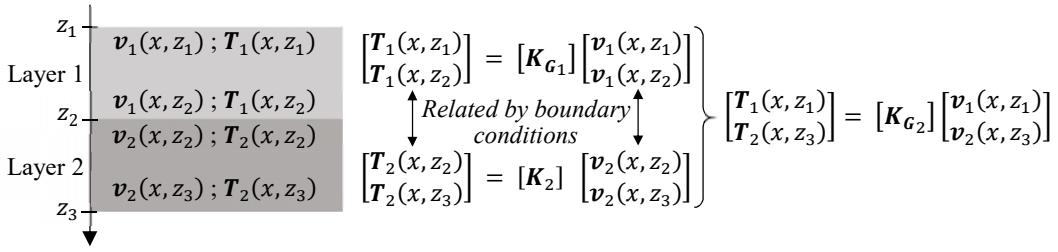

Figure 3-1: Merging of the stiffness matrices for the first two layers.

Thus, the coupling of $[\boldsymbol{K}_{\boldsymbol{G}_1}]$ and $[\boldsymbol{K}_2]$ will lead to the first two layers total stiffness matrix $[\boldsymbol{K}_{\boldsymbol{G}_2}]$. The same work can be done at the interface z_3 in order to combine the first two layers total stiffness matrix $[\boldsymbol{K}_{\boldsymbol{G}_2}]$ with the third layer stiffness matrix $[\boldsymbol{K}_3]$, and to obtain the first three layers total stiffness matrix $[\boldsymbol{K}_{\boldsymbol{G}_3}]$. Having $[\boldsymbol{K}_{\boldsymbol{G}_3}]$, it could be combined with $[\boldsymbol{K}_4]$ to obtain $[\boldsymbol{K}_{\boldsymbol{G}_4}]$. The procedure continues recursively until layer N is reached, where its stiffness matrix $[\boldsymbol{K}_N]$ is merged with the total stiffness matrix of the previous layers, $[\boldsymbol{K}_{\boldsymbol{G}_{N-1}}]$, to form the whole structure total stiffness matrix $[\boldsymbol{K}_{\boldsymbol{G}_N}]$ as illustrated in Figure 3-2. Thus, starting with $[\boldsymbol{K}_{\boldsymbol{G}_1}] = [\boldsymbol{K}_1]$, then using the recursive algorithm $N - 1$ times, leads to

the total stiffness matrix of the multilayer $[\boldsymbol{K}_{\boldsymbol{G}_N}]$ that relates the stresses and displacements at the top and bottom of the structure as follows:

$$\begin{bmatrix} \boldsymbol{T}_1(x,z_1) \\ \boldsymbol{T}_N(x,z_{N+1}) \end{bmatrix} = [\boldsymbol{K}_{\boldsymbol{G}_N}] \begin{bmatrix} \boldsymbol{v}_1(x,z_1) \\ \boldsymbol{v}_N(x,z_{N+1}) \end{bmatrix}. \tag{3.5}$$

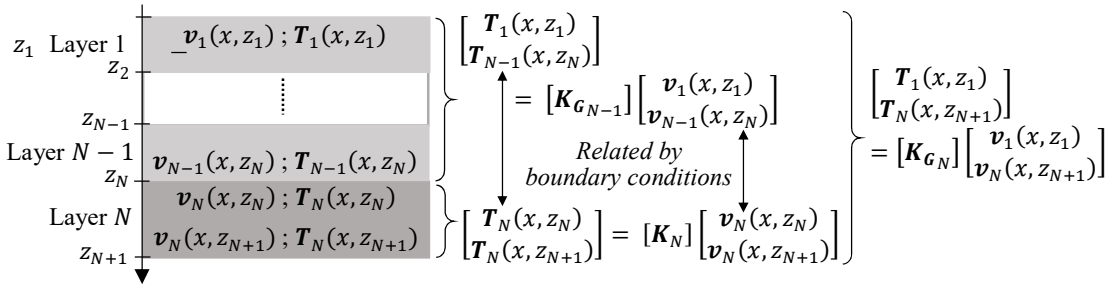

Figure 3-2: Coupling of the stiffness matrices at the level of layer *N*.

In general, for a given layer i with $2 \le i \le N$, if its $2n_i \times 2n_i$ stiffness matrix $[\boldsymbol{K}_i]$ is subdivided into $n_i \times n_i$ submatrices, i.e:

$$[\boldsymbol{K}_i]_{2n_i \times 2n_i} = \left[\begin{array}{ccc|ccc} K_{i,1;1} & \cdots & K_{i,1;n_i} & K_{i,1;(n_i+1)} & \cdots & K_{i,1;2n_i} \\ \vdots & \ddots & \vdots & \vdots & \ddots & \vdots \\ K_{i,n_i;1} & \cdots & K_{i,n_i;n_i} & K_{i,n_i;(n_i+1)} & \cdots & K_{i,n_i;2n_i} \\ \hline K_{i,(n_i+1);1} & \cdots & K_{i,(n_i+1);n_i} & K_{i,(n_i+1);(n_i+1)} & \cdots & K_{i,(n_i+1);2n_i} \\ \vdots & \ddots & \vdots & \vdots & \ddots & \vdots \\ K_{i,2n_i;1} & \cdots & K_{i,2n_i;n_i} & K_{i,2n_i;(n_i+1)} & \cdots & K_{i,2n_i;2n_i} \end{array}\right] \tag{3.6}$$

$$= \begin{bmatrix} [\boldsymbol{K}_i^{11}]_{n_i \times n_i} & [\boldsymbol{K}_i^{12}]_{n_i \times n_i} \\ [\boldsymbol{K}_i^{21}]_{n_i \times n_i} & [\boldsymbol{K}_i^{22}]_{n_i \times n_i} \end{bmatrix}$$

(the subscript notation $x;y$ denotes the element in the x^{th} row and y^{th} column, respectively), the stress-displacement relationship of that layer can be expressed as:

$$\begin{bmatrix} \boldsymbol{T}_i(x,z_i) \\ \boldsymbol{T}_i(x,z_{i+1}) \end{bmatrix} = \begin{bmatrix} [\boldsymbol{K}_i^{11}]_{n_i \times n_i} & [\boldsymbol{K}_i^{12}]_{n_i \times n_i} \\ [\boldsymbol{K}_i^{21}]_{n_i \times n_i} & [\boldsymbol{K}_i^{22}]_{n_i \times n_i} \end{bmatrix} \begin{bmatrix} \boldsymbol{v}_i(x,z_i) \\ \boldsymbol{v}_i(x,z_{i+1}) \end{bmatrix}. \tag{3.7}$$

Moreover, at the layer $i-1$, the displacement and stress components vectors $\boldsymbol{v}_{i-1}$ and $\boldsymbol{T}_{i-1}$, of length n_{i-1}, can be related to $\boldsymbol{v}_1$ and $\boldsymbol{T}_1$, the displacement and stress components vectors in the first layer with a length n_1, through the total stiffness matrix of the layers 1 up to $i-1$, $\left[\boldsymbol{K}_{\boldsymbol{G}_{i-1}}\right]$. If the latter is subdivided into four square matrices as follows:

$$\left[\boldsymbol{K}_{\boldsymbol{G}_{i-1}}\right]_{(n_1+n_{i-1})\times(n_1+n_{i-1})}$$

$$= \left[\begin{array}{ccc|ccc} K_{G\,i-1,1;1} & \cdots & K_{G\,i-1,1;n_1} & K_{G\,i-1,1;(n_1+1)} & \cdots & K_{G\,i-1,1;(n_1+n_{i-1})} \\ \vdots & \ddots & \vdots & \vdots & \ddots & \vdots \\ K_{G\,i-1,n_1;1} & \cdots & K_{G\,i-1,n_1;n_1} & K_{G\,i-1,n_1;(n_1+1)} & \cdots & K_{G\,i-1,n_1;(n_1+n_{i-1})} \\ \hline K_{G\,i-1,(n_1+1);1} & \cdots & K_{G\,i-1,(n_1+1);n_1} & K_{G\,i-1,(n_1+1);(n_1+1)} & \cdots & K_{G\,i-1,(n_1+1);(n_1+n_{i-1})} \\ \vdots & \ddots & \vdots & \vdots & \ddots & \vdots \\ K_{G\,i-1,(n_1+n_{i-1});1} & \cdots & K_{G\,i-1,(n_1+n_{i-1});n_1} & K_{G\,i-1,(n_1+n_{i-1});(n_1+1)} & \cdots & K_{G\,i-1,(n_1+n_{i-1});(n_1+n_{i-1})} \end{array}\right] \tag{3.8}$$

$$= \begin{bmatrix} \left[\boldsymbol{K}^{11}_{\boldsymbol{G}_{i-1}}\right]_{n_1\times n_1} & \left[\boldsymbol{K}^{12}_{\boldsymbol{G}_{i-1}}\right]_{n_1\times n_{i-1}} \\ \left[\boldsymbol{K}^{21}_{\boldsymbol{G}_{i-1}}\right]_{n_{i-1}\times n_1} & \left[\boldsymbol{K}^{22}_{\boldsymbol{G}_{i-1}}\right]_{n_{i-1}\times n_{i-1}} \end{bmatrix},$$

the corresponding stress-displacement relationship can be expressed as:

$$\begin{bmatrix} \boldsymbol{T}_1(x,z_1) \\ \boldsymbol{T}_{i-1}(x,z_i) \end{bmatrix} = \left[\boldsymbol{K}_{\boldsymbol{G}_{i-1}}\right]_{(n_1+n_{i-1})\times(n_1+n_{i-1})} \begin{bmatrix} \boldsymbol{v}_1(x,z_1) \\ \boldsymbol{v}_{i-1}(x,z_i) \end{bmatrix}$$

$$= \begin{bmatrix} \left[\boldsymbol{K}^{11}_{\boldsymbol{G}_{i-1}}\right]_{n_1\times n_1} & \left[\boldsymbol{K}^{12}_{\boldsymbol{G}_{i-1}}\right]_{n_1\times n_{i-1}} \\ \left[\boldsymbol{K}^{21}_{\boldsymbol{G}_{i-1}}\right]_{n_{i-1}\times n_1} & \left[\boldsymbol{K}^{22}_{\boldsymbol{G}_{i-1}}\right]_{n_{i-1}\times n_{i-1}} \end{bmatrix} \begin{bmatrix} \boldsymbol{v}_1(x,z_1) \\ \boldsymbol{v}_{i-1}(x,z_i) \end{bmatrix}. \tag{3.9}$$

In order to obtain the total stiffness matrix of the layers 1 up to i, the relationships in Eqs. (3.6) and (3.9) should be merged by eliminating the vectors at the interface z_i. This is achieved by expressing the displacement components vectors $\boldsymbol{v}_{i-1}(x,z_i)$ and $\boldsymbol{v}_i(x,z_i)$ in terms of $\boldsymbol{v}_1(x,z_1)$ and $\boldsymbol{v}_i(x,z_{i+1})$ through a matrix $[\boldsymbol{V}_i]$ using the boundary conditions at the interface z_i as presented in Section 3.2. The relationship involving the matrix $[\boldsymbol{V}_i]$ is:

$$\begin{bmatrix} \boldsymbol{v}_{i-1}(x,z_i) \\ \\ \boldsymbol{v}_i(x,z_i) \end{bmatrix} = [\boldsymbol{V}_i]_{(n_{i-1}+n_i)\times(n_1+n_i)} \begin{bmatrix} \boldsymbol{v}_1(x,z_1) \\ \\ \boldsymbol{v}_i(x,z_{i+1}) \end{bmatrix}$$
$$= \begin{bmatrix} [\boldsymbol{V}_i^{11}]_{n_{i-1}\times n_1} & [\boldsymbol{V}_i^{12}]_{n_{i-1}\times n_i} \\ \\ [\boldsymbol{V}_i^{21}]_{n_i\times n_1} & [\boldsymbol{V}_i^{22}]_{n_i\times n_i} \end{bmatrix} \begin{bmatrix} \boldsymbol{v}_1(x,z_1) \\ \\ \boldsymbol{v}_i(x,z_{i+1}) \end{bmatrix}. \tag{3.10}$$

The derivation of the matrix $[\boldsymbol{V}_i]$ will be detailed in the following section.

Then, using Eqs. (3.7), (3.9), and (3.10), the stress components vectors $\boldsymbol{T}_1(x,z_1)$ and $\boldsymbol{T}_i(x,z_{i+1})$ can also be expressed as a function of $\boldsymbol{v}_1(x,z_1)$ and $\boldsymbol{v}_i(x,z_{i+1})$ as follows:

$$\begin{bmatrix} \boldsymbol{T}_1(x,z_1) \\ \\ \boldsymbol{T}_i(x,z_{i+1}) \end{bmatrix} = \begin{bmatrix} \left[\boldsymbol{K}_{\boldsymbol{G}_{i-1}}^{11}\right] + \left[\boldsymbol{K}_{\boldsymbol{G}_{i-1}}^{12}\right][\boldsymbol{V}_i^{11}] & \left[\boldsymbol{K}_{\boldsymbol{G}_{i-1}}^{12}\right][\boldsymbol{V}_i^{12}] \\ \\ [\boldsymbol{K}_i^{21}][\boldsymbol{V}_i^{21}] & [\boldsymbol{K}_i^{21}][\boldsymbol{V}_i^{22}] + [\boldsymbol{K}_i^{22}] \end{bmatrix} \begin{bmatrix} \boldsymbol{v}_1(x,z_1) \\ \\ \boldsymbol{v}_i(x,z_{i+1}) \end{bmatrix}. \tag{3.11}$$

Thus, starting with $\left[\boldsymbol{K}_{\boldsymbol{G}_1}\right] = [\boldsymbol{K}_1]$, the i^{th} total stiffness matrix $\left[\boldsymbol{K}_{\boldsymbol{G}_i}\right]$ (i.e. the total stiffness matrix for the layers 1 up to i) with $2 \le i \le N$ is defined as:

$$\left[\boldsymbol{K}_{\boldsymbol{G}_i}\right]_{(n_1+n_i)\times(n_1+n_i)} = \begin{bmatrix} \left[\boldsymbol{K}_{\boldsymbol{G}_{i-1}}^{11}\right] + \left[\boldsymbol{K}_{\boldsymbol{G}_{i-1}}^{12}\right][\boldsymbol{V}_i^{11}] & \left[\boldsymbol{K}_{\boldsymbol{G}_{i-1}}^{12}\right][\boldsymbol{V}_i^{12}] \\ \\ [\boldsymbol{K}_i^{21}][\boldsymbol{V}_i^{21}] & [\boldsymbol{K}_i^{21}][\boldsymbol{V}_i^{22}] + [\boldsymbol{K}_i^{22}] \end{bmatrix}, \tag{3.12}$$

$$\text{for } 2 \le i \le N.$$

3.3.2 Computation of the Matrix $[\boldsymbol{V}_i]$

As defined in Section 3.3.1, for a layer i with $2 \le i \le N$, $[\boldsymbol{V}_i]$ is a matrix that relates the displacement components vectors $\boldsymbol{v}_{i-1}(x,z_i)$ and $\boldsymbol{v}_i(x,z_i)$ to the displacement components vectors $\boldsymbol{v}_1(x,z_1)$ and $\boldsymbol{v}_i(x,z_{i+1})$, depending on the boundary conditions at the the interface z_i. Given the three-layer natures, nine combinations are possible at the interface z_i, three of which correspond to same nature consecutive layers (i.e. layers i and $i-1$ are of the same nature) leading to the same expression of $[\boldsymbol{V}_i]$. As for the six other possible combinations, $[\boldsymbol{V}_i]$ should be obtained for each of them based on the corresponding boundary conditions. Thus, in total, seven different matrices $[\boldsymbol{V}_i]$ are to be derived in order to account

for all possible interfaces associated with the three-layer natures. The derivation of the matrix $[\boldsymbol{V}_i]$ for each case is detailed in the following subsections.

3.3.2.1 Interface Separating Two Layers of the Same Nature

Given an interface at z_i $(2 \leq i \leq N)$ that separates two layers i and $i-1$ of the same nature (i.e. fluid-fluid, solid-solid, or porous-porous interface), the boundary conditions imply the continuity of all the components of the displacement-stress vector at $z = z_i$, that is:

$$\begin{cases} \boldsymbol{v}_{i-1}(x, z_i) = \boldsymbol{v}_i(x, z_i) \\ \boldsymbol{T}_{i-1}(x, z_i) = \boldsymbol{T}_i(x, z_i) \end{cases}. \tag{3.13}$$

With reference to Eqs. (3.9) and (3.7), $\boldsymbol{T}_{i-1}(x, z_i)$ and $\boldsymbol{T}_i(x, z_i)$ are expressed respectively, as:

$$\begin{aligned} \boldsymbol{T}_{i-1}(x, z_i) &= \left[\boldsymbol{K}_{\boldsymbol{G}_{i-1}}^{21}\right]_{n_{i-1}\times n_1} \boldsymbol{v}_1(x, z_1) + \left[\boldsymbol{K}_{\boldsymbol{G}_{i-1}}^{22}\right]_{n_{i-1}\times n_{i-1}} \boldsymbol{v}_{i-1}(x, z_i), \\ \boldsymbol{T}_i(x, z_i) &= [\boldsymbol{K}_i^{11}]_{n_i\times n_i} \boldsymbol{v}_i(x, z_i) + [\boldsymbol{K}_i^{12}]_{n_i\times n_i} \boldsymbol{v}_i(x, z_{i+1}), \end{aligned} \tag{3.14}$$

where $n_{i-1} = n_i = 1,2,3$ for fluid, isotropic elastic solid, and isotropic poro-elastic medium respectively.

Applying the equalities in Eq. (3.13) into Eq. (3.14), $\boldsymbol{v}_{i-1}(x, z_i)$ or $\boldsymbol{v}_i(x, z_i)$ can be expressed in terms of $\boldsymbol{v}_1(x, z_1)$ and $\boldsymbol{v}_i(x, z_{i+1})$ as:

$$\begin{aligned} \boldsymbol{v}_i(x, z_i) &= \boldsymbol{v}_{i-1}(x, z_i) \\ &= \left[\left[\boldsymbol{K}_{\boldsymbol{G}_{i-1}}^{22}\right] - [\boldsymbol{K}_i^{11}]\right]_{n_i\times n_i}^{-1} \begin{bmatrix} -\left[\boldsymbol{K}_{\boldsymbol{G}_{i-1}}^{21}\right] & [\boldsymbol{K}_i^{12}] \end{bmatrix}_{n_i\times(n_1+n_i)} \begin{bmatrix} \boldsymbol{v}_1(x, z_1) \\ \boldsymbol{v}_i(x, z_{i+1}) \end{bmatrix}. \end{aligned} \tag{3.15}$$

Hence, the matrix $[\boldsymbol{V}_i]$ will be:

$$[\boldsymbol{V}_i]_{(2n_i)\times(n_1+n_i)} = \begin{bmatrix} \left[\left[\boldsymbol{K}_{\boldsymbol{G}_{i-1}}^{22}\right] - [\boldsymbol{K}_i^{11}]\right]^{-1} & \begin{bmatrix} -\left[\boldsymbol{K}_{\boldsymbol{G}_{i-1}}^{21}\right] & [\boldsymbol{K}_i^{12}] \end{bmatrix} \\ \left[\left[\boldsymbol{K}_{\boldsymbol{G}_{i-1}}^{22}\right] - [\boldsymbol{K}_i^{11}]\right]^{-1} & \begin{bmatrix} -\left[\boldsymbol{K}_{\boldsymbol{G}_{i-1}}^{21}\right] & [\boldsymbol{K}_i^{12}] \end{bmatrix} \end{bmatrix}. \tag{3.16}$$

3.3.2.2 Fluid - Isotropic Elastic Solid Interface

With reference to Eq. (3.1), in the case of a layer $i-1$ of fluid type followed by a layer i that is an isotropic elastic solid, the boundary conditions at the interface z_i imply that:

$$\begin{cases} u_{z_i}(x,z_i) = u_{z_{i-1}}(x,z_i), \\ \boldsymbol{T}_i(x,z_i) = \begin{bmatrix} 0 \\ \\ \boldsymbol{T}_{i-1}(x,z_i) \end{bmatrix}. \end{cases} \tag{3.17}$$

Using the expressions of $\boldsymbol{T}_i(x,z_i)$ and $\boldsymbol{T}_{i-1}(x,z_i)$ as defined in Eq. (3.14) with $n_{i-1} = 1$ and $n_i = 2$, and applying the conditions in Eq. (3.17), $\boldsymbol{v}_i(x,z_i)$ can be expressed in terms of $\boldsymbol{v}_1(x,z_1)$ and $\boldsymbol{v}_i(x,z_{i+1})$ as:

$$\begin{aligned} \boldsymbol{v}_i(x,z_i) &= \begin{bmatrix} u_{x_i}(x,z_i) \\ \\ u_{z_i}(x,z_i) \end{bmatrix} \\ &= \left[\begin{bmatrix} 0 & 0 \\ \\ 0 & \boldsymbol{K}^{22}_{\boldsymbol{G}_{i-1}} \end{bmatrix} - [\boldsymbol{K}_i^{11}] \right]^{-1}_{2\times 2} \left[\begin{bmatrix} [\boldsymbol{0}]_{1\times n_1} \\ \\ -[\boldsymbol{K}^{21}_{\boldsymbol{G}_{i-1}}] \end{bmatrix} \quad [\boldsymbol{K}_i^{12}] \right]_{2\times(n_1+2)} \begin{bmatrix} \boldsymbol{v}_1(x,z_1) \\ \\ \boldsymbol{v}_i(x,z_{i+1}) \end{bmatrix} \\ &= [\boldsymbol{W}_i]_{2\times(n_1+2)} \begin{bmatrix} \boldsymbol{v}_1(x,z_1) \\ \\ \boldsymbol{v}_i(x,z_{i+1}) \end{bmatrix}. \end{aligned} \tag{3.18}$$

Since $\boldsymbol{v}_{i-1}(x,z_i) = u_{z_{i-1}}(x,z_i) = u_{z_i}(x,z_i)$, then $\boldsymbol{v}_{i-1}(x,z_i)$ is the second component of $\boldsymbol{v}_i(x,z_i)$. Thus, if the matrix $[\boldsymbol{W}_i]$ as defined in Eq. (3.18) is subdivided as follows:

$$[\boldsymbol{W}_i]_{2\times(n_1+2)} = \begin{bmatrix} [\boldsymbol{W}_i^1]_{1\times(n_1+2)} \\ \\ [\boldsymbol{W}_i^2]_{1\times(n_1+2)} \end{bmatrix}, \tag{3.19}$$

$\boldsymbol{v}_{i-1}(x,z_i)$ can be expressed in terms of $\boldsymbol{v}_1(x,z_1)$ and $\boldsymbol{v}_i(x,z_{i+1})$ as:

$$\boldsymbol{v}_{i-1}(x,z_i) = u_{z_{i-1}}(x,z_i) = [\boldsymbol{W}_i^2] \begin{bmatrix} \boldsymbol{v}_1(x,z_1) \\ \\ \boldsymbol{v}_i(x,z_{i+1}) \end{bmatrix}. \tag{3.20}$$

Therefore, the matrix $[\boldsymbol{V}_i]$ will be:

$$[\boldsymbol{V}_i]_{3\times(n_1+2)} = \begin{bmatrix} [\boldsymbol{W}_i^2]_{1\times(n_1+2)} \\ [\boldsymbol{W}_i]_{2\times(n_1+2)} \end{bmatrix}. \tag{3.21}$$

3.3.2.3 Isotropic Elastic Solid - Fluid Interface

With reference to Eq. (3.1), in the case of a layer $i-1$ that is an isotropic elastic solid followed by a layer i of fluid type, the boundary conditions at the interface z_i imply that:

$$\begin{cases} u_{z_{i-1}}(x, z_i) = u_{z_i}(x, z_i), \\ \boldsymbol{T}_{i-1}(x, z_i) = \begin{bmatrix} 0 \\ \boldsymbol{T}_i(x, z_i) \end{bmatrix}. \end{cases} \tag{3.22}$$

Using the expressions of $\boldsymbol{T}_i(x, z_i)$ and $\boldsymbol{T}_{i-1}(x, z_i)$ as defined in Eq. (3.14) with $n_{i-1} = 2$ and $n_i = 1$, and applying the conditions in Eq. (3.22), $\boldsymbol{v}_{i-1}(x, z_i)$ can be expressed in terms of $\boldsymbol{v}_1(x, z_1)$ and $\boldsymbol{v}_i(x, z_{i+1})$ as:

$$\begin{aligned} \boldsymbol{v}_{i-1}(x, z_i) &= \begin{bmatrix} u_{x_{i-1}}(x, z_i) \\ u_{z_{i-1}}(x, z_i) \end{bmatrix} \\ &= \left[\begin{bmatrix} 0 & 0 \\ 0 & \boldsymbol{K}_i^{11} \end{bmatrix} - \left[\boldsymbol{K}_{\boldsymbol{G}_{i-1}}^{22}\right] \right]_{2\times 2}^{-1} \left[\left[\boldsymbol{K}_{\boldsymbol{G}_{i-1}}^{21}\right] \quad \begin{bmatrix} 0 \\ -\boldsymbol{K}_i^{12} \end{bmatrix} \right]_{2\times(n_1+1)} \begin{bmatrix} \boldsymbol{v}_1(x, z_1) \\ \boldsymbol{v}_i(x, z_{i+1}) \end{bmatrix} \\ &= [\boldsymbol{W}_i]_{2\times(n_1+1)} \begin{bmatrix} \boldsymbol{v}_1(x, z_1) \\ \boldsymbol{v}_i(x, z_{i+1}) \end{bmatrix} \end{aligned} \tag{3.23}$$

Since $\boldsymbol{v}_i(x, z_i) = u_{z_i}(x, z_i) = u_{z_{i-1}}(x, z_i)$, then $\boldsymbol{v}_i(x, z_i)$ is the second component of $\boldsymbol{v}_{i-1}(x, z_i)$. Thus, if the matrix $[\boldsymbol{W}_i]$ as defined in Eq. (3.23) is subdivided as follows:

$$[\boldsymbol{W}_i]_{2\times(n_1+1)} = \begin{bmatrix} [\boldsymbol{W}_i^1]_{1\times(n_1+1)} \\ [\boldsymbol{W}_i^2]_{1\times(n_1+1)} \end{bmatrix}, \tag{3.24}$$

$\boldsymbol{v}_i(x, z_i)$ can be expressed in terms of $\boldsymbol{v}_1(x, z_1)$ and $\boldsymbol{v}_i(x, z_{i+1})$ as:

$$\boldsymbol{v}_i(x, z_i) = u_{z_i}(x, z_i) = [\boldsymbol{W}_i^2] \begin{bmatrix} \boldsymbol{v}_1(x, z_1) \\ \\ \boldsymbol{v}_i(x, z_{i+1}) \end{bmatrix}. \tag{3.25}$$

Therefore, the matrix $[\boldsymbol{V}_i]$ will be:

$$[\boldsymbol{V}_i]_{3\times(n_1+1)} = \begin{bmatrix} [\boldsymbol{W}_i]_{2\times(n_1+1)} \\ \\ [\boldsymbol{W}_i^2]_{1\times(n_1+1)} \end{bmatrix}. \tag{3.26}$$

3.3.2.4 Fluid - Isotropic Poro-elastic Interface

With reference to Eq. (3.2), in the case of a layer $i-1$ of fluid type followed by a layer i that is an isotropic poro-elastic medium, the boundary conditions at the interface z_i imply that:

$$\begin{cases} u_{z_i}(x, z_i) + w_{z_i}(x, z_i) = u_{z_{i-1}}(x, z_i), \\ \\ \boldsymbol{T}_i(x, z_i) = \begin{bmatrix} 0 \\ \\ \boldsymbol{T}_{i-1}(x, z_i) \\ \\ -\boldsymbol{T}_{i-1}(x, z_i) \end{bmatrix}. \end{cases} \tag{3.27}$$

Using the expressions of $\boldsymbol{T}_i(x, z_i)$ and $\boldsymbol{T}_{i-1}(x, z_i)$ as defined in Eq. (3.14) with $n_{i-1} = 1$ and $n_i = 3$, and applying the conditions in Eq. (3.27), $\boldsymbol{v}_i(x, z_i)$ can be expressed in terms of $\boldsymbol{v}_1(x, z_1)$ and $\boldsymbol{v}_i(x, z_{i+1})$ as:

$$\boldsymbol{v}_i(x,z_i)=\begin{bmatrix}u_{x_i}(x,z_i)\\ u_{z_i}(x,z_i)\\ w_{z_i}(x,z_i)\end{bmatrix}$$

$$=\left[\begin{bmatrix}0 & 0 & 0\\ 0 & \boldsymbol{K}^{22}_{\boldsymbol{G}_{i-1}} & \boldsymbol{K}^{22}_{\boldsymbol{G}_{i-1}}\\ 0 & -\boldsymbol{K}^{22}_{\boldsymbol{G}_{i-1}} & -\boldsymbol{K}^{22}_{\boldsymbol{G}_{i-1}}\end{bmatrix}-[\boldsymbol{K}_i^{11}]\right]^{-1}_{3\times3}\begin{bmatrix}[\boldsymbol{0}]_{1\times n_1}\\ -\left[\boldsymbol{K}^{21}_{\boldsymbol{G}_{i-1}}\right]\\ \left[\boldsymbol{K}^{21}_{\boldsymbol{G}_{i-1}}\right]\end{bmatrix}\quad[\boldsymbol{K}_i^{12}]\Bigg]_{3\times(n_1+3)}\begin{bmatrix}\boldsymbol{v}_1(x,z_1)\\ \\ \boldsymbol{v}_i(x,z_{i+1})\end{bmatrix}\tag{3.28}$$

$$=[\boldsymbol{W}_i]_{3\times(n_1+3)}\begin{bmatrix}\boldsymbol{v}_1(x,z_1)\\ \\ \boldsymbol{v}_i(x,z_{i+1})\end{bmatrix}$$

As for the vector $\boldsymbol{v}_{i-1}(x,z_i)$, $\boldsymbol{v}_{i-1}(x,z_i)=u_{z_{i-1}}(x,z_i)=u_{z_i}(x,z_i)+w_{z_i}(x,z_i)$. Thus, if the matrix $[\boldsymbol{W_i}]$ as defined in Eq. (3.28) is subdivided as follows:

$$[\boldsymbol{W}_i]_{3\times(n_1+3)}=\begin{bmatrix}[\boldsymbol{W}_i^1]_{1\times(n_1+3)}\\ [\boldsymbol{W}_i^2]_{1\times(n_1+3)}\\ [\boldsymbol{W}_i^3]_{1\times(n_1+3)}\end{bmatrix},\tag{3.29}$$

$\boldsymbol{v}_{i-1}(x,z_i)$ can be expressed in terms of $\boldsymbol{v}_1(x,z_1)$ and $\boldsymbol{v}_i(x,z_{i+1})$ as:

$$\boldsymbol{v}_{i-1}(x,z_i)=\left[[\boldsymbol{W}_i^2]+[\boldsymbol{W}_i^3]\right]\begin{bmatrix}\boldsymbol{v}_1(x,z_1)\\ \\ \boldsymbol{v}_i(x,z_{i+1})\end{bmatrix}.\tag{3.30}$$

Therefore, the matrix $[\boldsymbol{V}_i]$ will be:

$$[\boldsymbol{V}_i]_{4\times(n_1+3)}=\begin{bmatrix}\left[[\boldsymbol{W}_i^2]+[\boldsymbol{W}_i^3]\right]_{1\times(n_1+3)}\\ \\ [\boldsymbol{W}_i]_{3\times(n_1+3)}\end{bmatrix}.\tag{3.31}$$

3.3.2.5 Isotropic Poro-elastic - Fluid Interface

With reference to Eq. (3.2), in the case of a layer $i-1$ that is an isotropic poro-elastic medium followed by a layer i of fluid type, the boundary conditions at the interface z_i imply that:

$$\begin{cases} u_{z_{i-1}}(x,z_i) + w_{z_{i-1}}(x,z_i) = u_{z_i}(x,z_i), \\ \boldsymbol{T}_{i-1}(x,z_i) = \begin{bmatrix} 0 \\ \boldsymbol{T}_i(x,z_i) \\ -\boldsymbol{T}_i(x,z_i) \end{bmatrix}. \end{cases} \tag{3.32}$$

Using the expressions of $\boldsymbol{T}_i(x,z_i)$ and $\boldsymbol{T}_{i-1}(x,z_i)$ as defined in Eq. (3.14) with $n_{i-1} = 3$ and $n_i = 1$, and applying the conditions in Eq. (3.32), $\boldsymbol{v}_{i-1}(x,z_i)$ can be expressed in terms of $\boldsymbol{v}_1(x,z_1)$ and $\boldsymbol{v}_i(x,z_{i+1})$ as:

$$\boldsymbol{v}_{i-1}(x,z_i) = \begin{bmatrix} u_{x_{i-1}}(x,z_i) \\ u_{z_{i-1}}(x,z_i) \\ w_{z_{i-1}}(x,z_i) \end{bmatrix}$$

$$= \left(\begin{bmatrix} 0 & 0 & 0 \\ 0 & \boldsymbol{K}_i^{11} & \boldsymbol{K}_i^{11} \\ 0 & -\boldsymbol{K}_i^{11} & -\boldsymbol{K}_i^{11} \end{bmatrix} - \left[\boldsymbol{K}_{\boldsymbol{G}_{i-1}}^{22}\right] \right]_{3\times 3}^{-1} \left[\left[\boldsymbol{K}_{\boldsymbol{G}_{i-1}}^{21}\right] \quad \begin{bmatrix} 0 \\ -\boldsymbol{K}_i^{12} \\ \boldsymbol{K}_i^{12} \end{bmatrix} \right]_{3\times(n_1+1)} \begin{bmatrix} \boldsymbol{v}_1(x,z_1) \\ \boldsymbol{v}_i(x,z_{i+1}) \end{bmatrix} \tag{3.33}$$

$$= [\boldsymbol{W}_i]_{3\times(n_1+1)} \begin{bmatrix} \boldsymbol{v}_1(x,z_1) \\ \boldsymbol{v}_i(x,z_{i+1}) \end{bmatrix}$$

As for the vector $\boldsymbol{v}_i(x,z_i)$, $\boldsymbol{v}_i(x,z_i) = u_{z_i}(x,z_i) = u_{z_{i-1}}(x,z_i) + w_{z_{i-1}}(x,z_i)$. Thus, if the matrix $[\boldsymbol{W_i}]$ as defined in Eq. (3.33) is subdivided as follows:

$$[\boldsymbol{W}_i]_{3\times(n_1+1)} = \begin{bmatrix} [\boldsymbol{W}_i^1]_{1\times(n_1+1)} \\ [\boldsymbol{W}_i^2]_{1\times(n_1+1)} \\ [\boldsymbol{W}_i^3]_{1\times(n_1+1)} \end{bmatrix}, \tag{3.34}$$

$\boldsymbol{v}_i(x,z_i)$ can be expressed in terms of $\boldsymbol{v}_1(x,z_1)$ and $\boldsymbol{v}_i(x,z_{i+1})$ as:

$$\boldsymbol{v}_i(x,z_i) = u_{z_i}(x,z_i) = \left[[\boldsymbol{W}_i^2] + [\boldsymbol{W}_i^3]\right] \begin{bmatrix} \boldsymbol{v}_1(x,z_1) \\ \boldsymbol{v}_i(x,z_{i+1}) \end{bmatrix}. \tag{3.35}$$

Therefore, the matrix $[\boldsymbol{V}_i]$ will be:

$$[\boldsymbol{V}_i]_{4\times(n_1+1)} = \begin{bmatrix} [\boldsymbol{W}_i]_{3\times(n_1+1)} \\ \left[[\boldsymbol{W}_i^2] + [\boldsymbol{W}_i^3]\right]_{1\times(n_1+1)} \end{bmatrix}. \tag{3.36}$$

3.3.2.6 Isotropic Elastic Solid - Isotropic Poro-elastic Interface

With reference to Eq. (3.3), in the case of a layer $i-1$ of solid type followed by a layer i that is an isotropic poro-elastic medium, the boundary conditions at the interface z_i imply that:

$$\begin{cases} \boldsymbol{v}_i(x,z_i) = \begin{bmatrix} \boldsymbol{v}_{i-1}(x,z_i) \\ 0 \end{bmatrix}, \\ \begin{bmatrix} \sigma_{xz_i}(x,z_i) \\ \sigma_{zz_i}(x,z_i) \end{bmatrix} = \boldsymbol{T}_{i-1}(x,z_i). \end{cases} \tag{3.37}$$

According to Eq. (3.37), the fluid phase pressure in the porous medium is excluded from the boundary conditions at the interface z_i (i.e. $\mathrm{P_{f_i}}(x,z_i)$); moreover, the relative fluid displacement in this medium should be zero at $z=z_i$ (i.e. $w_{z_i}(x,z_i)=0$). Hence, to calculate the matrix $[\boldsymbol{V}_i]$, the third row and column of the stiffness matrix $[\boldsymbol{K}_i]$ of the porous layer i will be excluded in this case. Consequently, referring to the stiffness matrix expansion in Eq. (3.6) with $n_i=3$, a 2×2 submatrix $\left[\boldsymbol{K}_i^{11'}\right]$ and a 2×3 submatrix $\left[\boldsymbol{K}_i^{12'}\right]$ are defined such that:

$$\begin{aligned} \left[\boldsymbol{K}_i^{11'}\right]_{2\times2} &= \begin{bmatrix} K_{i,1;1} & K_{i,1;2} \\ K_{i,2;1} & K_{i,2;2} \end{bmatrix}, \\ \left[\boldsymbol{K}_i^{12'}\right]_{2\times3} &= \begin{bmatrix} K_{i,1;4} & K_{i,1;5} & K_{i,1;6} \\ K_{i,2;4} & K_{i,2;5} & K_{i,2;6} \end{bmatrix} \end{aligned} \tag{3.38}$$

Then, with reference to Eq. (2.64), the normal and tangential stresses in the porous layer i at $z=z_i$ can be expressed in terms of $\left[\boldsymbol{K}_i^{11'}\right]$ and $\left[\boldsymbol{K}_i^{12'}\right]$ as:

$$\begin{bmatrix} \sigma_{xz_i}(x,z_i) \\ \\ \sigma_{zz_i}(x,z_i) \end{bmatrix} = \left[\boldsymbol{K}_i^{11'}\right]_{2\times 2} \begin{bmatrix} u_{x_i}(x,z_i) \\ \\ u_{z_i}(x,z_i) \end{bmatrix} + \left[\boldsymbol{K}_i^{12'}\right]_{2\times 3} \boldsymbol{v}_i(x,z_{i+1}). \tag{3.39}$$

Using the expression of $\boldsymbol{T}_{i-1}(x,z_i)$ as defined in Eq. (3.14) with $n_{i-1}=2$ along with the stresses expressed in Eq. (3.39), and applying the conditions in Eq. (3.37), $\boldsymbol{v}_{i-1}(x,z_i)$ can be expressed in terms of $\boldsymbol{v}_1(x,z_1)$ and $\boldsymbol{v}_i(x,z_{i+1})$ as:

$$\begin{aligned} \boldsymbol{v}_{i-1}(x,z_i) &= \begin{bmatrix} u_{x_{i-1}}(x,z_i) \\ \\ u_{z_{i-1}}(x,z_i) \end{bmatrix} \\ &= \left[\left[\boldsymbol{K}_{\boldsymbol{G}_{i-1}}^{22}\right] - \left[\boldsymbol{K}_i^{11'}\right]\right]_{2\times 2}^{-1} \left[-\left[\boldsymbol{K}_{\boldsymbol{G}_{i-1}}^{21}\right] \quad \left[\boldsymbol{K}_i^{12'}\right]\right]_{2\times(n_1+3)} \begin{bmatrix} \boldsymbol{v}_1(x,z_1) \\ \\ \boldsymbol{v}_i(x,z_{i+1}) \end{bmatrix} \\ &= \left[\boldsymbol{W}_i\right]_{2\times(n_1+3)} \begin{bmatrix} \boldsymbol{v}_1(x,z_1) \\ \\ \boldsymbol{v}_i(x,z_{i+1}) \end{bmatrix} \end{aligned} \tag{3.40}$$

As for the vector $\boldsymbol{v}_i(x,z_i)$, it can be expressed in terms of $\boldsymbol{v}_1(x,z_1)$ and $\boldsymbol{v}_i(x,z_{i+1})$ as:

$$\boldsymbol{v}_i(x,z_i) = \begin{bmatrix} u_{x_i}(x,z_i) \\ \\ u_{z_i}(x,z_i) \\ \\ w_{z_i}(x,z_i) \end{bmatrix} = \begin{bmatrix} \left[\boldsymbol{W}_i\right]_{2\times(n_1+3)} \\ \\ \left[\boldsymbol{0}\right]_{1\times(n_1+3)} \end{bmatrix} \begin{bmatrix} \boldsymbol{v}_1(x,z_1) \\ \\ \boldsymbol{v}_i(x,z_{i+1}) \end{bmatrix}. \tag{3.41}$$

Therefore, the matrix $[\boldsymbol{V}_i]$ will be:

$$\left[\boldsymbol{V}_i\right]_{5\times(n_1+3)} = \begin{bmatrix} \left[\boldsymbol{W}_i\right]_{2\times(n_1+3)} \\ \\ \left[\boldsymbol{W}_i\right]_{2\times(n_1+3)} \\ \\ \left[\boldsymbol{0}\right]_{1\times(n_1+3)} \end{bmatrix}. \tag{3.42}$$

3.3.2.7 Isotropic Poro-elastic - Isotropic Elastic Solid Interface

With reference to Eq. (3.3), in the case of a layer $i-1$ that is an isotropic poro-elastic medium followed by a layer i of solid type, the boundary conditions at the interface z_i imply that:

$$\begin{cases} \boldsymbol{v}_{i-1}(x,z_i) = \begin{bmatrix} \boldsymbol{v}_i(x,z_i) \\ \\ 0 \end{bmatrix}, \\ \begin{bmatrix} \sigma_{xz_{i-1}}(x,z_i) \\ \\ \sigma_{zz_{i-1}}(x,z_i) \end{bmatrix} = \boldsymbol{T}_i(x,z_i). \end{cases} \tag{3.43}$$

According to Eq. (3.37), the fluid phase pressure in the porous medium is excluded from the boundary conditions at the interface z_i (i.e. $P_{f_{i-1}}(x,z_i)$); moreover, the relative fluid displacement in this medium should be zero at $z = z_i$ (i.e. $w_{z_{i-1}}(x,z_i) = 0$). Hence, in this case, to calculate the matrix $[\boldsymbol{V}_i]$, the last row and last column of the total stiffness matrix $\left[\boldsymbol{K}_{\boldsymbol{G}i-1}\right]$ corresponding to the case of a porous layer $i-1$ will be excluded. Consequently, referring to the global stiffness matrix expansion in Eq. (3.8) with $n_{i-1} = 3$, a $2 \times n_1$ submatrix $\left[\boldsymbol{K}_{\boldsymbol{G}_{i-1}}^{21}{}'\right]$ and a 2×2 submatrix $\left[\boldsymbol{K}_{\boldsymbol{G}_{i-1}}^{22}{}'\right]$ are defined such that:

$$\begin{aligned} \left[\boldsymbol{K}_{\boldsymbol{G}_{i-1}}^{21}{}'\right]_{2\times n_1} &= \begin{bmatrix} K_{G\,i-1,(n_1+1);1} & \cdots & K_{G\,i-1,(n_1+1);n_1} \\ \\ K_{G\,i-1,(n_1+2);1} & \cdots & K_{G\,i-1,(n_1+2);n_1} \end{bmatrix}, \\ \left[\boldsymbol{K}_{\boldsymbol{G}_{i-1}}^{22}{}'\right]_{2\times 2} &= \begin{bmatrix} K_{G_{i-1,(n_1+1);(n_1+1)}} & K_{G_{i-1,(n_1+1);(n_1+2)}} \\ \\ K_{G_{i-1,(n_1+2);(n_1+1)}} & K_{G_{i-1,(n_1+2);(n_1+2)}} \end{bmatrix}. \end{aligned} \tag{3.44}$$

Then, with reference to Eq. (3.5), the normal and tangential stresses in the porous layer $i-1$ at $z = z_i$ can be expressed in terms of $\left[\boldsymbol{K}_{\boldsymbol{G}_{i-1}}^{21}{}'\right]$ and $\left[\boldsymbol{K}_{\boldsymbol{G}_{i-1}}^{22}{}'\right]$ as:

$$\begin{bmatrix} \sigma_{xz_{i-1}}(x,z_i) \\ \\ \sigma_{zz_{i-1}}(x,z_i) \end{bmatrix} = \left[\boldsymbol{K}_{\boldsymbol{G}_{i-1}}^{21}{}'\right]_{2\times n_1} \boldsymbol{v}_1(x,z_1) + \left[\boldsymbol{K}_{\boldsymbol{G}_{i-1}}^{22}{}'\right]_{2\times 2} \begin{bmatrix} u_{x_{i-1}}(x,z_i) \\ \\ u_{z_{i-1}}(x,z_i) \end{bmatrix}. \tag{3.45}$$

Using the expression of $\boldsymbol{T}_i(x,z_i)$ as defined in Eq. (3.14) with $n_i = 2$ along with the stresses expressed in Eq. (3.45), and applying the conditions in Eq. (3.43), $\boldsymbol{v}_i(x,z_i)$ can be expressed in terms of $\boldsymbol{v}_1(x,z_1)$ and $\boldsymbol{v}_i(x,z_{i+1})$ as:

$$\boldsymbol{v}_i(x,z_i)=\begin{bmatrix}u_{x_i}(x,z_i)\\ \\ u_{z_i}(x,z_i)\end{bmatrix}$$

$$=\left[\left[\boldsymbol{K}_{\boldsymbol{G}_{i-1}}^{22}{}'\right]-[\boldsymbol{K}_i^{11}]\right]_{2\times2}^{-1}\ \left[-\left[\boldsymbol{K}_{\boldsymbol{G}_{i-1}}^{21}{}'\right]\quad[\boldsymbol{K}_i^{12}]\right]_{2\times(n_1+2)}\ \begin{bmatrix}\boldsymbol{v}_1(x,z_1)\\ \\ \boldsymbol{v}_i(x,z_{i+1})\end{bmatrix}\tag{3.46}$$

$$=[\boldsymbol{W}_i]_{2\times(n_1+2)}\times\begin{bmatrix}\boldsymbol{v}_1(x,z_1)\\ \\ \boldsymbol{v}_i(x,z_{i+1})\end{bmatrix}$$

As for the vector $\boldsymbol{v}_{i-1}(x,z_i)$, it can be expressed in terms of $\boldsymbol{v}_1(x,z_1)$ and $\boldsymbol{v}_i(x,z_{i+1})$ as:

$$\boldsymbol{v}_{i-1}(x,z_i)=\begin{bmatrix}u_{x_{i-1}}(x,z_i)\\ \\ u_{z_{i-1}}(x,z_i)\\ \\ w_{z_{i-1}}(x,z_i)\end{bmatrix}=\begin{bmatrix}[\boldsymbol{W}_i]_{2\times(n_1+2)}\\ \\ [\boldsymbol{0}]_{1\times(n_1+2)}\end{bmatrix}\begin{bmatrix}\boldsymbol{v}_1(x,z_1)\\ \\ \boldsymbol{v}_i(x,z_{i+1})\end{bmatrix}.\tag{3.47}$$

Therefore, the matrix $[\boldsymbol{V}_i]$ will be:

$$[\boldsymbol{V}_i]_{5\times(n_1+2)}=\begin{bmatrix}[\boldsymbol{W}_i]_{2\times(n_1+2)}\\ \\ [\boldsymbol{0}]_{1\times(n_1+2)}\\ \\ [\boldsymbol{W}_i]_{2\times(n_1+2)}\end{bmatrix}.\tag{3.48}$$

3.4 Reflection and Transmission Coefficients

In this section, for a plane wave originating from the reference plane ($z=z_0$) with a frequency ω and an incidence angle θ_0 at the top of the multilayered structure whose total stiffness matrix is $\left[\boldsymbol{K}_{\boldsymbol{G}_N}\right]$, the reflection in the incidence medium and the transmission in the substrate will be calculated assuming a unity incidence.

It is to be noted that the term $e^{j(k_x x)}$ will be omitted intentionally in the following equations since it will be simplified in the calculations.

In the incidence medium (denoted by the subscript zero), n_0 partial plane waves propagate in the positive direction, and n_0 partial plane waves are reflected in the negative direction. Let $\boldsymbol{I}$ be a column vector of ones corresponding to the amplitudes of the incident partial plane waves, and $\boldsymbol{R}$ another column vector consisting of the amplitudes of the partial plane waves reflected back in the incidence medium at the interface z_1. For this medium, the local coordinate origin is selected at $z = z_1$ for waves traveling in both directions. Then, the displacement and stress components vector in this medium can be related to the incident and reflected partial plane waves amplitudes through the medium characteristic matrix $[\boldsymbol{B}_0]$ as follows:

$$\begin{bmatrix} \boldsymbol{v}_0(z) \\ \\ \boldsymbol{T}_0(z) \end{bmatrix} = [\boldsymbol{B}_0]_{2n_0 \times 2n_0} \, [\boldsymbol{E}_0(z)]_{2n_0 \times 2n_0} \begin{bmatrix} \boldsymbol{I} \\ \\ \boldsymbol{R} \end{bmatrix}, \tag{3.49}$$

where $[\boldsymbol{E}_0(z)]$ is a diagonal $2n_0 \times 2n_0$ matrix such that:

$$diag\,\{[\boldsymbol{E}_0(z)]\} = e^{jk_{z_0}^m (z - z_1)}. \tag{3.50}$$

If the characteristic matrix decomposition defined in Eq. (2.48) with $i = 0$ is used, expressing Eq. (3.49) at $z = z_1$ yields:

$$\begin{cases} \boldsymbol{v}_0(z_1) = [\boldsymbol{B}_0^{11}] + [\boldsymbol{B}_0^{12}]\boldsymbol{R} \\ \boldsymbol{T}_0(z_1) = [\boldsymbol{B}_0^{21}] + [\boldsymbol{B}_0^{22}]\boldsymbol{R} \end{cases}. \tag{3.51}$$

In the transmission medium (denoted by subscript $N + 1$), the partial plane waves propagate only in the positive direction and their amplitudes will be grouped in a vector $\boldsymbol{T_r}$ of length n_{N+1}. Then, the displacement and stress components vectors in this medium can be related to the transmitted partial plane waves amplitudes through the medium characteristic matrix $[\boldsymbol{B}_{N+1}]$. For this medium, the characteristic matrix will include only the coefficients corresponding to the waves propagating in the positive direction, i.e. $[\boldsymbol{B}_{N+1}]$ is only composed of the submatrices $[\boldsymbol{B}_{N+1}^{11}]$ and $[\boldsymbol{B}_{N+1}^{21}]$ that have been defined in Section 2.2. Consequently, by selecting the origin of the local coordinate system in this medium at $z =$

z_{N+1} for the propagating waves, the displacement-stress vector can be related to $\boldsymbol{T_r}$ as follows:

$$\begin{bmatrix} \boldsymbol{v}_{N+1}(z) \\ \boldsymbol{T}_{N+1}(z) \end{bmatrix} = \begin{bmatrix} [\boldsymbol{B}_{N+1}^{11}]_{n_{N+1}\times n_{N+1}} \\ [\boldsymbol{B}_{N+1}^{21}]_{n_{N+1}\times n_{N+1}} \end{bmatrix} [\boldsymbol{E}_{N+1}(z)]_{n_{N+1}\times n_{N+1}} \boldsymbol{T_r}, \tag{3.52}$$

where $[\boldsymbol{E}_{N+1}(z)]$ is a diagonal $n_{N+1} \times n_{N+1}$ matrix such that:

$$diag\ \{[\boldsymbol{E}_{N+1}(z)]\} = \left[e^{jk_{z_{N+1}}^{m+}(z-z_{N+1})}\right]. \tag{3.53}$$

Expressing Eq. (3.52) at $z = z_{N+1}$ yields:

$$\begin{cases} \boldsymbol{v}_{N+1}(z_{N+1}) = [\boldsymbol{B}_{N+1}^{11}]\, \boldsymbol{T_r} \\ \boldsymbol{T}_{N+1}(z_{N+1}) = [\boldsymbol{B}_{N+1}^{21}]\, \boldsymbol{T_r} \end{cases}. \tag{3.54}$$

Moreover, the multilayer total stiffness matrix relationship in Eq. (3.5) can be re-expressed using the total compliance matrix, $[\boldsymbol{S}_{\boldsymbol{G}_N}]$, as:

$$\begin{bmatrix} \boldsymbol{v}_1(z_1) \\ \boldsymbol{v}_N(z_{N+1}) \end{bmatrix} = [\boldsymbol{S}_{\boldsymbol{G}_N}] \begin{bmatrix} \boldsymbol{T}_1(z_1) \\ \boldsymbol{T}_N(z_{N+1}) \end{bmatrix}. \tag{3.55}$$

The multilayer global compliance matrix is related to the global stiffness matrix through:

$$[\boldsymbol{S}_{\boldsymbol{G}_N}] = [\boldsymbol{K}_{\boldsymbol{G}_N}]^{-1}. \tag{3.56}$$

The displacement and stress components vectors in the incidence medium and the layer 1 of the structure around the interface z_1 (i.e. $\boldsymbol{v}_0(z_1)$, $\boldsymbol{v}_1(z_1)$, $\boldsymbol{T}_0(z_1)$, and $\boldsymbol{T}_1(z_1)$) can be related through the boundary conditions at that interface.

Similarly, the displacement and stress components vectors in the layer N of the structure and the transmission medium around the interface z_{N+1} (i.e. $\boldsymbol{v}_N(z_{N+1})$, $\boldsymbol{v}_{N+1}(z_{N+1})$, $\boldsymbol{T}_N(z_{N+1})$, and $\boldsymbol{T}_{N+1}(z_{N+1})$) can be related through the boundary conditions at that interface.

Consequently, the system of equations in Eqs. (3.51), (3.54), and (3.55) can be solved and the reflection and transmission coefficients are thus obtained.

At this stage, fluid incidence and transmission media will be considered. Hence, Eqs. (3.51) and (3.54) can be reduced to:

$$\begin{cases} u_{z_0}(z_1) = B_0^{11} + RB_0^{12} \\ -P_{f_0}(z_1) = B_0^{21} + RB_0^{22} \end{cases},$$
$$\begin{cases} u_{z_{N+1}}(z_{N+1}) = T_r B_{N+1}^{11} \\ -P_{f_{N+1}}(z_{N+1}) = T_r B_{N+1}^{21} \end{cases}. \tag{3.57}$$

Since the calculation of the reflection and transmission coefficients depends on the boundary conditions at the interfaces z_1 and z_{N+1}, these coefficients depend on the natures of the layers around these interfaces. Having considered the incidence and transmission media both fluids, then, for the three possible layer natures for each of the first and last layers of the multilayer, nine different cases will be developed for the computation of the reflection-transmission coefficients. The boundary conditions at the interfaces z_1 and z_{N+1} are summarized in Table 3-1.

Table 3-1: Boundary Conditions at the Upper Surface of the Multilayer ($z = z_1$) for a Fluid Incidence Medium.

Layer 1 Fluid	$\begin{cases} u_{z_1}(z_1) = u_{z_0}(z_1) \\ P_{f_1}(z_1) = P_{f_0}(z_1) \end{cases}$	(3.58)
Layer 1 Isotropic Elastic Solid	$\begin{cases} u_{z_1}(z_1) = u_{z_0}(z_1) \\ \sigma_{xz_1}(z_1) = 0 \\ \sigma_{zz_1}(z_1) = -P_{f_0}(z_1) \end{cases}$	(3.59)
Layer 1 Isotropic Poroelastic Medium	$\begin{cases} u_{z_1}(z_1) + w_{z_1}(z_1) = u_{z_0}(z_1) \\ \sigma_{xz_1}(z_1) = 0 \\ \sigma_{zz_1}(z_1) = -P_{f_0}(z_1) \\ P_{f_1}(z_1) = P_{f_0}(z_1) \end{cases}$	(3.60)

Table 3-2: Boundary Conditions at the Lower Surface of the Multilayer ($z = z_{N+1}$) for a Fluid Transmission Medium.

Layer N Fluid	$\begin{cases} u_{z_N}(z_{N+1}) = u_{z_{N+1}}(z_{N+1}) \\ P_{f_N}(z_{N+1}) = P_{f_{N+1}}(z_{N+1}) \end{cases}$	(3.61)
Layer N Isotropic Elastic Solid	$\begin{cases} u_{z_N}(z_{N+1}) = u_{z_{N+1}}(z_{N+1}) \\ \sigma_{xz_N}(z_{N+1}) = 0 \\ \sigma_{zz_N}(z_{N+1}) = -P_{f_{N+1}}(z_{N+1}) \end{cases}$	(3.62)
Layer N Isotropic Poroelastic Medium	$\begin{cases} u_{z_N}(z_{N+1}) + w_{z_N}(z_{N+1}) = u_{z_{N+1}}(z_{N+1}) \\ \sigma_{xz_N}(z_{N+1}) = 0 \\ \sigma_{zz_N}(z_{N+1}) = -P_{f_{N+1}}(z_{N+1}) \\ P_{f_N}(z_{N+1}) = P_{f_{N+1}}(z_{N+1}) \end{cases}$	(3.63)

3.4.1 Layer 1 Fluid – Layer *N* Fluid

Given a multilayer whose first ($i = 1$) and last ($i = N$) layers are fluids, the compliance matrix relationship in Eq. (3.55) can be expressed as:

$$\begin{bmatrix} u_{z_1}(z_1) \\ u_{z_N}(z_{N+1}) \end{bmatrix} = \left[\boldsymbol{S}_{\boldsymbol{G}_N}\right]_{2\times 2} \begin{bmatrix} -P_{f_1}(z_1) \\ -P_{f_N}(z_{N+1}) \end{bmatrix}. \tag{3.64}$$

By applying the boundary conditions in Eqs. (3.58) and (3.61) into Eq. (3.57) and substituting the resulting displacement and stress expressions into Eq. (3.64), the following system of equations is obtained:

$$\begin{cases} B_0^{11} + RB_0^{12} = S_{G_{N,1;1}}(B_0^{21} + RB_0^{22}) + S_{G_{N,1;2}} T_r B_{N+1}^{21} \\ T_r B_{N+1}^{11} = S_{G_{N,2;1}}(B_0^{21} + RB_0^{22}) + S_{G_{N,2;2}} T_r B_{N+1}^{21} \end{cases} \tag{3.65}$$

where $S_{G_{N,x;y}}$ corresponds to the element in the x^{th} row and y^{th} column of the matrix $\left[\boldsymbol{S}_{\boldsymbol{G}_N}\right]$.

Solving for the reflection and transmission coefficients leads to:

$$\begin{bmatrix} R \\ T_r \end{bmatrix} = \begin{bmatrix} B_0^{12} - S_{G_{N,1;1}} B_0^{22} & -S_{G_{N,1;2}} B_{N+1}^{21} \\ -S_{G_{N,2;1}} B_0^{22} & B_{N+1}^{11} - S_{G_{N,2;2}} B_{N+1}^{21} \end{bmatrix}^{-1} \begin{bmatrix} S_{G_{N,1;1}} B_0^{21} - B_0^{11} \\ S_{G_{N,2;1}} B_0^{21} \end{bmatrix}. \quad (3.66)$$

3.4.2 Layer 1 Fluid – Layer *N* Isotropic Elastic Solid

Given a multilayer whose first layer is a fluid and last layer is an isotropic elastic solid, the compliance matrix relationship in Eq. (3.55) can be expressed as:

$$\begin{bmatrix} u_{z_1}(z_1) \\ u_{x_N}(z_{N+1}) \\ u_{z_N}(z_{N+1}) \end{bmatrix} = \left[\boldsymbol{S}_{\boldsymbol{G}_N}\right]_{3\times 3} \begin{bmatrix} -P_{f_1}(z_1) \\ \sigma_{xz_N}(z_{N+1}) \\ \sigma_{zz_N}(z_{N+1}) \end{bmatrix}. \quad (3.67)$$

By applying the boundary conditions in Eqs. (3.58) and (3.62) into Eq. (3.57) and substituting the resulting displacement and stress expressions into Eq. (3.67), the following system of equations is obtained:

$$\begin{cases} B_0^{11} + RB_0^{12} = S_{G_{N,1;1}}(B_0^{21} + RB_0^{22}) + S_{G_{N,1;3}} T_r B_{N+1}^{21} \\ T_r B_{N+1}^{11} = S_{G_{N,3;1}}(B_0^{21} + RB_0^{22}) + S_{G_{N,3;3}} T_r B_{N+1}^{21} \end{cases}. \quad (3.68)$$

Solving for the reflection and transmission coefficients leads to:

$$\begin{bmatrix} R \\ T_r \end{bmatrix} = \begin{bmatrix} B_0^{12} - S_{G_{N,1;1}} B_0^{22} & -S_{G_{N,1;3}} B_{N+1}^{21} \\ -S_{G_{N,3;1}} B_0^{22} & B_{N+1}^{11} - S_{G_{N,3;3}} B_{N+1}^{21} \end{bmatrix}^{-1} \begin{bmatrix} S_{G_{N,1;1}} B_0^{21} - B_0^{11} \\ S_{G_{N,3;1}} B_0^{21} \end{bmatrix}. \quad (3.69)$$

3.4.3 Layer 1 Fluid – Layer *N* Isotropic Poro-elastic Medium

Given a multilayer whose first layer is a fluid and last layer is an isotropic poro-elastic medium, the compliance matrix relationship in Eq. (3.55) can be expressed as:

$$\begin{bmatrix} u_{z_1}(z_1) \\ u_{x_N}(z_{N+1}) \\ u_{z_N}(z_{N+1}) \\ w_{z_N}(z_{N+1}) \end{bmatrix} = \left[\boldsymbol{S}_{\boldsymbol{G}_N}\right]_{4\times4} \begin{bmatrix} -P_{f_1}(z_1) \\ \sigma_{xz_N}(z_{N+1}) \\ \sigma_{zz_N}(z_{N+1}) \\ P_{f_N}(z_{N+1}) \end{bmatrix}. \tag{3.70}$$

By applying the boundary conditions in Eqs. (3.58) and (3.63) into Eq. (3.57) and substituting the resulting displacement and stress expressions into Eq. (3.70), the following system of equations is obtained:

$$\begin{cases} B_0^{11} + RB_0^{12} = S_{G_N,1;1}(B_0^{21} + RB_0^{22}) + \left(S_{G_N,1;3} - S_{G_N,1;4}\right) T_r B_{N+1}^{21} \\ T_r B_{N+1}^{11} = \left(S_{G_N,3;1} + S_{G_N,4;1}\right)(B_0^{21} + RB_0^{22}) \\ \qquad\qquad + \left(S_{G_N,3;3} - S_{G_N,3;4} + S_{G_N,3;3} - S_{G_N,3;4}\right) T_r B_{N+1}^{21} \end{cases}. \tag{3.71}$$

Solving for the reflection and transmission coefficients leads to:

$$\begin{bmatrix} R \\ T_r \end{bmatrix}$$

$$= \begin{bmatrix} B_0^{12} - S_{G_N,1;1}B_0^{22} & -\left(S_{G_N,1;3} - S_{G_N,1;4}\right)B_{N+1}^{21} \\ -\left(S_{G_N,3;1} + S_{G_N,4;1}\right)B_0^{22} & B_{N+1}^{11} - \left(S_{G_N,3;3} - S_{G_N,3;4} + S_{G_N,3;3} - S_{G_N,3;4}\right)B_{N+1}^{21} \end{bmatrix}^{-1} \tag{3.72}$$

$$\begin{bmatrix} S_{G_N,1;1}B_0^{21} - B_0^{11} \\ \left(S_{G_N,3;1} + S_{G_N,4;1}\right)B_0^{21} \end{bmatrix}.$$

3.4.4 Layer 1 Isotropic Elastic Solid – Layer *N* Fluid

Given a multilayer having whose first layer is an isotropic elastic solid and last layer is a fluid, the compliance matrix relationship in Eq. (3.55) can be expressed as:

$$\begin{bmatrix} u_{x_1}(z_1) \\ u_{z_1}(z_1) \\ u_{z_N}(z_{N+1}) \end{bmatrix} = \left[\boldsymbol{S}_{\boldsymbol{G}_N}\right]_{3\times 3} \begin{bmatrix} \sigma_{xz_1}(z_1) \\ \sigma_{zz_1}(z_1) \\ -P_{f_N}(z_{N+1}) \end{bmatrix}. \tag{3.73}$$

By applying the boundary conditions in Eqs. (3.59) and (3.61) into Eq. (3.57) and substituting the resulting displacement and stress expressions into Eq. (3.73), the following system of equations is obtained:

$$\begin{cases} B_0^{11} + RB_0^{12} = S_{G_N,2;2}(B_0^{21} + RB_0^{22}) + S_{G_N,2;3}T_r B_{N+1}^{21} \\ T_r B_{N+1}^{11} = S_{G_N,3;2}(B_0^{21} + RB_0^{22}) + S_{G_N,3;3}T_r B_{N+1}^{21} \end{cases}. \tag{3.74}$$

Solving for the reflection and transmission coefficients leads to:

$$\begin{bmatrix} R \\ T_r \end{bmatrix} = \begin{bmatrix} B_0^{12} - S_{G_N,2;2}B_0^{22} & -S_{G_N,2;3}B_{N+1}^{21} \\ -S_{G_N,3;2}B_0^{22} & B_{N+1}^{11} - S_{G_N,3;3}B_{N+1}^{21} \end{bmatrix}^{-1} \begin{bmatrix} S_{G_N,2;2}B_0^{21} - B_0^{11} \\ S_{G_N,3;2}B_0^{21} \end{bmatrix}. \tag{3.75}$$

3.4.5 Layer 1 Isotropic Elastic Solid – Layer *N* Isotropic Elastic Solid

Given a multilayer whose first and last layers are isotropic elastic solids, the compliance matrix relationship in Eq. (3.55) can be expressed as:

$$\begin{bmatrix} u_{x_1}(z_1) \\ u_{z_1}(z_1) \\ u_{x_N}(z_{N+1}) \\ u_{z_N}(z_{N+1}) \end{bmatrix} = \left[\boldsymbol{S}_{\boldsymbol{G}_N}\right]_{4\times 4} \begin{bmatrix} \sigma_{xz_1}(z_1) \\ \sigma_{zz_1}(z_1) \\ \sigma_{xz_N}(z_{N+1}) \\ \sigma_{zz_N}(z_{N+1}) \end{bmatrix}. \tag{3.76}$$

By applying the boundary conditions in Eqs. (3.59) and (3.62) into Eq. (3.57) and substituting the resulting displacement and stress expressions into Eq. (3.76), the following system of equations is obtained:

$$\begin{cases} B_0^{11} + RB_0^{12} = S_{G_{N,2;2}}(B_0^{21} + RB_0^{22}) + S_{G_{N,2;4}} T_r B_{N+1}^{21} \\ T_r B_{N+1}^{11} = S_{G_{N,4;2}}(B_0^{21} + RB_0^{22}) + S_{G_{N,4;4}} T_r B_{N+1}^{21} \end{cases}. \tag{3.77}$$

Solving for the reflection and transmission coefficients leads to:

$$\begin{bmatrix} R \\ T_r \end{bmatrix} = \begin{bmatrix} B_0^{12} - S_{G_{N,2;2}} B_0^{22} & -S_{G_{N,2;4}} B_{N+1}^{21} \\ -S_{G_{N,4;2}} B_0^{22} & B_{N+1}^{11} - S_{G_{N,4;4}} B_{N+1}^{21} \end{bmatrix}^{-1} \begin{bmatrix} S_{G_{N,2;2}} B_0^{21} - B_0^{11} \\ S_{G_{N,4;2}} B_0^{21} \end{bmatrix}. \tag{3.78}$$

3.4.6 Layer 1 Isotropic Elastic Solid – Layer *N* Isotropic Poro-elastic Medium

Given a multilayer whose first layer is an isotropic elastic solid and last layer is an isotropic poro-elastic medium, the compliance matrix relationship in Eq. (3.55) can be expressed as:

$$\begin{bmatrix} u_{x_1}(z_1) \\ u_{z_1}(z_1) \\ u_{x_N}(z_{N+1}) \\ u_{z_N}(z_{N+1}) \\ w_{z_N}(z_{N+1}) \end{bmatrix} = \left[\boldsymbol{S}_{\boldsymbol{G}_N}\right]_{5\times 5} \begin{bmatrix} \sigma_{xz_1}(z_1) \\ \sigma_{zz_1}(z_1) \\ \sigma_{xz_N}(z_{N+1}) \\ \sigma_{zz_N}(z_{N+1}) \\ P_{f_N}(z_{N+1}) \end{bmatrix}. \tag{3.79}$$

By applying the boundary conditions in Eqs. (3.59) and (3.63) into Eq. (3.57) and substituting the resulting displacement and stress expressions into Eq. (3.79), the following system of equations is obtained:

$$\begin{cases} B_0^{11} + RB_0^{12} = S_{G_{N,2;2}}(B_0^{21} + RB_0^{22}) + \left(S_{G_{N,2;4}} - S_{G_{N,2;5}}\right) T_r B_{N+1}^{21} \\ T_r B_{N+1}^{11} = \left(S_{G_{N,4;2}} + S_{G_{N,5;2}}\right)(B_0^{21} + RB_0^{22}) \\ \qquad\qquad + \left(S_{G_{N,4;4}} - S_{G_{N,4;5}} + S_{G_{N,5;4}} - S_{G_{N,5;5}}\right) T_r B_{N+1}^{21} \end{cases}. \tag{3.80}$$

Solving for the reflection and transmission coefficients leads to:

$$\begin{bmatrix} R \\ T_r \end{bmatrix}$$

$$= \begin{bmatrix} B_0^{12} - S_{G_{N,2;2}} B_0^{22} & -\left(S_{G_{N,2;4}} - S_{G_{N,2;5}}\right) B_{N+1}^{21} \\ -\left(S_{G_{N,4;2}} + S_{G_{N,5;2}}\right) B_0^{22} & B_{N+1}^{11} - \left(S_{G_{N,4;4}} - S_{G_{N,4;5}} + S_{G_{N,5;4}} - S_{G_{N,5;5}}\right) B_{N+1}^{21} \end{bmatrix}^{-1} \begin{bmatrix} S_{G_{N,2;2}} B_0^{21} - B_0^{11} \\ \left(S_{G_{N,4;2}} + S_{G_{N,5;2}}\right) B_0^{21} \end{bmatrix}. \quad (3.81)$$

3.4.7 Layer 1 Isotropic Poro-elastic Medium – Layer *N* Fluid

Given a multilayer whose first layer is an isotropic poro-elastic medium and last layer is a fluid, the compliance matrix relationship in Eq. (3.55) can be expressed as:

$$\begin{bmatrix} u_{x_1}(z_1) \\ u_{z_1}(z_1) \\ w_{z_1}(z_1) \\ u_{z_N}(z_{N+1}) \end{bmatrix} = \left[\boldsymbol{S_{G_N}}\right]_{4\times 4} \begin{bmatrix} \sigma_{xz_1}(z_1) \\ \sigma_{zz_1}(z_1) \\ P_{f_1}(z_1) \\ P_{f_N}(z_{N+1}) \end{bmatrix}. \quad (3.82)$$

By applying the boundary conditions in Eqs. (3.60) and (3.61) into Eq. (3.57) and substituting the resulting displacement and stress expressions into Eq. (3.82), the following system of equations is obtained:

$$\begin{cases} B_0^{11} + RB_0^{12} = \left(S_{G_{N,2;2}} - S_{G_{N,2;3}} + S_{G_{N,3;2}} - S_{G_{N,3;3}}\right)\left(B_0^{21} + RB_0^{22}\right) \\ \qquad\qquad + \left(S_{G_{N,2;4}} + S_{G_{N,3;4}}\right) T_r B_{N+1}^{21} \\ T_r B_{N+1}^{11} = \left(S_{G_{N,4;2}} - S_{G_{N,4;3}}\right)\left(B_0^{21} + RB_0^{22}\right) + S_{G_{N,4;4}} T_r B_{N+1}^{21} \end{cases}. \quad (3.83)$$

Solving for the reflection and transmission coefficients leads to:

$$\begin{bmatrix} R \\ T_r \end{bmatrix}$$

$$= \begin{bmatrix} B_0^{12} - \left(S_{G_{N,2;2}} - S_{G_{N,2;3}} + S_{G_{N,3;2}} - S_{G_{N,3;3}}\right)B_0^{22} & -\left(S_{G_{N,2;4}} + S_{G_{N,3;4}}\right)B_{N+1}^{21} \\ -\left(S_{G_{N,4;2}} - S_{G_{N,4;3}}\right)B_0^{22} & B_{N+1}^{11} - S_{G_{N,4;4}}B_{N+1}^{21} \end{bmatrix}^{-1} \tag{3.84}$$

$$\begin{bmatrix} \left(S_{G_{N,2;2}} - S_{G_{N,2;3}} + S_{G_{N,3;2}} - S_{G_{N,3;3}}\right)B_0^{21} - B_0^{11} \\ \left(S_{G_{N,4;2}} - S_{G_{N,4;3}}\right)B_0^{21} \end{bmatrix}.$$

3.4.8 Layer 1 Isotropic Poro-elastic Medium – Layer *N* Isotropic Elastic Solid

Given a multilayer whose first layer is an isotropic poro-elastic medium and last layer is an isotropic elastic solid, the compliance matrix relationship in Eq. (3.55) can be expressed as:

$$\begin{bmatrix} u_{x_1}(z_1) \\ u_{z_1}(z_1) \\ w_{z_1}(z_1) \\ u_{x_N}(z_{N+1}) \\ u_{z_N}(z_{N+1}) \end{bmatrix} = \left[\boldsymbol{S}_{\boldsymbol{G}_N}\right]_{5\times5} \begin{bmatrix} \sigma_{xz_1}(z_1) \\ \sigma_{zz_1}(z_1) \\ P_{f_1}(z_1) \\ \sigma_{xz_N}(z_{N+1}) \\ \sigma_{zz_N}(z_{N+1}) \end{bmatrix}. \tag{3.85}$$

By applying the boundary conditions in Eqs. (3.60) and (3.62) into Eq. (3.57) and substituting the resulting displacement and stress expressions into Eq. (3.85), the following system of equations is obtained:

$$\begin{cases} B_0^{11} + RB_0^{12} = \left(S_{G_{N,2;2}} - S_{G_{N,2;3}} + S_{G_{N,3;2}} - S_{G_{N,3;3}}\right)(B_0^{21} + RB_0^{22}) \\ \qquad\qquad + \left(S_{G_{N,2;5}} + S_{G_{N,3;5}}\right)T_r B_{N+1}^{21} \\ T_r B_{N+1}^{11} = \left(S_{G_{N,5;2}} - S_{G_{N,5;3}}\right)(B_0^{21} + RB_0^{22}) + S_{G_{N,5;5}} T_r B_{N+1}^{21} \end{cases}. \tag{3.86}$$

Solving for the reflection and transmission coefficients leads to:

$$\begin{bmatrix} R \\ T_r \end{bmatrix}$$

$$= \begin{bmatrix} B_0^{12} - \left(S_{G_N,2;2} - S_{G_N,2;3} + S_{G_N,3;2} - S_{G_N,3;3}\right)B_0^{22} & -\left(S_{G_N,2;5} + S_{G_N,3;5}\right)B_{N+1}^{21} \\ -\left(S_{G_N,5;2} - S_{G_N,5;3}\right)B_0^{22} & B_{N+1}^{11} - S_{G_N,5;5}B_{N+1}^{21} \end{bmatrix}^{-1} \tag{3.87}$$

$$\begin{bmatrix} \left(S_{G_N,2;2} - S_{G_N,2;3} + S_{G_N,3;2} - S_{G_N,3;3}\right)B_0^{21} - B_0^{11} \\ \left(S_{G_N,5;2} - S_{G_N,5;3}\right)B_0^{21} \end{bmatrix}.$$

3.4.9 Layer 1 Isotropic Poro-elastic Medium – Layer *N* Isotropic Poro-elastic Medium

Given a multilayer whose first and last layers are isotropic poro-elastic media, the compliance matrix relationship in Eq. (3.55) can be expressed as:

$$\begin{bmatrix} u_{x_1}(z_1) \\ u_{z_1}(z_1) \\ w_{z_1}(z_1) \\ u_{x_N}(z_{N+1}) \\ u_{z_N}(z_{N+1}) \\ w_{z_N}(z_{N+1}) \end{bmatrix} = \left[\boldsymbol{S}_{\boldsymbol{G}_N}\right]_{6\times 6} \begin{bmatrix} \sigma_{xz_1}(z_1) \\ \sigma_{zz_1}(z_1) \\ P_{f_1}(z_1) \\ \sigma_{xz_N}(z_{N+1}) \\ \sigma_{zz_N}(z_{N+1}) \\ P_{f_N}(z_{N+1}) \end{bmatrix}. \tag{3.88}$$

By applying the boundary conditions in Eqs. (3.60) and (3.63) into Eq. (3.57) and substituting the resulting displacement and stress expressions into Eq. (3.88), the following system of equations is obtained:

$$\begin{cases} B_0^{11} + RB_0^{12} = \left(S_{G_{N,2;2}} - S_{G_{N,2;3}} + S_{G_{N,3;2}} - S_{G_{N,3;3}}\right)(B_0^{21} + RB_0^{22}) \\ \qquad\qquad + \left(S_{G_{N,2;5}} - S_{G_{N,2;6}} + S_{G_{N,3;5}} - S_{G_{N,3;6}}\right) T_r B_{N+1}^{21} \\ T_r B_{N+1}^{11} = \left(S_{G_{N,5;2}} - S_{G_{N,5;3}} + S_{G_{N,6;2}} - S_{G_{N,6;3}}\right)(B_0^{21} + RB_0^{22}) \\ \qquad\qquad + \left(S_{G_{N,5;5}} - S_{G_{N,5;6}} + S_{G_{N,6;5}} - S_{G_{N,6;6}}\right) T_r B_{N+1}^{21} \end{cases} . \tag{3.89}$$

Solving for the reflection and transmission coefficients leads to:

$$\begin{bmatrix} R \\ T_r \end{bmatrix}$$

$$= \begin{bmatrix} B_0^{12} - \left(S_{G_{N,2;2}} - S_{G_{N,2;3}} + S_{G_{N,3;2}} - S_{G_{N,3;3}}\right) B_0^{22} & -\left(S_{G_{N,2;5}} - S_{G_{N,2;6}} + S_{G_{N,3;5}} - S_{G_{N,3;6}}\right) B_{N+1}^{21} \\ -\left(S_{G_{N,5;2}} - S_{G_{N,5;3}} + S_{G_{N,6;2}} - S_{G_{N,6;3}}\right) B_0^{22} & B_{N+1}^{11} - \left(S_{G_{N,5;5}} - S_{G_{N,5;6}} + S_{G_{N,6;5}} - S_{G_{N,6;6}}\right) B_{N+1}^{21} \end{bmatrix}^{-1} \tag{3.90}$$

$$\begin{bmatrix} \left(S_{G_{N,2;2}} - S_{G_{N,2;3}} + S_{G_{N,3;2}} - S_{G_{N,3;3}}\right) B_0^{21} - B_0^{11} \\ \left(S_{G_{N,5;2}} - S_{G_{N,5;3}} + S_{G_{N,6;2}} - S_{G_{N,6;3}}\right) B_0^{21} \end{bmatrix}.$$

3.5 Wave Amplitudes Inside the Structure Layers

In this section, a back recursive algorithm is developed in order to determine the displacement amplitudes of the partial plane waves inside any layer i of the multilayered structure.

Having obtained the reflection coefficient $\boldsymbol{R}$ in Section 3.4, $\boldsymbol{T}_0(z_1)$ and $\boldsymbol{v}_0(z_1)$ in Eq. (3.51) can be evaluated. Then, $\boldsymbol{T}_1(z_1)$ and $\boldsymbol{v}_1(z_1)$ can be deduced according to the corresponding boundary conditions at the interface z_1. Similarly, having the transmission coefficient $\boldsymbol{T_r}$, $\boldsymbol{T}_{N+1}(z_{N+1})$ and $\boldsymbol{v}_{N+1}(z_{N+1})$ in Eq. (3.54) can be evaluated, then, $\boldsymbol{T}_N(z_{N+1})$ and $\boldsymbol{v}_N(z_{N+1})$ can be deduced using the boundary conditions at the interface z_{N+1}.

Let $\boldsymbol{Q}_i$ be a column vector such that:

$$\boldsymbol{Q}_i = \begin{bmatrix} \boldsymbol{v}_1(z_1) \\ \\ \boldsymbol{v}_i(z_{i+1}) \end{bmatrix}. \tag{3.91}$$

In the following, in the characteristic matrix relationship as expressed in Eq. (2.7), the exponential term $e^{j(k_x x-\omega t)}$ will not be shown. Hence, when it will be mentioned that the displacement amplitudes of the partial plane waves in a layer i are being evaluated, what is implicitly calculated is not just the vector $\boldsymbol{A}_i$, but indeed the product $\boldsymbol{A}_i\, e^{j(k_x x-\omega t)}$. However, the latter product will be referred to as $\boldsymbol{A}_i$ for simplicity. Therefore Eq. (2.7) will be regarded as:

$$\boldsymbol{U}_i(z) = \begin{bmatrix} \boldsymbol{v}_i(z) \\ \\ \boldsymbol{T}_i(z) \end{bmatrix} = [\boldsymbol{B}_i][\boldsymbol{E}_i(z)]\, \boldsymbol{A}_i, \quad \text{for } z_i \le z \le z_{i+1}. \tag{3.92}$$

3.5.1 Wave Amplitudes Inside Layer *N*

Starting with $i = N$, $\boldsymbol{Q}_N$ can be obtained using Eq. (3.55) having the multilayer total compliance matrix $[\boldsymbol{S}_{\boldsymbol{G}_N}]$, and the vectors $\boldsymbol{T}_1(z_1)$, and $\boldsymbol{T}_N(z_{N+1})$:

$$\boldsymbol{Q}_N = \begin{bmatrix} \boldsymbol{v}_1(z_1) \\ \\ \boldsymbol{v}_N(z_{N+1}) \end{bmatrix} = [\boldsymbol{S}_{\boldsymbol{G}_N}] \begin{bmatrix} \boldsymbol{T}_1(z_1) \\ \\ \boldsymbol{T}_N(z_{N+1}) \end{bmatrix}. \tag{3.93}$$

Then, using the characteristic matrix relationship as expressed in Eq. (3.92) for the layer N at $z = z_N$, the following can be written:

$$\boldsymbol{U}_N(z_N) = \begin{bmatrix} \boldsymbol{v}_N(z_N) \\ \\ \boldsymbol{T}_N(z_N) \end{bmatrix} = [\boldsymbol{B}_N][\boldsymbol{E}_N(z_N)]\, \boldsymbol{A}_N. \tag{3.94}$$

In order to get the displacement amplitudes of the partial plane waves in the layer N, (i.e. $\boldsymbol{A}_N$), the vectors $\boldsymbol{v}_N(z_N)$ and $\boldsymbol{T}_N(z_N)$ are needed.

With reference to Eq. (3.10), $\boldsymbol{v}_N(z_N)$ could be expressed in terms of $\boldsymbol{Q}_N$ using the matrix $[\boldsymbol{V}_N]$ as follows:

$$\boldsymbol{v}_N(z_N) = [[\boldsymbol{V}_N^{21}] \quad [\boldsymbol{V}_N^{22}]]\, \boldsymbol{Q}_N. \tag{3.95}$$

Then, using the stiffness matrix relationship of the layer N,

$$\begin{bmatrix} \boldsymbol{T}_N(z_N) \\ \boldsymbol{T}_N(z_{N+1}) \end{bmatrix} = [\boldsymbol{K}_N] \begin{bmatrix} \boldsymbol{v}_N(z_N) \\ \boldsymbol{v}_N(z_{N+1}) \end{bmatrix} = \begin{bmatrix} [\boldsymbol{K}_N^{11}] & [\boldsymbol{K}_N^{12}] \\ [\boldsymbol{K}_N^{21}] & [\boldsymbol{K}_N^{22}] \end{bmatrix} \begin{bmatrix} \boldsymbol{v}_N(z_N) \\ \boldsymbol{v}_N(z_{N+1}) \end{bmatrix}, \tag{3.96}$$

$\boldsymbol{T}_N(z_N)$ can be also expressed in terms of $\boldsymbol{Q}_N$ using Eqs. (3.95) and (3.96):

$$\begin{aligned} \boldsymbol{T}_N(z_N) &= [[\boldsymbol{K}_N^{11}] \quad [\boldsymbol{K}_N^{12}]] \begin{bmatrix} \boldsymbol{v}_N(z_N) \\ \boldsymbol{v}_N(z_{N+1}) \end{bmatrix} \\ &= [[\boldsymbol{K}_N^{11}][\boldsymbol{V}_N^{21}] \quad [\boldsymbol{K}_N^{11}][\boldsymbol{V}_N^{22}] + [\boldsymbol{K}_N^{12}]]\, \boldsymbol{Q}_N. \end{aligned} \tag{3.97}$$

Therefore, back to Eq. (3.94), the partial plane waves displacement amplitudes $\boldsymbol{A}_N$ in the layer N are found to be:

$$\begin{aligned} \boldsymbol{A}_N &= \{[\boldsymbol{B}_N][\boldsymbol{E}_N(z_N)]\}^{-1} \begin{bmatrix} \boldsymbol{v}_N(z_N) \\ \boldsymbol{T}_N(z_N) \end{bmatrix} \\ &= \{[\boldsymbol{B}_N][\boldsymbol{E}_N(z_N)]\}^{-1} \begin{bmatrix} [\boldsymbol{V}_N^{21}] & [\boldsymbol{V}_N^{22}] \\ [\boldsymbol{K}_N^{11}][\boldsymbol{V}_N^{21}] & [\boldsymbol{K}_N^{11}][\boldsymbol{V}_N^{22}] + [\boldsymbol{K}_N^{12}] \end{bmatrix} \boldsymbol{Q}_N. \end{aligned} \tag{3.98}$$

3.5.2 Wave Amplitudes Inside Layers $N-1$ to 2

At the layer $N-1$, the vector $\boldsymbol{Q}_{N-1}$ is:

$$\boldsymbol{Q}_{N-1} = \begin{bmatrix} \boldsymbol{v}_1(z_1) \\ \boldsymbol{v}_{N-1}(z_N) \end{bmatrix}. \tag{3.99}$$

With reference to Eq. (3.10), $\boldsymbol{v}_{N-1}(z_N)$ can be expressed in terms of $\boldsymbol{Q}_N$ using the matrix $[\boldsymbol{V}_N]$ as follows:

$$\boldsymbol{v}_{N-1}(z_N) = \left[[\boldsymbol{V}_N^{11}]_{n_{N-1} \times n_1} \quad [\boldsymbol{V}_N^{12}]_{n_{N-1} \times n_N}\right] \boldsymbol{Q}_N. \tag{3.100}$$

Therefore, $\boldsymbol{Q}_{N-1}$ can be deduced from $\boldsymbol{Q}_N$ using the relationship:

$$\boldsymbol{Q}_{N-1} = \begin{bmatrix} [\boldsymbol{I}]_{n_1 \times n_1} & [\boldsymbol{0}]_{n_1 \times n_N} \\ [\boldsymbol{V}_N^{11}]_{n_{N-1} \times n_1} & [\boldsymbol{V}_N^{12}]_{n_{N-1} \times n_N} \end{bmatrix} \boldsymbol{Q}_N, \tag{3.101}$$

where $[\boldsymbol{I}]$ is an identity matrix. Then, similarly to the process performed at the layer N, the displacement stress components vector in layer $N-1$ at $z = z_{N-1}$ can be expressed in terms of $\boldsymbol{Q}_{N-1}$, $[\boldsymbol{K}_{N-1}]$ and $[\boldsymbol{V}_{N-1}]$ as:

$$\boldsymbol{U}_{N-1} = \begin{bmatrix} \boldsymbol{v}_{N-1}(z_{N-1}) \\ \boldsymbol{T}_{N-1}(z_{N-1}) \end{bmatrix} = \begin{bmatrix} [\boldsymbol{V}_{N-1}^{21}] & [\boldsymbol{V}_{N-1}^{22}] \\ [\boldsymbol{K}_{N-1}^{11}][\boldsymbol{V}_{N-1}^{21}] & [\boldsymbol{K}_{N-1}^{11}][\boldsymbol{V}_{N-1}^{22}] + [\boldsymbol{K}_{N-1}^{12}] \end{bmatrix} \boldsymbol{Q}_{N-1}. \tag{3.102}$$

Thus, the displacement amplitudes of the partial plane waves of the layer $N-1$, $\boldsymbol{A}_{N-1}$, are:

$$\boldsymbol{A}_{N-1} = \{[\boldsymbol{B}_{N-1}][\boldsymbol{E}_{N-1}(z_{N-1})]\}^{-1} \begin{bmatrix} [\boldsymbol{V}_{N-1}^{21}] & [\boldsymbol{V}_{N-1}^{22}] \\ [\boldsymbol{K}_{N-1}^{11}][\boldsymbol{V}_{N-1}^{21}] & [\boldsymbol{K}_{N-1}^{11}][\boldsymbol{V}_{N-1}^{22}] + [\boldsymbol{K}_{N-1}^{12}] \end{bmatrix} \boldsymbol{Q}_{N-1}. \tag{3.103}$$

The displacement amplitudes of the partial plane waves of the other layers can be obtained by applying the same procedure recursively from the layer $N-2$ back to layer 2.

Hence, in general, for any layer i with $2 \leq i \leq N-1$, and having already determined the vector $\boldsymbol{Q}_{i+1}$ of the layer $i+1$, $\boldsymbol{Q}_i$ can be deduced recursively from the latter according to the following recursive relationship:

$$\boldsymbol{Q}_i = \begin{bmatrix} [\boldsymbol{I}]_{n_1 \times n_1} & [\boldsymbol{0}]_{n_1 \times n_{i+1}} \\ [\boldsymbol{V}_{i+1}^{11}] & [\boldsymbol{V}_{i+1}^{12}] \end{bmatrix} \boldsymbol{Q}_{i+1}, \quad 2 \leq i \leq N-1. \tag{3.104}$$

Then, having obtained $\boldsymbol{Q}_i$, the displacement amplitudes of the partial plane waves inside the layer i can be expressed as:

$$\boldsymbol{A}_i = \{[\boldsymbol{B}_i][\boldsymbol{E}_i(z_i)]\}^{-1} \begin{bmatrix} [\boldsymbol{V}_i^{21}] & [\boldsymbol{V}_i^{22}] \\ [\boldsymbol{K}_i^{11}][\boldsymbol{V}_i^{21}] & [\boldsymbol{K}_i^{11}][\boldsymbol{V}_i^{22}] + [\boldsymbol{K}_i^{12}] \end{bmatrix} \boldsymbol{Q}_i, \quad 2 \leq i \leq N-1. \tag{3.105}$$

3.5.3 Wave Amplitudes Inside Layer 1

With respect to the first layer $\boldsymbol{T}_0(z_1)$ and $\boldsymbol{v}_0(z_1)$ can be obtained by substituting the reflection coefficients $\boldsymbol{R}$ into Eq. (3.51). Consequently, $\boldsymbol{T}_1(z_1)$ and $\boldsymbol{v}_1(z_1)$ can be deduced using the corresponding boundary conditions at the interface z_1. Then, applying the characteristic matrix relationship as expressed in Eq. (3.94) for layer 1 at $z = z_1$, the displacement amplitudes of the partial plane waves inside the layer 1 are found to be:

$$\boldsymbol{A}_1 = \{[\boldsymbol{B}_1][\boldsymbol{E}_1(z_1)]\}^{-1} \begin{bmatrix} \boldsymbol{v}_1(z_1) \\ \\ \boldsymbol{T}_1(z_1) \end{bmatrix}. \tag{3.106}$$

3.6 Conclusion

The propagation of a plane wave into a multilayer whose layers could be of any of the three natures, fluid, isotropic solid, or isotropic poro-elastic materials, has been modeled based on the recursive stiffness matrix method. First, a total stiffness matrix has been constructed through a recursive algorithm that combines all the structure layers into one single layer based on their physical parameters and the boundary conditions at the interface separating every two adjacent layers. Having obtained the multilayer total stiffness matrix, the reflection coefficient in the incidence medium and the transmission coefficient in the substrate can be obtained. Their calculations have been presented in details for the case of fluid incidence and transmission media. Then, a back recursive algorithm has been implemented to determine the displacement amplitudes of the partial plane waves propagating inside each layer.

CHAPTER 4

WAVE BEAM PROPAGATION THROUGH LAYERED MEDIA USING THE ANGULAR SPECTRUM METHOD

4.1 Introduction

In the previous chapter, the propagation of a plane wave incident on a multilayered medium bounded by fluid media has been developed. After calculating the reflection and transmission coefficients of the plane wave in terms of the incidence angle and frequency, the displacement amplitudes of the partial plane waves inside each layer of the multilayered structure has been determined.

However, in real situations, an incident wave generated by an acoustic source is usually not a plane wave, but rather a bounded beam. In this case, an efficient solution to study the reflection-transmission of an acoustic beam and its propagation in the multilayered medium is by the implementation of the angular spectrum technique that is based on the superposition of plane waves.

4.2 Modeling of the Wave Beam Propagation

In this section, the propagation inside a multilayer of a wave field created by a planar acoustic source will be modeled based on the angular spectrum approach [68, 69, 70, 71, 72]. In this method, in order to model the propagation of a monochromatic wave field from a

plane surface to another parallel plane at a distance z, this wave field is first decomposed by the discrete Fourier transform into an equivalent spectrum of plane waves. Then, to account for the wave propagation, each component of the spectrum is multiplied by a suitable phase factor depending on the distance z and the medium characteristics. An inverse Fourier transform is applied to the resulting propagated spectrum in order to reconstruct the wave field at the plane z. The method will be applied in order to obtain the incident wave field generated by the acoustic source, the corresponding reflected and transmitted wave fields, as well as the displacement and stress components distributions inside the layers of the structure.

4.2.1 Incident Wave Field

Consider a planar monochromatic acoustic source located at the reference plane ($z = z_0 = 0$) and generating a pressure wave field with a frequency ω in a fluid medium. The coordinate system is chosen so that the incident plane coincides with the (x, z) plane and the wave is propagating in the $+z$ direction. Let $p_0(x, z_0)$ represent the pressure field distribution of the source wave at the z_0 plane. The objective is to find the resulting incident field distribution (for the waves propagating in the $+z$ direction) at any parallel plane in the incidence medium, i.e. at any plane z such that $z_0 \leq z \leq z_1$. Thus, first, the discrete Fourier transform is applied to the source pressure wave field $p_0(x, z_0)$, and the transform is denoted by $P_0(k_x, z_0)$:

$$P_0(k_x, z_0) = \mathcal{F}\big(p_0(x, z_0)\big) = \int_{-\infty}^{+\infty} p_0(x, z_0)\, e^{-jk_x x}\, dx. \tag{4.1}$$

where k_x is the x component of the incident plane wave vector $\boldsymbol{k}_0$. The Fourier transform decomposes the source pressure wave field into a spectrum in which the magnitude and phase at every k_x represent the magnitude and phase of a plane wave traveling at a given directional angle θ_0, k_x and θ_0 being related with reference to Eqs. (2.3) and (2.8) by:

$$k_x = \frac{\omega}{c_0} \sin\theta_0, \tag{4.2}$$

where c_0 is the wave speed in the incidence medium.

The propagation of the plane wave spectrum can be modeled by multiplying each component by a phase propagation factor to account for the plane wave propagation in its corresponding direction. For the case of a propagation in the $+z$ direction, this factor is expressed as:

$$G(k_x, z - z_0) = e^{j\sqrt{k_0^2 - k_x^2}\,(z - z_0)} = e^{jk_{z_0}(z - z_0)}, \tag{4.3}$$

where $k_{z_0} = \sqrt{k_0^2 - k_x^2}$ is the z component of the incident plane wave vector $\boldsymbol{k}_0$.

Hence, if the angular spectrum of the field at z_0 for every k_x is multiplied by its corresponding phase factor, the resultant wave spectrum in the incidence medium at any plane z, denoted by $P_I(k_x, z)$, will be:

$$P_I(k_x, z) = P_0(k_x, z_0) e^{jk_{z_0}(z - z_0)}, \qquad z_0 \le z \le z_1. \tag{4.4}$$

Then, the incident pressure wave field $p_I(x, z)$ at the plane z can be reconstructed by applying the inverse Fourier transform of the angular spectrum $P_I(k_x, z)$:

$$p_I(x, z) = \mathcal{F}^{-1}\big(P_I(k_x, z)\big) = \frac{1}{2\pi} \int_{-\infty}^{+\infty} P_I(k_x, z)\, e^{jk_x x}\, dk_x, \qquad z_0 \le z \le z_1. \tag{4.5}$$

The steps for obtaining the incident pressure wave field distribution in the incidence medium, $p_I(x, z)$, knowing the pressure field distribution of the source wave at z_0, $p_I(x, z)$, are summarized in the diagram of Figure 4-1, where FT denotes the Fourier transform, and IFT its inverse.

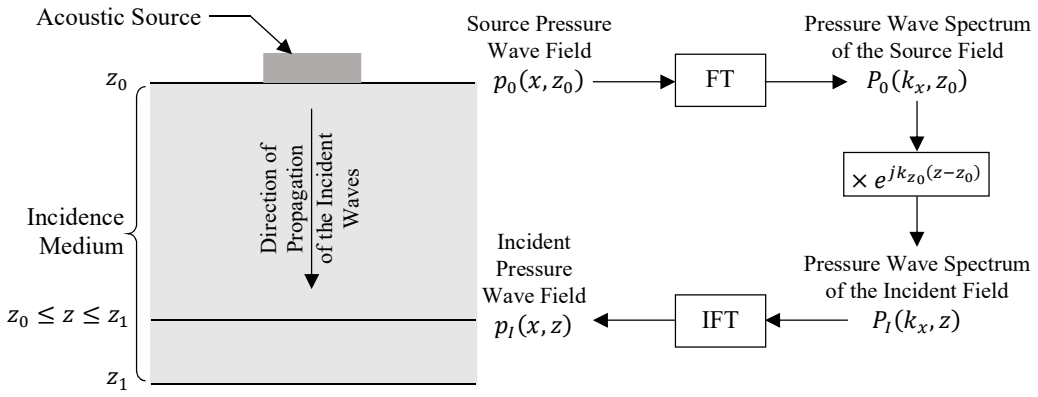

Figure 4-1: Diagram of the steps followed for obtaining the incident pressure wave field in the incidence medium ($\mathbf{z_0 \leq z \leq z_1}$).

4.2.2 Reflected and Transmitted Wave Fields

In Section 3.4, the reflection and transmission coefficients have been obtained for a plane wave originating from the reference plane ($z = z_0$) with a frequency ω and incident with an incidence angle θ_0 at the top of a multilayered structure. Thus, the obtained expressions for these coefficients are functions of the incidence, layered, and transmission media physical parameters, as well as the incident plane wave frequency and incidence angle. This means that one can find the reflection and transmission coefficients for an incident plane wave traveling in any direction angle θ_0 or correspondingly having any wavenumber k_x, θ_0 and k_x being related by the expression in Eq. (4.1). Hence the expressions found for these coefficients are nothing but angular spectra. The reflection coefficient angular spectrum at the plane z_1 will be denoted by $R(\theta_0, z_1)$ or equivalently $R(k_x, z_1)$, and the angular spectrum of the transmission coefficient at the plane z_{N+1} by $T_r(\theta_0, z_{N+1})$ or equivalently $T_r(k_x, z_{N+1})$.

The main goal is to determine the reflected pressure wave field in the incidence medium, $p_R(x, z)$, and the transmitted pressure wave field in the transmission medium, $p_{T_r}(x, z)$, due to the incident pressure wave field at the top of the multilayer (i.e. at the plane z_1), $p_I(x, z_1)$. The latter can be decomposed into a spectrum of plane waves $P_I(k_x, z_1)$. Then,

to each component of this spectrum (i.e. at every k_x), or equivalently to every plane wave of the spectrum incident with the directional angle θ_0, one can associate the appropriate reflection and transmission coefficients expressed at the same angle θ_0 (or equivalently same value of k_x).

Therefore, the corresponding reflected pressure wave spectrum at the plane z_1, $P_R(k_x, z_1)$, will be the incident pressure wave spectrum at the plane z_1, $P_I(k_x, z_1)$, weighted by the reflection coefficient spectrum $R(k_x, z_1)$. Similarly, the transmitted pressure wave spectrum at the plane z_{N+1}, $P_{T_r}(k_x, z_{N+1})$, will be $P_I(k_x, z_1)$ weighted by the transmission coefficient spectrum $T_r(k_x, z_{N+1})$.

However, the reflection and transmission coefficients have been calculated in terms of the displacement amplitude of the incident partial plane wave and not its pressure. Thus, the reflected and transmitted spectra will be first calculated in the form of displacement amplitude spectra denoted by $A_R(k_x, z_1)$ and $A_{T_r}(k_x, z_{N+1})$ respectively, and then will be converted into the corresponding pressure wave spectra. $A_R(k_x, z_1)$ and $A_{T_r}(k_x, z_{N+1})$ are found by multiplying the incident displacement amplitude wave spectrum $A_I(k_x, z_1)$ by $R(k_x, z_1)$ and $T_r(k_x, z_{N+1})$, respectively.

A relationship between the pressure spectrum and the amplitude spectrum for each of the incident, reflected, and transmitted waves is needed for the conversion. Referring to Eq. (2.16), for a plane wave propagating in a fluid medium, its pressure can be related to the corresponding displacement amplitude through:

$$P_{f_i}^{L^\pm} = -jK_f\left(p_{z_i}^{L^\pm} k_{z_i}^{L^\pm} + p_{x_i}^{L^\pm} k_i\right) a_i^{L^\pm} = -jK_{f_i} \frac{\omega}{c_i} a_i^{L^\pm}. \tag{4.6}$$

Hence, for the incident plane wave at $z = z_1$, $A_I(k_x, z_1)$ and $P_I(k_x, z_1)$ can be related through:

$$P_I(k_x, z_1) = -jK_{f_0} \frac{\omega}{c_0} A_I(k_x, z_1). \tag{4.7}$$

Thus, the reflected displacement amplitude wave spectrum at the plane z_1 will be:

$$A_R(k_x, z_1) = R(k_x, z_1) \times A_I(k_x, z_1). \tag{4.8}$$

Then, the reflected displacement amplitude wave spectrum is converted into a pressure wave spectrum using Eq. (4.6) as follows:

$$P_R(k_x, z_1) = -jK_{f_0} \frac{\omega}{c_0} \times A_R(k_x, z_1). \tag{4.9}$$

Substituting the expression of $A_R(k_x, z_1)$ in Eq. (4.8) into Eq. (4.9) yields:

$$P_R(k_x, z_1) = -jK_{f_0} \frac{\omega}{c_0} \times R(k_x, z_1) \times A_I(k_x, z_1). \tag{4.10}$$

Then, using Eq. (4.7) to express $A_I(k_x, z_1)$ in terms of $P_I(k_x, z_1)$, the reflected pressure wave spectrum is found to be related to the incident pressure wave spectrum and to the reflection coefficient spectrum through:

$$P_R(k_x, z_1) = R(k_x, z_1) \times P_I(k_x, z_1). \tag{4.11}$$

Similarly, for the transmitted plane waves at the surface z_{N+1}, if a fluid transmission medium is considered, their displacement amplitude spectrum is:

$$A_{T_r}(k_x, z_{N+1}) = T_r(k_x, z_{N+1}) \times A_I(k_x, z_1). \tag{4.12}$$

Using the relationship in Eq. (4.6), the transmitted displacement amplitude wave spectrum is converted into a pressure wave spectrum as follows:

$$P_{T_r}(k_x, z_{N+1}) = -jK_{f_{N+1}} \frac{\omega}{c_{N+1}} A_{T_r}(k_x, z_{N+1}). \tag{4.13}$$

Substituting the expression of $A_{T_r}(k_x, z_1)$ in Eq. (4.12) into Eq. (4.13) leads to:

$$P_{T_r}(k_x, z_{N+1}) = -jK_{f_{N+1}} \frac{\omega}{c_{N+1}} T_r(k_x, z_{N+1}) \times A_I(k_x, z_1). \tag{4.14}$$

Then, using Eq. (4.7) to express $A_I(k_x, z_1)$ in terms of $P_I(k_x, z_1)$, the transmitted pressure wave spectrum becomes related to the incident pressure wave spectrum and to the transmission coefficient spectrum by:

$$P_{T_r}(k_x, z_{N+1}) = \frac{c_0\, K_{f_{N+1}}}{c_{N+1}\, K_{f_0}}\, T_r(k_x, z_{N+1}) \times P_I(k_x, z_1). \tag{4.15}$$

If the incidence and transmission media were identical, Eq. (4.15) can be reduced to:

$$P_{T_r}(k_x, z_{N+1}) = T_r(k_x, z_{N+1}) \times P_I(k_x, z_1). \tag{4.16}$$

It is to be noted that all the spectra multiplications are performed term by term for every k_x.

Having obtained the reflected pressure wave spectrum at the plane z_1, $P_R(k_x, z_1)$, the corresponding propagated pressure wave spectrum in the incidence medium, $P_R(k_x, z)$ (i.e. the pressure wave spectrum at any parallel plane z such that $z_0 < z < z_1$) is found by multiplying each component of the spectrum at $z = z_1$ by the appropriate phase propagation factor to account for the plane wave propagation in the $-z$ direction, that is:

$$P_R(k_x, z) = P_R(k_x, z_1) \times e^{-jk_{z_0}(z - z_1)}, \qquad z_0 \le z \le z_1. \tag{4.17}$$

Similarly, having the transmitted pressure wave spectrum at the plane z_{N+1}, $P_{T_r}(k_x, z_{N+1})$, the corresponding propagated pressure wave spectrum in the transmission medium, $P_{T_r}(k_x, z)$ (i.e. the pressure wave spectrum at any parallel plane z such that $z_{N+1} < z$) is found by multiplying each component of the spectrum at $z = z_{N+1}$ by the appropriate phase propagation factor to account for the plane wave propagation in the $+z$ direction, that is:

$$P_{T_r}(k_x, z) = P_{T_r}(k_x, z_{N+1}) \times e^{jk_{z_{N+1}}(z - z_{N+1})}, \qquad z_{N+1} \le z\,. \tag{4.18}$$

Thus, finally, the reflected pressure wave field in the incidence medium, and the transmitted pressure wave field in the transmission medium, due to the source incident pressure wave field, are reconstructed by applying the inverse Fourier transform to their angular spectra, and they are expressed respectively as:

$$p_R(x,z) = \mathcal{F}^{-1}\big(P_R(k_x,z)\big) = \frac{1}{2\pi}\int_{-\infty}^{+\infty} P_R(k_x,z)\, e^{jk_x x}\, dk_x, \qquad z_0 \le z_1\,,$$
$$p_{T_r}(x,z) = \mathcal{F}^{-1}\left(P_{T_r}(k_x,z)\right) = \frac{1}{2\pi}\int_{-\infty}^{+\infty} P_{T_r}(k_x,z)\, e^{jk_x x}\, dk_x, \qquad z_{N+1} \le z\,. \tag{4.19}$$

The steps for obtaining the reflected pressure wave field distribution in the incidence medium, $p_R(x,z)$, and the transmitted pressure wave field in the transmission medium, $p_{T_r}(x,z)$, knowing the incident pressure wave field at the plane z_1, $p_I(x,z_1)$, the reflection coefficient spectrum at the plane z_1, $R(k_x,z_1)$, as well as the transmission coefficient angular spectrum at the plane z_{N+1}, $T_r(k_x,z_{N+1})$, are summarized in the diagram of Figure 4-2.

4.2.3 Displacement and Stress Distribution in the Multilayer

In Section 3.5, the partial plane waves displacement amplitudes vector, $\boldsymbol{A}_i$, has been obtained for all the layers of the structure. Subsequently, using Eq. (3.92), the displacement and stress components defined in the displacement-stress vector $\boldsymbol{U}_i(z)$ can be found in any layer and at any plane surface z. The resulting vector $\boldsymbol{U}_i(z)$ corresponds to an incident plane wave with a given incidence direction angle (i.e. given θ_0 or k_x) and a unity amplitude.

In the case of an incident beam on the multilayer, the displacement and stress distribution inside the multilayer can be also obtained using the concept of angular spectrum. In fact, the incident beam being the superposition of planes waves traveling in many directions, the distribution of each component of $\boldsymbol{U}_i(z)$ will be the summation of the contribution of each plane wave component of that incident beam. Hence, if the value of the plane wave incidence angle θ_0, or equivalently k_x, is considered as a variable in the calculation of the displacement-stress vector, then, $\boldsymbol{U}_i(k_x,z)$ is nothing but a vector whose

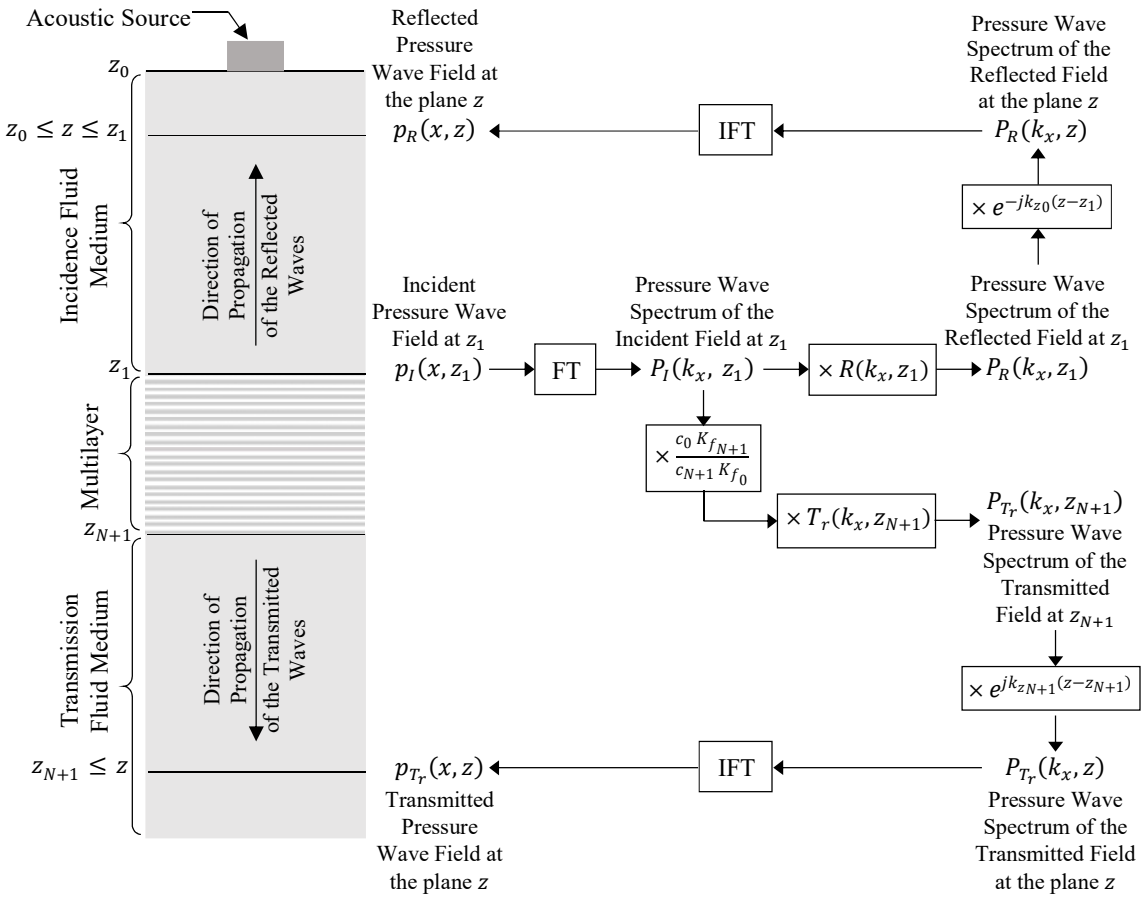

Figure 4-2: Diagram of the steps followed for obtaining the reflected pressure wave field in the incidence medium ($\mathbf{z_0 \leq z \leq z_1}$), and the transmitted pressure wave field in the transmission medium ($\mathbf{z_{N+1} \leq z}$).

components are the displacement and stress amplitudes spectrum at any plane z in the multilayer.

In order to account for the incident plane waves amplitudes, $\boldsymbol{U}_i(k_x,z)$ is weighted by the incident displacement amplitude wave spectrum at the top of the multilayer, i.e. $A_I(k_x,z_1)$. Thus, each component of $\boldsymbol{U}_i(k_x,z)$, at every k_x, is multiplied by the corresponding component of the spectrum $A_I(k_x,z_1)$ (i.e. at the same value of k_x). The resulting displacement-stress spectrum vector, denoted by $\boldsymbol{A}_{\boldsymbol{U}_i}(k_x,z)$ is:

$$\begin{aligned}\boldsymbol{A}_{\boldsymbol{U}_i}(k_x, z) &= \boldsymbol{U}_i(k_x, z) \times A_I(k_x, z_1) \\ &= j\frac{c_0}{\omega K_{f_0}} \boldsymbol{U}_i(k_x, z) \times P_I(k_x, z_1),\end{aligned} \tag{4.20}$$

where $P_I(k_x, z_1)$ is the incident pressure wave spectrum at z_1, related to $A_I(k_x, z_1)$ according to Eq. (4.7).

The field distributions of the displacement and stress components in the multilayer at any plane z, grouped in a column vector $\boldsymbol{a}_{\boldsymbol{U}_i}(x, z)$, are obtained consequently by applying the inverse Fourier transform of each component of $\boldsymbol{A}_{\boldsymbol{U}_i}(k_x, z)$, i.e.:

$$\begin{gathered}\boldsymbol{a}_{\boldsymbol{U}_i}(x, z) = \mathcal{F}^{-1}\left(\boldsymbol{A}_{\boldsymbol{U}_i}(k_x, z)\right) = \frac{1}{2\pi}\int_{-\infty}^{+\infty} \boldsymbol{A}_{\boldsymbol{U}_i}(k_x, z) e^{jk_x x}\, dk_x\,, \\ 1 \le i \le N, \qquad z_1 \le z \le z_{N+1}.\end{gathered} \tag{4.21}$$

4.3 Numerical Application

In this section, an acoustic monochromatic wave beam with a frequency of 1 MHz incident on a three-layered structure immersed in water is simulated. This multilayer consists of a water-filled poro-elastic layer sandwiched between two elastic solid layers having the same mechanical properties as the solid grains of the porous material. The physical parameters of the media are listed in Table 4-1. In order to obtain the corresponding reflected and transmitted beams, as well as the distributions of the displacements and stresses inside the multilayer, the angular spectrum method will be applied as detailed in Section 4.2.

Therefore, at a first stage, the algorithm developed in Section 3.3 is applied in order to obtain the three-layered structure total stiffness matrix for incident plane waves traveling with various directional angles θ_0. Then, the multilayer having its first and last layers elastic solids, the corresponding reflection and transmission coefficients are obtained for every value

of θ_0 as per Section 3.4.5. Figure 4-3 shows the magnitude and phase of the reflection and transmission coefficients as a function of the incidence propagation angle. The results reveal the stability of the method for all the incidence angle values.

Table 4-1 Parameters for the simulated medium layers.

Incidence/Transmission Medium (Water)	Bulk modulus, K_f	2.25 GPa
	Density, ρ_f	1000 Kg/m^3
Elastic Solid Layers	**Thickness, h**	**3 mm**
	Bulk modulus, K_s	37 GPa
	Shear modulus, μ_s	6.5 GPa
	Density, ρ_s	2650 Kg/m^3
Poro-elastic Layer	**Thickness, h**	**5 mm**
Solid Grains	Bulk modulus, K_s	37 GPa
	Shear modulus, μ_s	6.5 GPa
	Density, ρ_s	2650 Kg/m^3
Matrix	Bulk modulus, K_m	8.66 GPa
	Permeability, κ_m	1.9 darcy
	Porosity, ϕ	0.297
Fluid	Bulk modulus, K_f	2.25 GPa
	Viscosity η_f	0.01 Poise
	Density, ρ_f	1000 Kg/m^3

Having obtained the reflection and transmission coefficients of all the incident plane waves directions, the partial plane waves displacement amplitudes vector, $\boldsymbol{A_i}$, can be consequently evaluated inside all the layers of the structure, and for all the incidence angles, by the back recursive algorithm as presented in Section 3.5. Afterwards, the displacement and stress components can be found in any layer, at any plane surface z, and for the corresponding incident plane wave direction by using Eq. (3.92). In order to test the developed algorithm, the magnitudes of the displacement and stress components $u_x(z)$, $u_z(z)$, $w_z(z)$, $\sigma_{xz}(z)$, $\sigma_{zz}(z)$, and $P_f(z)$ corresponding to the plane wave incident on the

three-layered structure with an incidence angle $\theta_0 = 30^o$ are plotted inside the whole structure and shown in Figure 4-4.

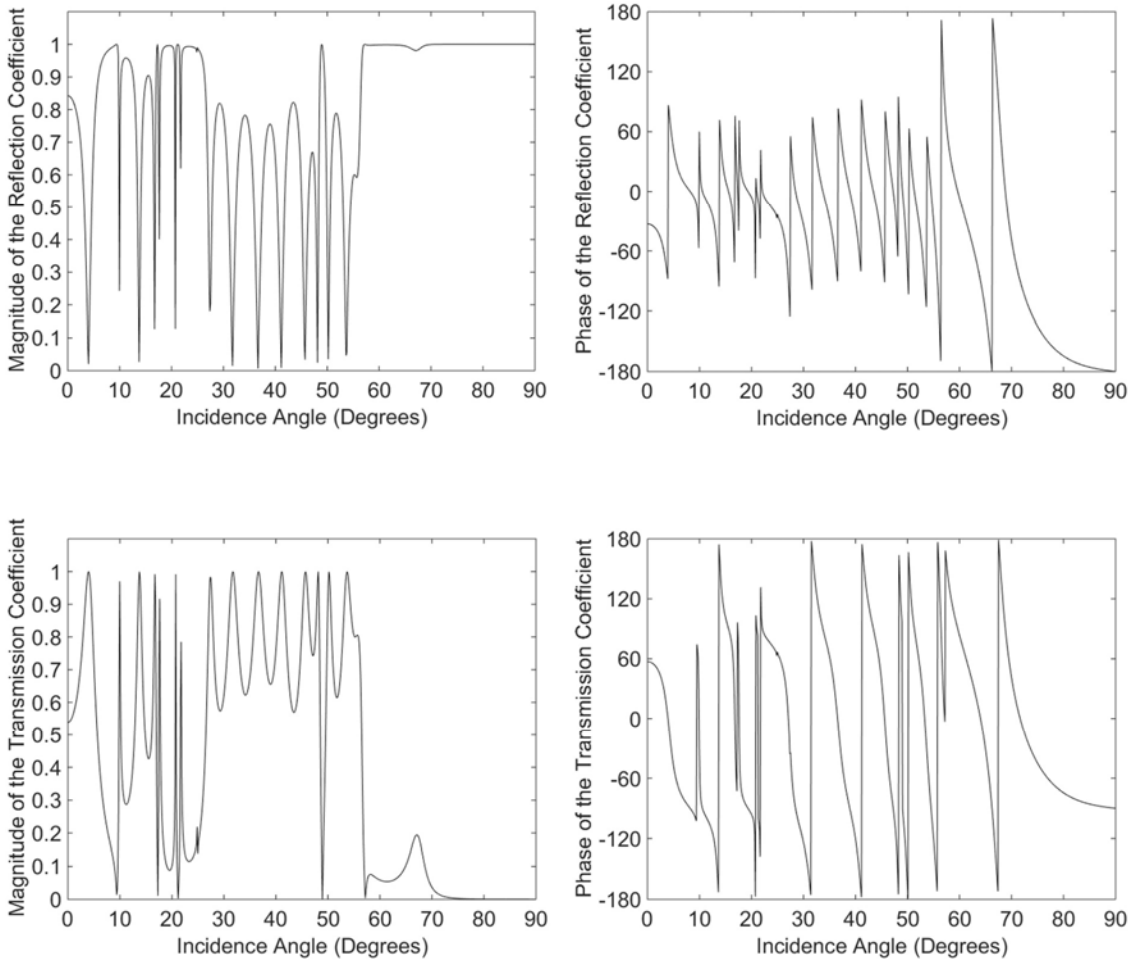

Figure 4-3: Magnitude and phase of the Reflection and Transmission coefficients as a function of the plane waves incidence angles for the three-layered medium and for $f = 1$ MHz.

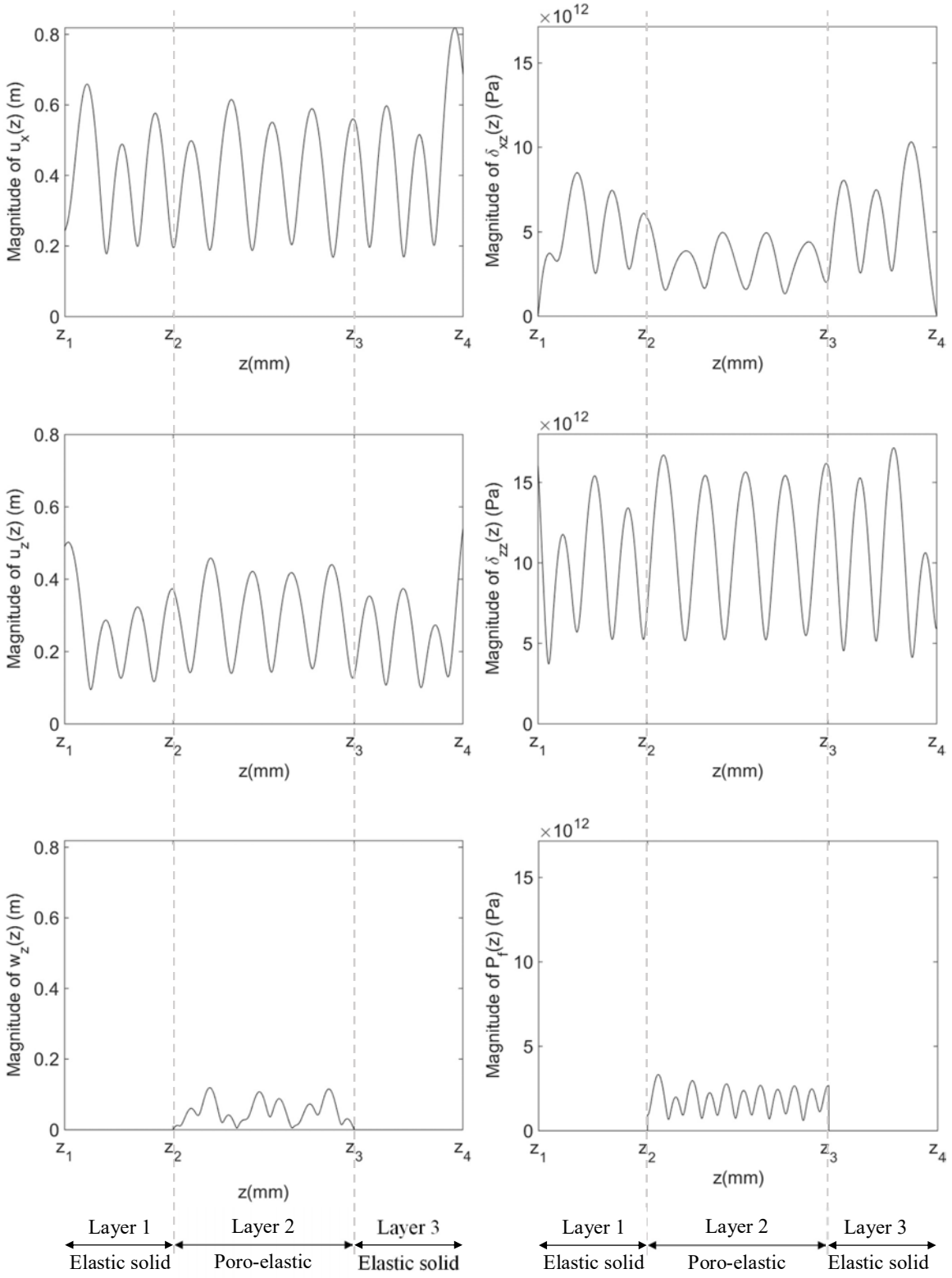

Figure 4-4: Displacement-stress vector components magnitudes inside the three-layered structure for a plane wave incident on the multilayer with a frequency of 1 MHz and an incidence angle $\theta_0 = 30^{\circ}$.

The results plotted in Figure 4-4 show the continuity of all the displacement and stress components at each of the solid-porous interfaces, i.e. at z_2 and z_3. It is to be noted that the z component of the average relative fluid displacement, $w_z(z)$, and fluid phase pressure, $P_f(z)$, are nonzero only in the poro-elastic layer.

Figure 4-5 illustrates the real part of the displacement-stress vector components inside the whole multilayer corresponding to the incident plane waves traveling at various directional angles θ_0, with $0 \leq \theta_0 \leq 90°$. The graphs are plotted in gray scale, with the black and white colors corresponding to the minimum and maximum values, respectively. The plotted results also show a continuity of the displacement and stress components at the interfaces and for all values of the plane wave incidence angle.

Having calculated, for all the incident plane waves directions, the reflection and transmission coefficients as well as the displacement and stress components inside the multilayer, the reflected and transmitted wave fields, as well as the displacements and stresses distributions inside the multilayer can be obtained by applying the angular spectrum method as presented in Section 4.2. Figure 4-6 to Figure ***4-10*** show in gray scale the incident pressure fields for a beam generated by the acoustic source with the steering angles, 15°, 30°, 45°, 60°, and 75°, respectively. These figures show the evolutions of the corresponding reflected pressure fields in the incidence medium, and the transmitted pressure fields in the transmission medium, along with corresponding displacements and stresses distributions resulting inside the structure layers. The acoustic source size is 7.5 mm and it is placed at 40mm from the multilayer, i.e. $h_0 = 40$ mm. Similarly, the black and white colors correspond to the minimum and maximum values, respectively.

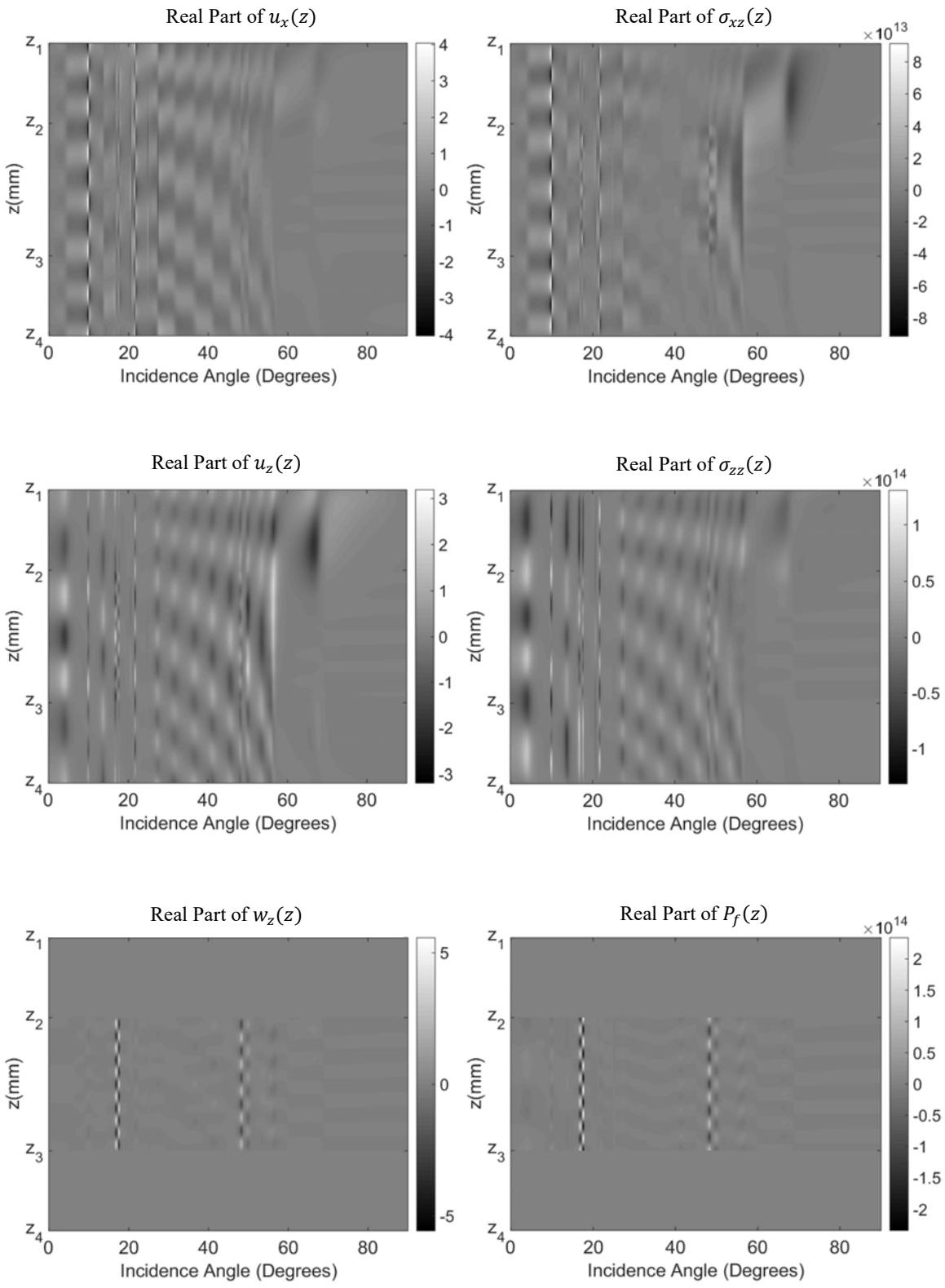

Figure 4-5: The variation of the real parts of the displacement-stress vector components inside the three-layered structure as a function of the plane waves incidence angles.

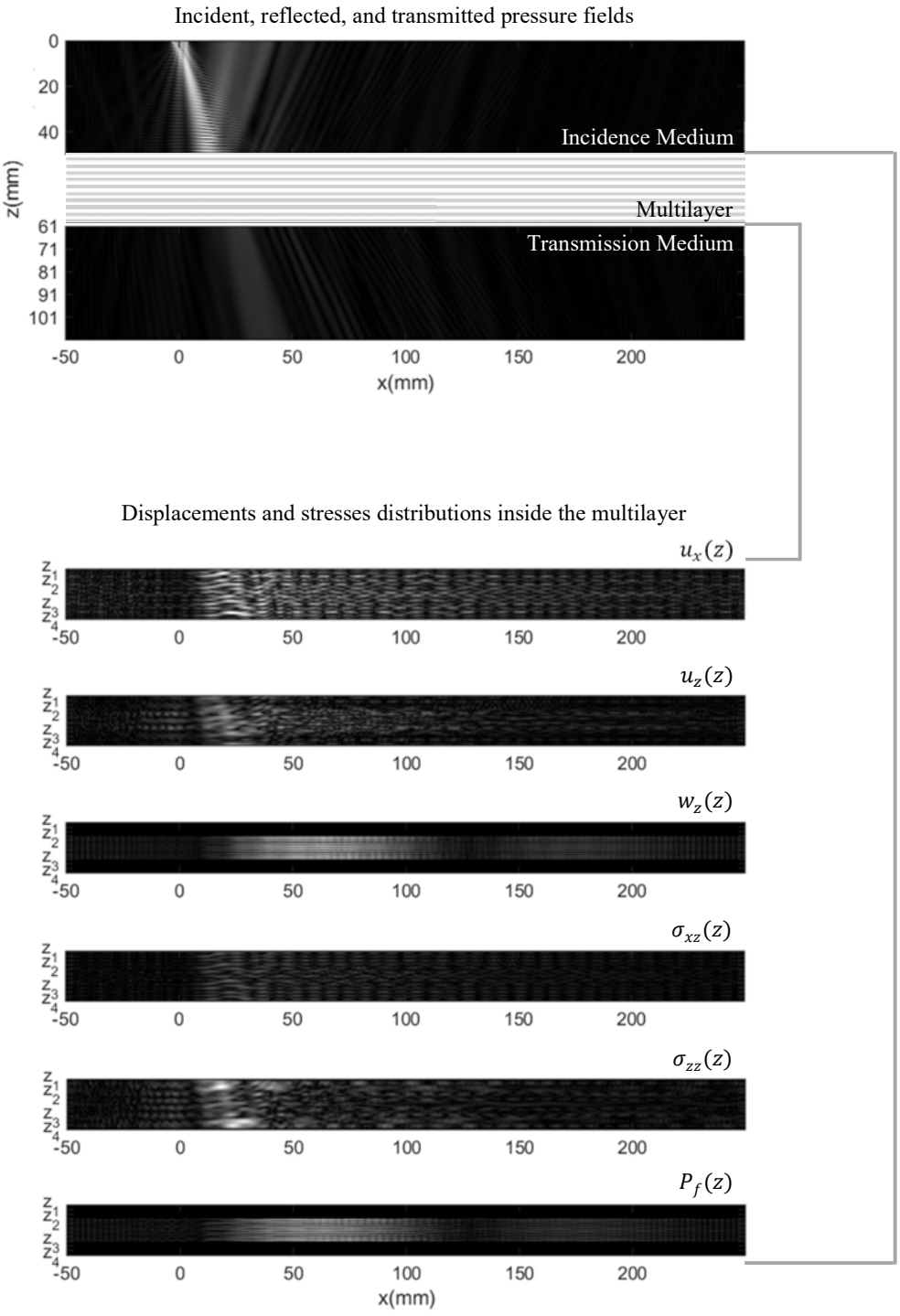

Figure 4-6: The magnitude of the incident pressure field with the corresponding magnitudes of the reflected and transmitted pressure fields, along with the corresponding displacements and stresses distributions in magnitudes inside the multilayer, for an acoustic source with a steering angle of 15°.

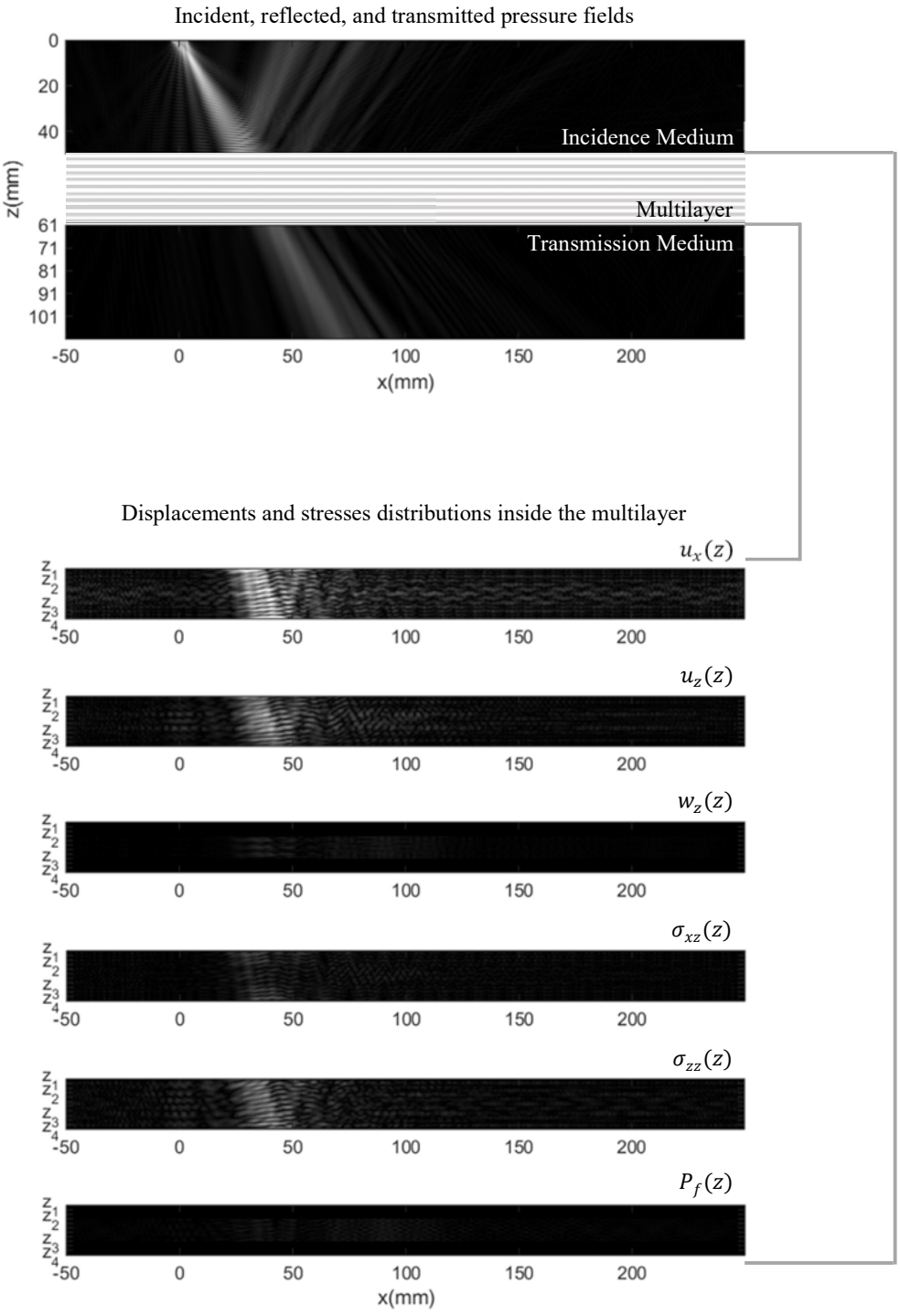

Figure 4-7: The magnitude of the incident pressure field with the corresponding magnitudes of the reflected and transmitted pressure fields, along with the corresponding displacements and stresses distributions in magnitudes inside the multilayer, for an acoustic source with a steering angle of 30°.

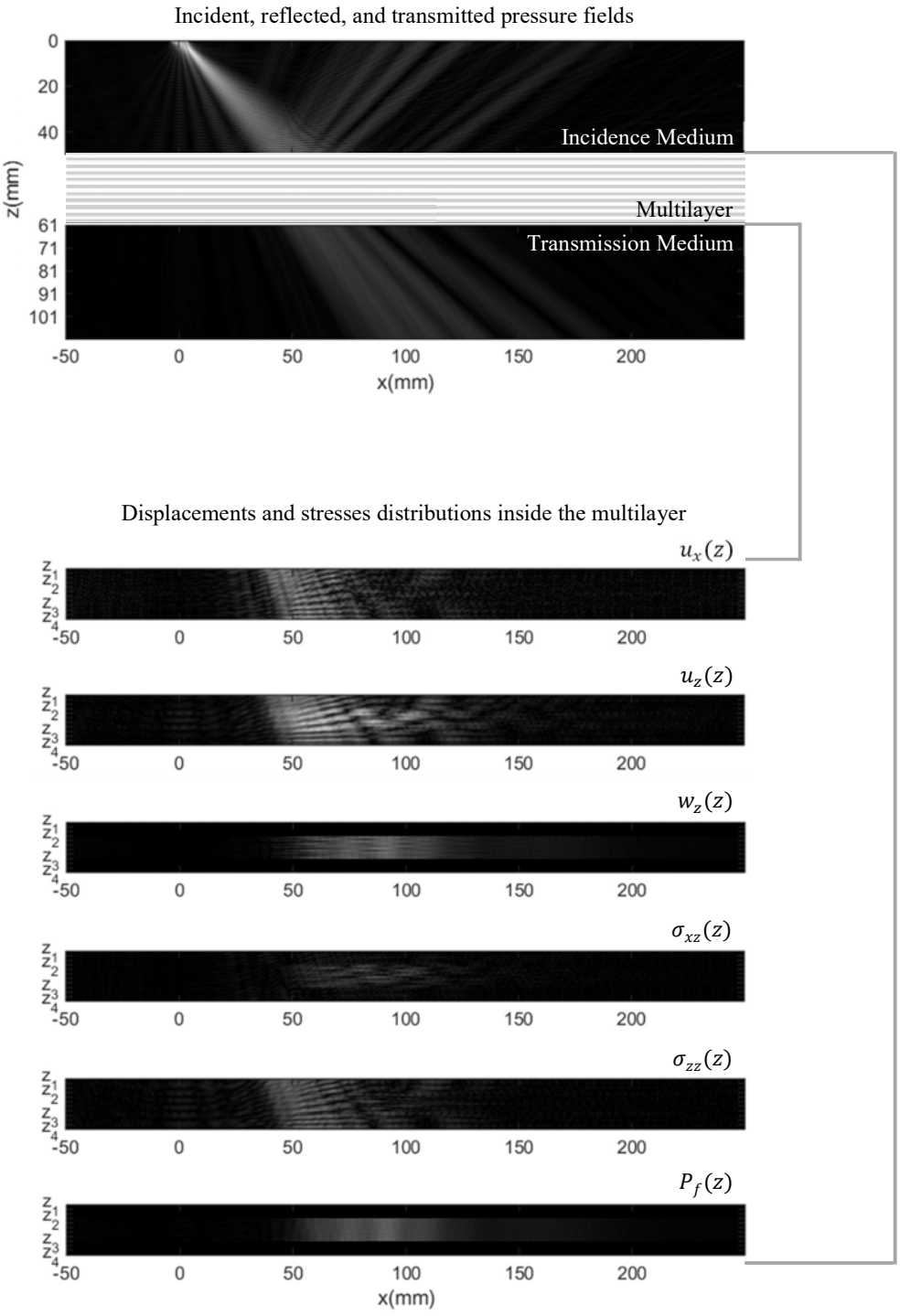

Figure 4-8: The magnitude of the incident pressure field with the corresponding magnitudes of the reflected and transmitted pressure fields, along with the corresponding displacements and stresses distributions in magnitudes inside the multilayer, for an acoustic source with a steering angle of 45°.

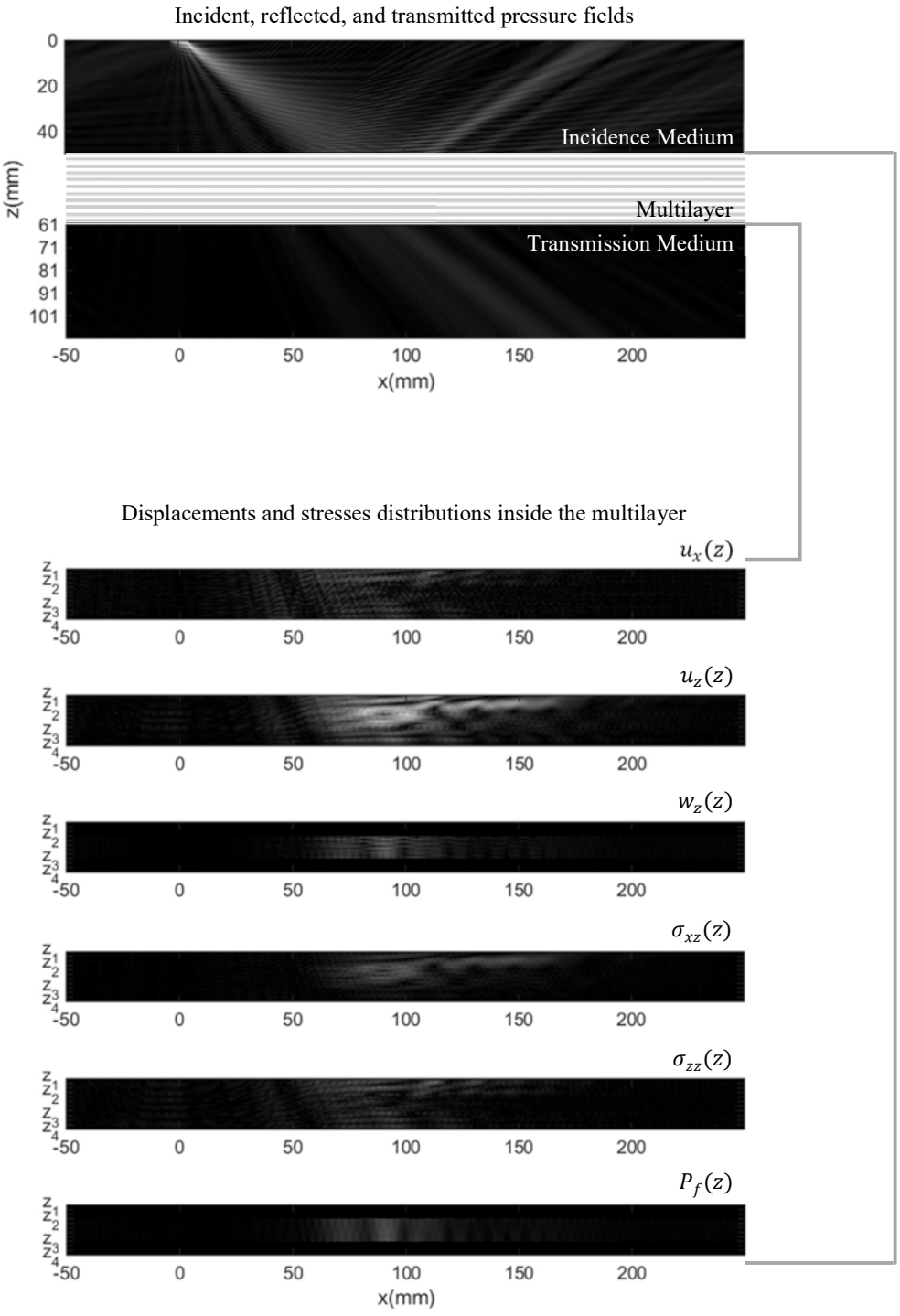

Figure 4-9: The magnitude of the incident pressure field with the corresponding magnitudes of the reflected and transmitted pressure fields, along with the corresponding displacements and stresses distributions in magnitudes inside the multilayer, for an acoustic source with a steering angle of 60°.

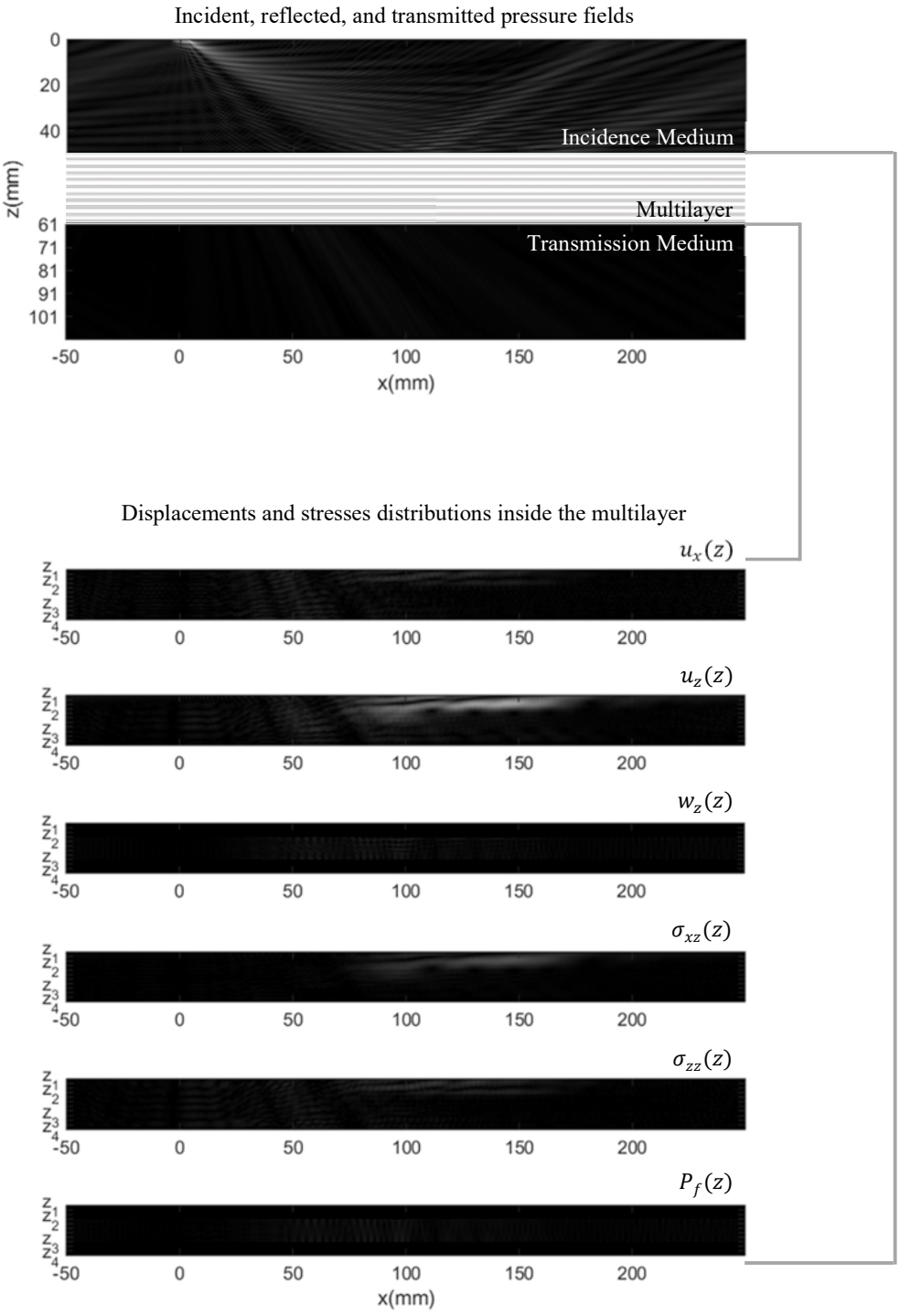

Figure 4-10: The magnitude of the incident pressure field with the corresponding magnitudes of the reflected and transmitted pressure fields, along with the corresponding displacements and stresses distributions in magnitudes inside the multilayer, for an acoustic source with a steering angle of 75°.

The algorithm is furthermore tested to investigate the behavior of the propagating modes in a multilayered medium. Hence, the same three-layered medium immersed in water is considered, but with a varying porosity of the porous layer solid matrix. Figure 4-11 shows the magnitudes of the reflection coefficient diagrams with varying frequency and incidence angle and for various porosities, namely ≅0, 0.3, 0.6 and 1. The graphs are plotted in gray scale the black and white colors corresponding to a zero and a one, respectively.

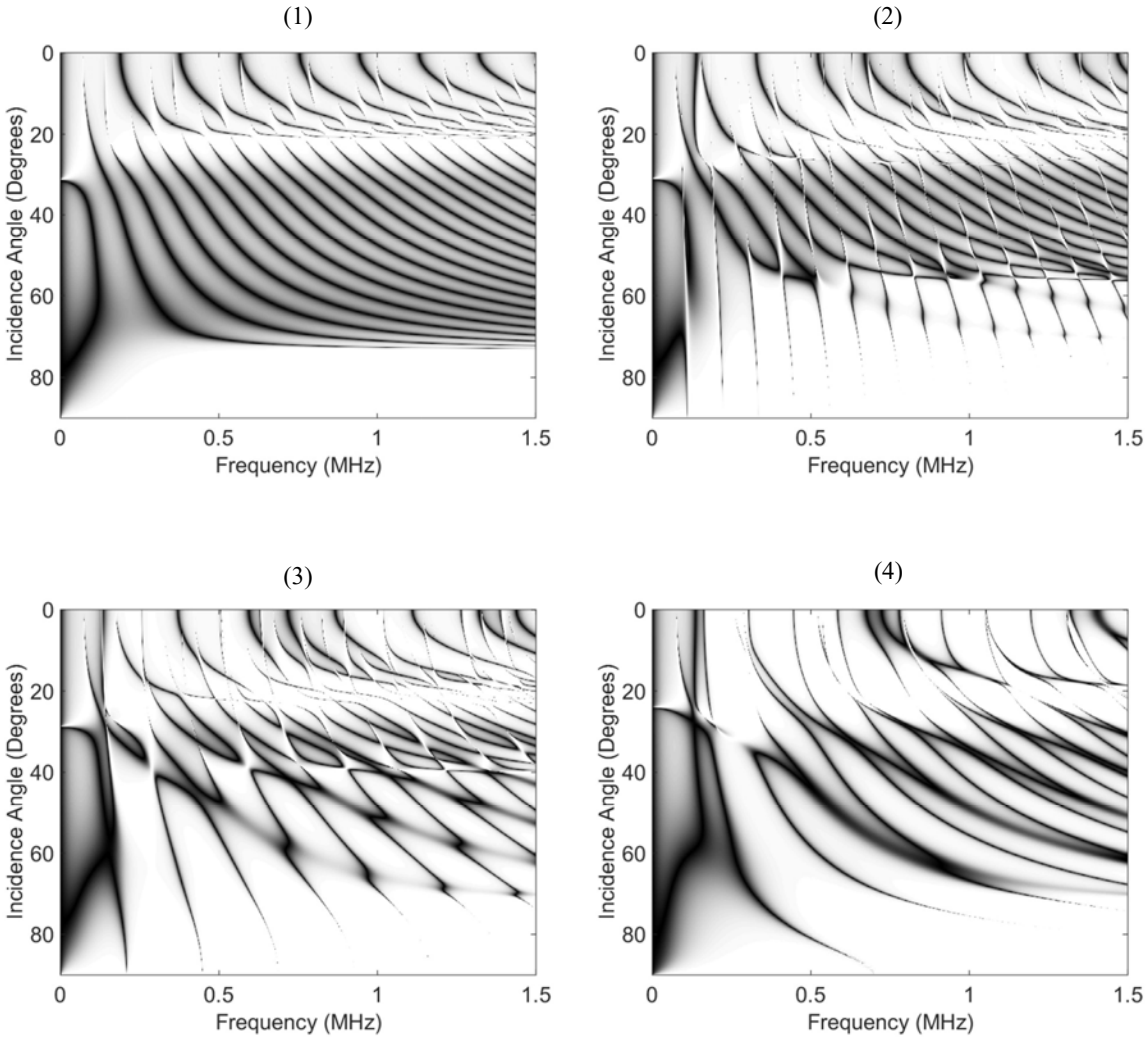

Figure 4-11. Magnitude of the reflection coefficient in terms of the frequency and incidence angle of the incident plane wave on the three-layered structure with porosities: (1) $\phi \cong 0$, (2) 0.3, (3) 0.6, and (4) 1.

With a very negligible porosity (i.e. $\phi \cong 0$), the porous medium tends towards a solid with the same properties as the surrounding solid layers. Hence, the three-layers structure becomes like a single solid layer with its thickness equal to the total thickness of the three layers. Figure 4-11 (1) reflects the guided wave modes dispersion of that single solid layer. Since in the case of a zero porosity the fluid phase or the slow longitudinal mode in the poro-solid vanishes, the modes observed in the diagram (1) of Figure 4-11 are only formed by the longitudinal and shear modes of the solid. The longitudinal mode can be verified at normal incidence (for theta $= 0$) by the resonance periodicity in frequency.

The guided wave modes evolution with a progressive increase of the porosity of the middle layer (for $\phi = 0.3$, 0.6 and 1) is illustrated in the subplots (2) to (4) of Figure 4-11. When the porosity is increased to 0.3, the long light vertical lines appear as shown in the subplot (2) of Figure 4-11, reflecting the additional propagating mode relative to the fluid phase in the porous medium. As the porosity increases furthermore to 0.6, the effect of the fluid phase becomes stronger, which is reflected by the darker vertical lines as shown in subplot (3) of Figure 4-11. When the porosity reaches a value of 1, the middle porous layer tends to behave as a fluid medium, and the effect of the fluid phase in this case is the strongest which is illustrated in subplot (4) of Figure 4-11. Moreover, the speed of the various propagating modes increases with an increase of the porosity, this is reflected by the progressive increase of the periodicity of the frequency of the corresponding modes in the subplots (1) to (4) of Figure 4-11.

4.4 Conclusion

The propagation of an acoustic beam incident on a multilayer consisting of any combination of fluid – isotropic elastic solid – and isotropic fluid-filled poro-elastic materials

has been modeled based on the angular spectrum technique. In this method, in order to model the propagation of a monochromatic wave field, the latter is decomposed into its spectrum of plane waves traveling in different directions. Then, the propagation of each plane wave is treated separately based on the algorithm developed in the previous chapter. In order to reconstruct any resulting wave field distribution, the contributions of all these plane waves are superposed. In this way, the reflected and transmitted waves fields have been obtained, along with the displacement and stress components distributions inside the multilayer.

Then, in order to test the developed algorithm, a numerical example of a three-layered solid-porous-solid medium has been simulated. The algorithm has been first applied on plane waves traveling in different directions. So, first, the global stiffness matrix has been obtained for every incidence directional angle. Then, the reflection and transmission coefficients have been calculated and the displacement and stress components have been evaluated afterwards at any plane inside the multilayer, for every value of a plane wave incidence angle as well. The plots of the displacement and stress components at a particular value of the incidence angle, and in general for all the values of incidence angles, have showed a continuity of each of these components at the interfaces which validates the algorithm. Then by superposing the contributions of the plane waves traveling in various directions, the reflected and transmitted pressure wave fields, as well as the displacement and stress components distributions inside the multilayer have been obtained and plotted for two steering angles of the acoustic source. Furthermore, the effect of the porosity of the porous layer on the partial modes propagating in the three-layered structure has been investigated by simulating the reflection coefficient as a function of the frequency and incidence angle of the incident plane wave.

CONCLUSION

In this work, a general method has been developed to model the acoustic wave field propagation inside a multilayer that consists of any combination of fluid, isotropic elastic solid, and isotropic fluid-filled poro-elastic materials. The propagation of a bounded incident wave beam has been modeled using the angular spectrum method which is based on the decomposition of this field into an equivalent spectrum of plane waves traveling in different directions. The corresponding reflected wave beam in the incidence medium, and the transmitted wave beam in the transmission medium, as well as the displacement and stress components distributions inside the multilayer can be found by adding the contributions of the plane waves traveling in different directions.

Hence, at a first stage a stable and general algorithm has been developed, based on the recursive stiffness matrix approach, to model the propagation of a plane wave incident on the multilayer with a given incidence angle. So, first, each layer of the structure has been characterized: the characteristic and stiffness matrices have been obtained for every layer in terms of the incident plane wave frequency and incidence angle. Three layer-natures have been considered: fluid, isotropic elastic solid, and isotropic poro-elastic material. Then, a recursive algorithm has been implemented to merge the whole multilayer into a single layer characterized by its total stiffness matrix obtained in terms of the incident plane wave frequency and incidence angle. Having the multilayer total stiffness matrix, the reflection and transmission coefficients have been calculated considering fluid incidence and transmission media, which allows then to evaluate the partial waves displacement amplitudes inside every layer of the structure. Consequently, the displacement and stress components could be

deduced at every point of the multilayer corresponding to every plane wave incidence direction.

Afterwards, using the angular spectrum method, the contributions of the plane waves traveling in all the directions are superposed to find the reflected and transmitted wave fields, along with the displacement and stress components distributions.

Finally, the method has been simulated on a three-layered solid-porous-solid structure immersed in water and different results have been plotted.

It is true that the algorithm developed in this work has included only three layer-natures, however, the fact that all the displacements and stresses are expressed in terms of waves amplitudes, rather than potentials, makes it a general and extensible method. Indeed, this allows a future expansion of the formalism to include other material natures, such as anisotropic solids, anisotropic porous media, or piezoelectric materials. The introduction of an additional layer nature to the formalism requires defining its characteristic matrix, and then deriving additional matrices $[\boldsymbol{V}_i]$ corresponding to the interfaces separating this layer nature from the others. In general, for n layer-natures, the number of required matrices $[\boldsymbol{V}_i]$ for the formalism is $n^2 - (n-1)$, and n^2 cases are needed to be developed in order to compute the reflection and transmission coefficients for fluid incidence and transmission media. A further development of this algorithm would be by considering other natures for incidence and transmission media, which would lead to additional cases development for the reflection and transmission coefficients.

LIST OF REFERENCES

[1] S. I. Rokhlin and L. Wang, "Stable recursive algorithm for elastic wave propagation in layered anisotropic media: Stiffness matrix method," *The Journal of the Acoustical Society of America,* vol. 112, no. 3, pp. 822-834, 2002a.

[2] Stoneley, Robert, "Elastic waves at the surface of separation of two solids," *Proc. R. Soc. Lond. A,* vol. 106, no. 738, pp. 416-428, 1924.

[3] R. B. Lindsay, C. R. Lewis and R. D. Albright, "Acoustic Filtration in Non-Homogeneous Media," *The Journal of the Acoustical Society of America,* vol. 5, no. 3, pp. 202-205, 1934.

[4] R. B. Lindsay, "Filtration of oblique elastic waves in stratified media," *The Journal of the Acoustical Society of America,* vol. 11, no. 2, pp. 178-183, 1939.

[5] J. B. Smyth and R. B. Lindsay, "Supersonic Transmission at Oblique Incidence Through a Solid Plate in Water," *The Journal of the Acoustical Society of America,* vol. 16, no. 1, pp. 20-25, 1944.

[6] W. T. Thomson, "Transmission of Elastic Waves through a Stratified Solid Medium," *Journal of applied Physics,* vol. 21, no. 2, pp. 89-93, 1950.

[7] N. A. Haskell, "The dispersion of surface waves on multilayered media," *Bulletin of the Seismological Society of America,* vol. 43, no. 1, pp. 17-34, 1953.

[8] R. P. Shaw and P. Bugl, "Transmission of plane waves through layered linear viscoelastic media," *The Journal of the Acoustical Society of America,* vol. 46, no. 3B, pp. 649-654, 1969.

[9] L. Brekhovskikh, Waves in Layered Media, vol. 16, Elsevier, 2012.

[10] D. L. Folds and C. D. Loggins, "Transmission and reflection of ultrasonic waves in layered media," *The Journal of the Acoustical Society of America,* vol. 62, no. 5, pp. 1102-1109, 1977.

[11] J. W. Dunkin, "Computation of modal solutions in layered, elastic media at high frequencies," *Bulletin of the Seismological Society of America,* vol. 55, no. 2, pp. 335-358, 1965.

[12] T. Kundu and A. K. Mal, "Elastic waves in a multilayered solid due to a dislocation source," *Wave Motion,* vol. 7, no. 5, pp. 459-47, 1985.

[13] D. Lévesque and L. Piché, "A robust transfer matrix formulation for the ultrasonic response of multilayered absorbing media," *The Journal of the Acoustical Society of America,* vol. 92, no. 1, pp. 452-467, 1992.

[14] M. Castaings and B. Hosten, "Transmission coefficient of multilayered absorbing anisotropic media. A solution to the numerical limitations of the Thomson-Haskell method," *Ultrasonics International ,* vol. 93, pp. 431-434, 1993.

[15] M. Castaings and B. Hosten, "Delta operator technique to improve the Thomson–Haskell-method stability for propagation in multilayered anisotropic absorbing plates," *The Journal of the Acoustical Society of America,* vol. 95, no. 4, pp. 1931-1941, 1994.

[16] K. Balasubramaniam, "On a numerical truncation approximation algorithm for transfer matrix method," *Journal of the Acoustical Society of America,* vol. 107, no. 2, pp. 1053-1056, 2000.

[17] K. Balasubramaniam, V. Mukaundan and M. V. Reddy, "A Comparison of Ultrasonic Wave Reflection/transmission Models from Isotropic Multi-Layered Structures by Transfer-Matrix and Stiffness-Matrix Recursive Algorithms," in *AIP Conference Proceedings*, 2003.

[18] L. Knopoff, "A matrix method for elastic wave problems," *Bulletin of the Seismological Society of America,* vol. 54, no. 1, pp. 431-438, 1964.

[19] M. J. Randall, "Fast programs for layered half-space problems," *Bulletin of the Seismological Society of America,* vol. 57, no. 6, pp. 1299-1315, 1967.

[20] F. Schwab, "Surface wave dispersion computations: Knopoff's method," *Bulletin of the Seismological Society of America,* vol. 60, no. 5, pp. 1491-1520, 1970.

[21] H. Schmidt and F. B. Jensen, "A full wave solution for propagation in multilayered viscoelastic media with application to Gaussian beam reflection at fluid–solid interfaces," *The Journal of the Acoustical Society of America,* vol. 77, no. 3, pp. 813-825, 1985.

[22] H. Schmidt and G. Tango, "Efficient global matrix approach to the computation of synthetic seismograms," *Geophysical Journal of the Royal Astronomical Society,* vol. 84, no. 2, pp. 331-359, 1986.

[23] A. K. Mal, "Wave propagation in layered composite laminates under periodic surface loads," *Wave Motion,* vol. 10, no. 3, pp. 257-266, 1988.

[24] E. Storheim, K. D. Lohne and T. Hergum, "Transmission and reflection from a layered medium in water. Simulations and measurements," in *38th Scandinavian Symposium on Physical Acoustics*, Geilo, Norway, 2015.

[25] M. J. Lowe, "Matrix techniques for modeling ultrasonic waves in multilayered media," *IEEE Transactions on Ultrasonics, Ferroelectrics, and Frequency Control,* vol. 42, no. 4, pp. 525-542, 1995.

[26] E. Kausel and J. M. Roesset, "Stiffness matrices for layered soils," *Bulletin of the Seismological Society of America,* vol. 71, no. 6, pp. 1743-1761, 1981.

[27] B. N. Kennett and N. J. Kerry, "Seismic waves in a stratified half space," *Geophysical Journal International,* vol. 57, no. 3, pp. 557-583, 1979.

[28] B. N. Kennett, Seismic Wave Propagation in Stratified Media, ANU Press, 2009.

[29] G. J. Fryer and L. N. Frazer, "Seismic waves in stratified anisotropic media," *Geophysical Journal International,* vol. 78, no. 3, pp. 691-710, 1984.

[30] G. Fryer and L. N. Frazer, "Seismic waves in stratified anisotropic media-II. Elastodynamic eigensolutions for some anisotropic systems," *Geophysical Journal of the Royal Astronomical Society,* vol. 91, no. 1, pp. 73-101, 1987.

[31] S. I. Rokhlin and W. Huang, "Ultrasonic wave interaction with a thin anisotropic layer between two anisotropic solids. II. Second-order asymptotic boundary conditions," *The Journal of the Acoustical Society of America,* vol. 94, no. 6, pp. 3405-3420, 1993.

[32] L. Wang and S. I. Rokhlin, "Stable reformulation of transfer matrix method for wave propagation in layered anisotropic media," *Ultrasonics,* vol. 39, no. 6, pp. 413-424, 2001.

[33] S. I. Rokhlin and L. Wang, "Ultrasonic waves in layered anisotropic media: characterization of multidirectional composites," *International Journal of Solids and Structures,* vol. 39, no. 21-22, pp. 5529-5545, 2002b.

[34] J.-F. Allard, R. Bourdier and C. Depolier, "Biot waves in layered media," *Journal of Applied Physics,* vol. 60, no. 6, pp. 1926-1929, 1986.

[35] J.-F. Allard, C. Depolier, P. Rebillard, W. Lauriks and A. Cops, "Inhomogeneous Biot waves in layered media," *Journal of Applied Physics,* vol. 66, no. 6, pp. 2278-2284, 1989.

[36] D. P. Schmitt, "Acoustic multipole logging in transversely isotropic poroelastic formations," *The Journal of the Acoustical Society of America,* vol. 86, no. 6, pp. 2397-2421, 1989.

[37] W. Lauriks, J. F. Allard, C. Depollier and A. Corps, "Inhomogeneous plane waves in layered materials including fluid, solid and porous layers," *Wave Motion,* vol. 13, no. 4, pp. 329-336, 1991.

[38] A. K. Vashishth and P. Khurana, "Waves in stratified anisotropic poroelastic media: a transfer matrix approach," *Journal of Sound and Vibration,* vol. 277, no. 1-2, pp. 239-275, 2004.

[39] J. Jocker, D. Smeulders, G. Drijkoningen, C. van der Lee and A. Kalfsbeek, "Matrix propagator method for layered porous media: Analytical expressions and stability criteria," *Geophysics,* vol. 69, no. 4, pp. 1071-1081, 2004.

[40] J. O. Parra and P. C. Xu, "Dispersion and attenuation of acoustic guided waves in layered fluid-filled porous media," *The Journal of the Acoustical Society of America,* vol. 95, no. 1, pp. 91-98, 1994.

[41] B. Brouard, D. Lafarge and J. F. Allard, "A general method of modelling sound propagation in layered media," *Journal of Sound and Vibration,* vol. 183, no. 1, pp. 129-142, 1995.

[42] J. Allard and N. Atalla, Propagation of sound in porous media: modelling sound absorbing materials 2e, John Wiley & Sons, 2009.

[43] R. K. N. D. Rajapakse and T. Senjuntichai, "Dynamic response of a multi-layered poroelastic medium," *Earthquake Engineering & Structural Dynamics,* vol. 24, no. 5, pp. 703-722, 1995.

[44] T. Senjuntichai and R. K. N. D. Rajapakse, "Exact stiffness method for quasi-statics of a multi-layered poroelastic medium," *International Journal of Solids and Structures,* vol. 32, no. 11, pp. 1535-1553, 1995.

[45] G. Degrande, G. De Roeck, P. Van den Broeck and D. Smeulders, "Wave propagation in layered dry, saturated and unsaturated poroelastic media," *International Journal of Solids and Structures,* vol. 35, no. 34-35, pp. 4753-4778, 1998.

[46] S. J. Feng, Z. L. Chen and H. X. Chen, "Reflection and transmission of plane waves at an interface of water/multilayered porous sediment overlying solid substrate," *Ocean Engineering,* vol. 126, pp. 217-231, 2016.

[47] D. Royer and E. Dieulesaint, Elastic Waves in Solids I: Free and Guided Propagation, translated by DP Morgan, New York: Springer-Verlag, 2000.

[48] Z. E. A. Fellah, M. Fellah and C. Depollier, "Transient Acoustic Wave Propagation in Porous Media," in *Modeling and Measurement Methods for Acoustic Waves and for Acoustic Microdevices*, M. G. Beghi, Ed., Rijeka, Croatia, InTech, 2013, pp. 127-160.

[49] C. Zwikker and C. W. Kosten, Sound absorbing materials, New York: Elsevier, 1949.

[50] M. A. Biot, "Theory of Propagation of Elastic waves in a Fluid-Saturated Porous Solid. I. Low-Frequency Range," *The Journal of the Acoustical Society of America,* vol. 28, no. 2, pp. 168-178, 1956a.

[51] M. A. Biot, "Theory of propagation of elastic waves in a fluid-saturated porous solid. II. Higher frequency range," *The Journal of the Acoustical Society of America,* vol. 28, no. 2, pp. 179-191, 1956b.

[52] K. Attenborough, "Acoustical characteristics of porous materials," *Physics Reports,* vol. 82, no. 3, pp. 179-227, 1982.

[53] K. Attenborough, "Acoustical characteristics of rigid fibrous absorbents and granular materials," *he Journal of the Acoustical Society of America,* vol. 73, no. 3, pp. 785-799,

1983.

[54] D. L. Johnson, J. Koplik and R. Dashen, "Theory of dynamic permeability and tortuosity in fluid-saturated porous media," *Journal of Fluid Mechanics,* vol. 176, pp. 379-402, 1987.

[55] Y. Champoux and J. F. Allard, "Dynamic tortuosity and bulk modulus in air-saturated porous media," *Journal of Applied Physics,* vol. 70, no. 4, pp. 1975-1979, 1991.

[56] D. Lafarge, P. Lemarinier, J. F. Allard and V. Tarnow, "Dynamic compressibility of air in porous structures at audible frequencies," *The Journal of the Acoustical Society of America,* vol. 102, no. 4, pp. 1995-2006, 1997.

[57] N. Sebaa, "Propagation des ondes acoustiques dans les milieux poreux saturés: application du modèle de Biot à détermination des paramètres de mousses plast iques et de l'os trabéculaire," 2006.

[58] M. A. Biot, "Mechanics of Deformation and Acoustic Propagation in Porous Media," *Journal of Applied Physics,* vol. 33, no. 4, pp. 1482-1498, 1962.

[59] J. G. Berryman, "Elastic wave propagation in fluid-saturated porous media," *he Journal of the Acoustical Society of America,* vol. 69, no. 2, pp. 416-424, 1981.

[60] N. C. Dutta and H. Ode, "Seismic reflections from a gas-water contact," *Geophysics,* vol. 48, no. 2, pp. 148-162, 1983.

[61] J. M. Carcione, Wave fields in real media: Wave propagation in anisotropic, anelastic, porous and electromagnetic media, Elsevier, 2007.

[62] R. M. Corredor, J. E. Santos, P. M. Gauzellino and J. M. Carcione, "Reflection and transmission coefficients of a single layer," *The Journal of the Acoustical Society of America,* vol. 135, no. 6, pp. 3151-3162, 2014.

[63] J. G. Berryman, "Confirmation of Biot's theory," *Applied Physics Letters,* vol. 37, no. 4, pp. 382-384, 1980.

[64] J. E. Santos, J. M. Corbero, C. L. Ravazolli and J. L. Hensley, "Reflection and transmission coefficients in fluid-saturated porous media," *The Journal of the Acoustical Society of America,* vol. 91, no. 4, pp. 1911-1923, 1992.

[65] B. Bianco, A. Cambiaso and T. Tommasi, "On the boundary conditions for acoustic waves at a solid–solid or fluid–solid interface," *The Journal of the Acoustical Society of America,* vol. 95, no. 1, pp. 40-44, 1994.

[66] W. Kunyu, Q. Xue and L. Adler, "Reflection and transmission of elastic waves from a fluid-saturated porous solid boundary," *The Journal of the Acoustical Society of America,* vol. 87, no. 6, pp. 2349-2358, 1990.

[67] J. T. Wang, F. Fin and C. H. Zhang, "Reflection and transmission of plane waves at an interface of water/porous sediment with underlying solid substrate," *Ocean*

Engineering, vol. 63, pp. 8-16, 2013.

[68] J. W. Goodman, Introduction to Fourier optics, Roberts and Company Publishers, 2005.

[69] P. R. Stepanishen and K. C. Benjamin, "Forward and backward projection of acoustic fields using FFT methods," *The Journal of the Acoustical Society of America,* vol. 71, no. 4, pp. 803-812, 1982.

[70] M. E. Schafer and P. A. Lewin, "Transducer characterization using the angular spectrum method," *The Journal of the Acoustical Society of America,* vol. 85, no. 5, pp. 2202-2214, 1989.

[71] C. J. Vecchio, M. E. Schafer and P. A. Lewin, "Prediction of ultrasonic field propagation through layered media using the extended angular spectrum method," *Ultrasound in Medicine & Biology,* vol. 20, no. 7, pp. 611-622, 1994.

[72] C. J. Vecchio and P. A. Lewin, "Finite amplitude acoustic propagation modeling using the extended angular spectrum method," *The Journal of the Acoustical Society of America,* vol. 95, no. 5, pp. 2399-2408, 1994.